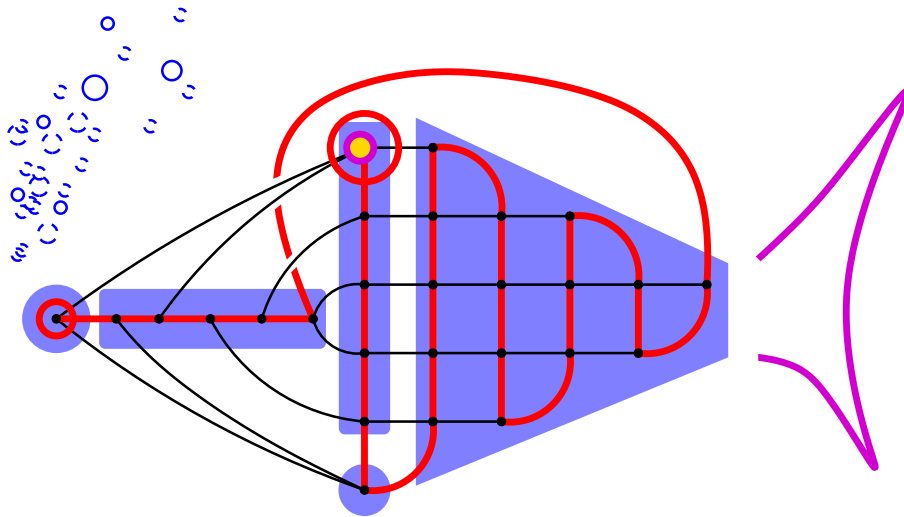


# Extremal Constructions for Polytopes and Spheres



Julian Pfeifle

.

PhD Dissertation, TU Berlin

April, 2003

D83





Paradys vischje. Le Poisson de Paradis, tres-beau et dont  
 il y a de differentes grandeurs et couleurs dans les Reservoirs de Loeven.  
 Il est familier, se plaît à entendre le son des flutes et flageolets, sautant souvent  
 un pied hors de l'eau comme pour se montrer et faire admirer ses belles  
 couleurs.

Louis Renard, *Poissons, Ecrevisses et Crabes, de Diverses Couleurs et Figures Extraordinaires ...*  
(Fishes, Crayfishes, and Crabs of Diverse Coloration and Extraordinary Form ...)  
Amsterdam, 1754

# Extremal Constructions for Polytopes and Spheres

vorgelegt von  
Mag. rer. nat. Julian Pfeifle  
aus Innsbruck

Von der Fakultät II – Mathematik und Naturwissenschaften  
der Technischen Universität Berlin  
zur Erlangung des akademischen Grades

Doktor der Naturwissenschaften  
– Dr. rer. nat. –

genehmigte Dissertation

Berichter  
Prof. Günter M. Ziegler · TU Berlin  
Prof. Francisco Santos · Universidad de Cantabria

Tag der wissenschaftlichen Aussprache: 4. April 2003

gefördert durch die DFG im Rahmen des Europäischen Graduiertenkollegs  
‘Combinatorics, Geometry, and Computation’ (GRK 588/2)

Berlin, April 2003  
D83



## Acknowledgements

It is only fitting to continue the tradition and cite Manuel Abellanas [1] in first place. Without him and his constant encouragement, none of this would have happened.

## Thank you,

all `combis` in Berlin, for all the support and the excellent working environment

christoph eyrich, for myśliwska and teaching me all the  $\lambda^{\alpha_{\mathcal{T}\mathcal{E}}\chi}$  i know (and then some)

Volker Kaibel, for the strongly non-polynomial patience in going through endless details in my manuscripts, and the expertise in shortening or lengthening my proofs

Paco Santos, not least for leaving Iñigo a day longer than necessary to come to my exam

Ewgenij Gawrilow and Michael Joswig, for `polymake`

the staff and outfitters of the Molotov-cocktail depot, for volatile cakes & coffee

Jörg Rambau, for coauthoring Chapter 6

Alexander Schwartz, for reading the manuscript and fixing all the software just in time

Bettina Felsner, for making it all work smoothly

Lourdes, que tú sabes muy bien todo lo que te tengo que agradecer

The place of honor, of course, goes to my PhD advisor, Günter M. Ziegler. He knows better than anyone else just how many wonderful things I learned in these three exciting years in Berlin. Thank you so much for everything, Günter.





# Contents

1	Introduction	3
2	Definitions: Complexes, polytopes, spheres	11
 <b>I Polytopes</b>		
3	The monotone upper bound problem: Overview	17
3.1	Solution status of the problems . . . . .	20
3.1.1	The combinatorial realizability problem . . . . .	20
3.1.2	The monotone realizability problem . . . . .	20
3.2	New results in this thesis . . . . .	22
3.3	Open problems . . . . .	24
4	An exhaustive analysis of a small polytope	27
4.1	A very brief introduction to the Gale transform . . . . .	27
4.2	The polar-Gale transform . . . . .	29
4.3	Three nonrealizable Hamiltonian AOF Holt-Klee orientations . . . . .	32
4.4	Realizing ascending Hamiltonian paths . . . . .	39
5	Long ascending paths in dimension 4	43
5.1	Introduction . . . . .	43
5.2	A family of polar-to-neighborly $d$ -polytopes . . . . .	44
5.3	A Hamiltonian path in dimension 4 . . . . .	50
5.4	Realizing the ascending Hamiltonian paths . . . . .	52
5.4.1	Outline of the inductive construction . . . . .	53
5.4.2	Properties of the family of polytopes . . . . .	54
5.4.3	Start of the induction and inductive invariant . . . . .	55
5.4.4	Induction step I: Positioning the polytope . . . . .	56
5.4.5	Induction step II: Finding the cutting plane . . . . .	57
5.4.6	Induction step III: The projective transformation . . . . .	59
6	Secondary Polytopes: An Invitation	63
6.1	The convex hull of triangulations: Secondary polytopes . . . . .	64
6.2	Hypergeometric Differential Equations . . . . .	67
6.3	The GKZ vectors . . . . .	68
6.4	Implementation: How to find the face lattice of the secondary . . . . .	69

## II Spheres

7	Overview	77
7.1	Many triangulated 3-spheres . . . . .	77
7.1.1	The $g$ -Theorem . . . . .	78
7.1.2	Many triangulated $d$ -spheres . . . . .	78
7.2	New results in this thesis . . . . .	80
7.3	Open problems . . . . .	80
8	Kalai's squeezed 3-spheres are polytopal	83
8.1	Kalai's 3-spheres . . . . .	83
8.2	Interlude: Some facts on cyclic polytopes . . . . .	84
8.3	A bird's-eye view of the realization construction . . . . .	86
8.4	How to realize Kalai's 3-spheres . . . . .	87
8.5	A shorter proof that squeezed 3-spheres are Hamiltonian . . . . .	90
9	Many triangulated 3-spheres	95
9.1	Heffter's embedding of the complete graph . . . . .	95
9.2	The E-construction . . . . .	97
9.3	Heegaard splittings . . . . .	97
9.4	Many triangulated 3-spheres . . . . .	98
10	Neighborly centrally symmetric fans	101
10.1	Introduction . . . . .	101
10.2	The number of facets of a cs-neighborly cs-fan . . . . .	103
10.3	Centrally symmetric Gale diagrams . . . . .	105
10.3.1	Centrally symmetric Gale diagrams on few vertices . . . . .	108
10.4	No cs-neighborly cs-fans on few rays . . . . .	109
10.4.1	Even dimension . . . . .	110
10.4.2	Odd dimension . . . . .	111
11	Zusammenfassung	125





## Chapter 1

### Introduction

This thesis provides some new constructions for extremal polytopes and spheres. You will find all relevant definitions in Chapter 2, but to set the stage, here are two 2-dimensional convex polytopes (also called *convex polygons*, of course) and two 1-dimensional spheres:

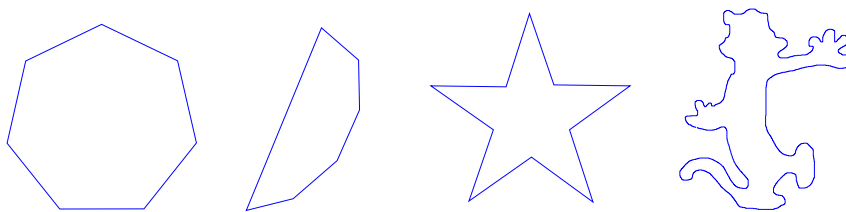


FIGURE 1.1: Two 2-dimensional polytopes and two 1-dimensional spheres

The first polytope is interesting because it is *regular* (in just about every sense of the word), and the second one because it is possible to traverse it from ‘bottom’ to ‘top’ along edges in such a way that we visit *every* vertex of the polytope. As you can see in the next picture, *spheres* arise by dropping the convexity requirement, and the last picture suggests that in some ways, spheres may be the more interesting objects.

Of course, the story continues in dimension 3, so let’s see some examples:

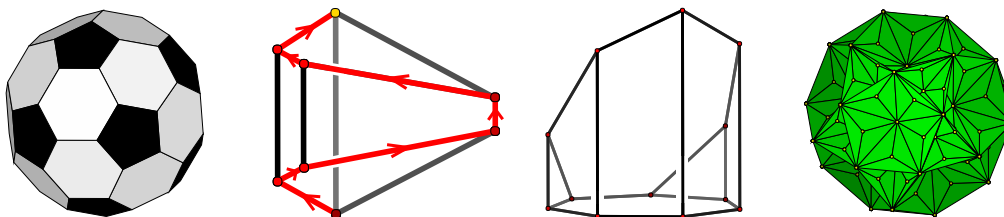


FIGURE 1.2: Three 3-dimensional polytopes and a 2-dimensional sphere

The soccer ball [81], or *truncated icosahedron*, is one of the thirteen *Archimedean* or *semi-regular solids*: all faces are regular polygons and all vertices are ‘surrounded’ in the same way (i.e., the vertex figures are congruent), but not all faces are congruent. The second polytope is the 3-dimensional *Klee-Minty cube* [54], which is combinatorially equivalent to a regular 3-cube (i.e., it has the same vertex-facet incidences), but is realized in such a way as to admit an ascending path along edges passing through all vertices, just like the second

polytope in Figure 1.1. The third, a wedge over a 7-gon, can also be viewed as a *polar of a cyclic polytope*; we will soon meet this polytope again. The last picture is a *simplicial sphere*, consisting of triangles pasted together along edges, such that the union is homeomorphic to  $S^2$  but not necessarily convex.

Polytopes have been around for quite a while—long before the peak of Greek geometry:



FIGURE 1.3: Neolithic carved stone balls from Scotland [34], dating from about 2000 BC

This thesis is mostly about polytopes and spheres in 4-dimensional space. Showing pictures becomes a little more difficult, but is still possible: to draw a *Schlegel diagram* over a *base facet*  $F$  of a polytope  $P$ , choose a viewpoint  $v$  just beyond  $F$ , and intersect (a hyperplane  $H$  parallel to)  $F$  with the cones with apex  $v$  over the other faces of  $P$  (Figure 1.4):

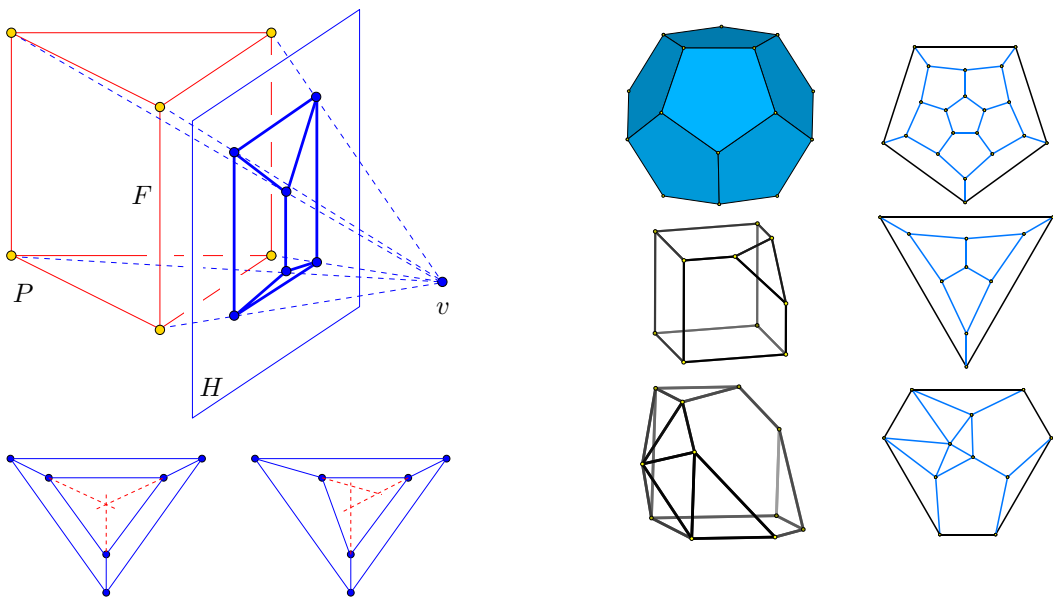


FIGURE 1.4: *Left:* Schlegel diagrams of a triangular prism. Caution: not everything that ‘looks like’ a Schlegel diagram of a prism actually is one, as the lower right drawing shows! In any projective image of a triangular prism  $P$ , the (images of the) carrier lines of the indicated edges intersect in a point, possibly at infinity. Therefore, the lower right image is *not* a Schlegel diagram of  $P$ . Note that taking Schlegel diagrams over different facets may result in combinatorially different images. *Right:* While the dodecahedron is quite straightforward to recognize from its Schlegel diagram, the truncated 3-cube may take a little more time. Stellar subdivisions of faces are again easy to see.

Already before 1855, Schläfli ([85]; see the discussion in [17]) had discovered that in addition to the five regular convex polytopes in  $\mathbb{R}^3$  and the infinite series of regular  $d$ -dimensional cubes, cross-polytopes (‘high-dimensional octahedra’) and simplices, there exist exactly three more regular polytopes, all of them in dimension 4. They are the self-dual *24-cell*, all of whose 24 facets are regular octahedra, and the dual pair of *120-cell* (with 120 regular dodecahedra as facets) and *600-cell*, whose facets are 600 regular tetrahedra.

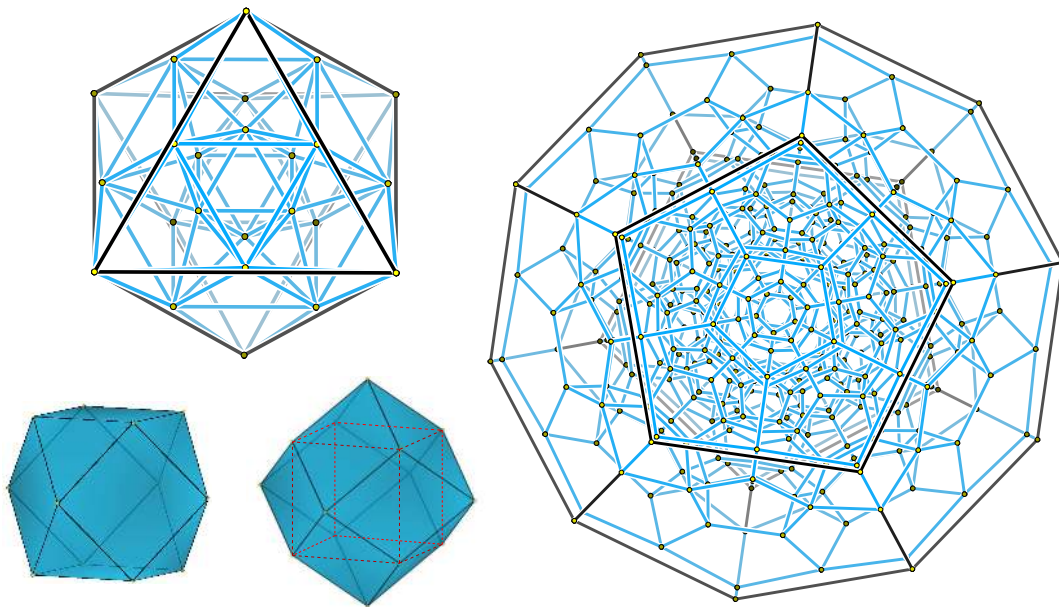


FIGURE 1.5: *Left:* A Schlegel diagram the regular 24-cell. The outer octahedron is the facet that the diagram is based on. Below are two 3-dimensional ‘analoga’ of the 24-cell [17]: The lower left picture shows the convex hull of the midpoints of the edges of an octahedron; in other words, the vertices of the octahedron are truncated in such a way that the truncating planes intersect in the midpoints of the edges of the octahedron. The lower right picture shows a regular 3-cube with 6 pyramids stacked on its facets. The heights of the pyramids are the same as the distance from the center of the cube to the facets. The volume of the resulting polytope (a *rhombic dodecahedron*) is therefore exactly twice the volume of the cube. In dimension 4, both of these constructions give the same polytope, namely the 24-cell. *Right:* The regular 120-cell, all of whose facets are regular dodecahedra.

It is now time to end the commercial on polytopes and begin discussing the main results of this thesis. Put briefly, we solve two extremal problems in polytope theory: We find 4-dimensional polytopes that admit *long ascending paths* along edges, and we construct far more simplicial 3-spheres than there are combinatorial types of 4-dimensional polytopes.

**Part I** of this thesis focuses on the *monotone upper bound problem* for polytopes. The setting of this problem is linear programming theory, so let us quickly review the background.

In many applications (see for example [10], [88] and the references therein) it is important to find the maximal value of a linear *objective function*  $f : \mathbb{R}^d \rightarrow \mathbb{R}$ ,  $\mathbf{x} \mapsto \mathbf{c}^T \mathbf{x}$ , where  $\mathbf{c} \in \mathbb{R}^d$ , subject to  $n$  linear *constraints* of the form  $\mathbf{a}^T \mathbf{x} \leq b$ , with  $\mathbf{a} \in \mathbb{R}^d$  and  $b \in \mathbb{R}$ . One possible canonical form for this *linear programming problem* is the following (see, e.g., [88]):

$$\begin{aligned} & \text{maximize} && \mathbf{c}^T \mathbf{x} \\ & \text{subject to} && A \mathbf{x} \leq \mathbf{b} \ , \end{aligned}$$

where  $\mathbf{x} \in \mathbb{R}^d$  is the *vector of variables*,  $\mathbf{c} \in \mathbb{R}^d$  the *objective function*, and  $A \in \mathbb{R}^{n \times d}$  and  $\mathbf{b} \in \mathbb{R}^n$  represent the  $n$  constraints of the problem. We may suppose that the *feasible region*  $P$  defined by  $A \mathbf{x} \leq \mathbf{b}$  is nonempty and bounded, so that  $P$  is a *polytope*.

The *simplex algorithm* for linear programming was developed by Kantorovich in the 1920s [47]; however, his work did not become generally known (see [48] for an autobiographical account). Around 1947, Dantzig (see [19] and [20] for the history) independently rediscovered and implemented the method. (As an aside, the 2-dimensional case goes back to work by Fourier in 1823; see the references in [88].)

The simplex algorithm starts at any vertex of  $P$ , and according to some *pivot rule* chooses an incident edge  $e$  of  $P$  such that the neighboring vertex of  $P$  along  $e$  improves the value of the objective function. Passing to this neighboring vertex is called making a *pivot step*. An easy lemma (which uses the convexity of  $P$  in an essential way) implies that if no locally improving vertex is found, then the current vertex is already the global optimum.

The *monotone upper bound problem* asks for the maximal number of pivot steps that the simplex algorithm might execute on a particular linear program. In other words, it asks for the maximal number of vertices in a strictly increasing path on a given polytope, where *increase* is measured with respect to some linear objective function.

This problem showcases the enormous difference between our theoretical and practical understanding of the simplex algorithm: On the practitioner's side, a recent study by Bixby [10] informs us that the huge increase in memory capacity and processing speed over the last decades, combined with the development of superior algorithms, makes it possible today to routinely solve linear programs with up to several million variables and constraints. At the same time, Bixby comes to the conclusion that the simplex algorithm is one of the practically most viable approaches towards solving linear programs.

On the other hand, nobody has yet been able to prove a *strongly* polynomial upper bound on the running time of any algorithm for linear programming at all. To elaborate this briefly, there *do* exist so-called *weakly polynomial* algorithms (e.g., the *ellipsoid method* by Khachiyan [50], the *interior point method* by Karmarkar [49] and their variants), whose running time is polynomial in the number  $d$  of variables, the number  $n$  of constraints, and the bit complexity  $L$  of the input. Interior point methods perform quite well in practice [10], while “computational experiments with the [ellipsoid] method are very discouraging” [88, p.170]. Part of the problem seems to be precisely the dependence of the number of iterations on the length of the numbers involved in the input, and the resulting explosion in memory required for storing ever longer numbers, respectively numerical instability in case of rounding.



It remains a major challenge in linear programming theory to prove or disprove the existence of a *strongly polynomial* algorithm, i.e., one whose number of arithmetic operations depends only on  $d$  and  $n$ , but not on  $L$ . In particular, is the simplex algorithm strongly polynomial with an appropriate pivot rule? See Chapter 3 for more on the state of the art.

Our approach in Chapters 4 and 5 is much more modest: we focus on bounding the worst-case behavior of the simplex algorithm in dimension 4. A naive approach in general dimension would be to show that there can be no *long paths* on a polytope, i.e., that the maximal number of pivot steps is bounded by a polynomial in the dimension and the number of facets of the polytope. This could be true for several reasons:

- ▷ If the maximal number  $f_0(d, n)$  of vertices of any  $d$ -dimensional polytope  $P$  defined by  $n$  linear inequalities were polynomial in  $d$  and  $n$ , then obviously the simplex algorithm would only take a polynomial number of steps. However, the existence of *polar-to-neighborly polytopes* shows that  $f_0(d, n)$  may in fact be exponential in  $d$ . (That polar-to-neighborly polytopes in fact have the greatest possible number of vertices among all polytopes with the same dimension and number of facets is the essence of McMullen’s *upper bound theorem* [64] from 1971; cf. Theorem 3.6.)
- ▷ Even though  $P$  may have exponentially many vertices, it could be hoped that the maximal length of a path along edges is bounded by a polynomial in  $d$  and  $n$ . However, Klee [52] provides a Hamiltonian path in the graph of polar-to-cyclic polytopes (the paradigmatic examples of polar-to-neighborly polytopes).
- ▷ A third possibility is that the maximum length of a *strictly ascending* path along edges could be bounded by a polynomial in  $d$  and  $n$ . Such hopes were however dashed in 1972, when Klee and Minty exhibited the first examples of ‘bad’ linear programs, the by now classical *Klee-Minty cubes* [54]; see Figure 1.2 for the 3-dimensional instance. These polytopes have the same combinatorics as a regular  $d$ -dimensional cube, so in particular they have an exponential number  $2^d$  of vertices in terms of their number  $2d$  of facets, and on them (and their variants) several commonly used pivot rules are fooled into exponential running times—in fact, they are made to visit *every* vertex of the cube.

To reiterate, in this thesis we investigate the worst-case behavior of the simplex algorithm in dimension 4. Chapter 4 is devoted to a complete analysis of the smallest interesting 4-dimensional polar-to-neighborly polytope, namely the polar-to-cyclic polytope  $P = C_4(7)^\Delta$ , which has 7 facets and 14 vertices. We show that worst-case behavior can arise on  $P$ , in the sense that  $P$  can be realized in such a way as to admit a strictly ascending path along edges passing through *all* vertices. Moreover, we give a complete classification with respect to realizability of all isomorphism classes (with respect to graph isomorphism) of ‘candidate orientations’ of the graph of  $P$ ; see Definition 3.16 and Theorem 4.1 for the exact statements.

In Chapter 5, we build on this example and show that this worst possible behavior may in fact arise in dimension 4 for polytopes on *any* number of facets: For all  $n \geq 5$ , we inductively construct a 4-dimensional polytope with  $n$  facets and maximally many vertices that admits an ascending path along edges passing through *all* of the vertices. This is partly joint work with Volker Kaibel and Günter M. Ziegler.

Chapter 6 is devoted to *secondary polytopes*, an intriguing construction of polytopes from certain triangulations of point configurations. This chapter does not contain any new research results, but does try to give at least a glimpse of some of the surprisingly diverse mathematics related to secondary polytopes. We will see polyhedral fans and rings of differential operators, and not least some very nice pictures generated by TOPCOM [79, 77], polymake [41, 40] and javaview [76]. This is joint work with Jörg Rambau.

In **Part II** of this thesis, we concentrate more on combinatorial than on geometric properties of simplicial complexes. A central concept is the *combinatorial type* of a polytope or sphere, by which we mean the equivalence class of all polytopes or spheres whose face lattice is isomorphic to that of a given one.

Chapters 8 and 9 resolve a problem left open by Kalai in his 1988 construction of “*many triangulated  $d$ -spheres*” [44]. The origin of this problem may be found in Goodman and Pollack’s 1986 paper with the suggestive title, “*There are asymptotically far fewer polytopes than we thought*” [29], [30], in which they expressed everyone’s surprise at the fact that asymptotically, there are no more than

$$2^{d(d+1)n \log n}$$

combinatorial types of simplicial  $d$ -dimensional polytopes on  $n$  vertices! The surprise stems from the fact that the only previously known upper bound on this number was the huge expression

$$2^{O(n^{\lfloor d/2 \rfloor} \log n)} \tag{1.1}$$

(for fixed  $d \geq 3$ ), derived via an easy application of McMullen’s upper bound theorem [64]. Goodman and Pollack proved their result using a theorem of Oleinik–Petrovsky–Milnor–Thom from algebraic geometry that bounds the sum of the Betti numbers of real algebraic varieties; still in 1986, Alon [2] extended their proof to non-simplicial polytopes.

By Stanley’s 1975 extension [94] of the upper bound theorem to spheres, the bound (1.1) also holds for the number of combinatorial types of simplicial  $(d-1)$ -dimensional PL-spheres. In his 1988 paper, Kalai came quite close to realizing this many spheres; in fact, he builds

$$2^{\Omega(n^{\lfloor (d-1)/2 \rfloor})}$$

simplicial  $(d-1)$ -spheres, for fixed  $d-1 \geq 2$ . Note that for  $d \geq 5$ , this construction implies that asymptotically, there are indeed *far* more  $(d-1)$ -spheres than  $d$ -polytopes, but for 3-spheres and 4-polytopes, the question remained undecided. (By a classical theorem of Steinitz [98], *every* 2-sphere, simplicial or not, is isomorphic to the boundary complex of some 3-polytope.) Two natural questions arise:

- ▷ How many of Kalai’s 3-spheres are non-polytopal, i.e., they do *not* correspond to the boundary complex of any 4-dimensional polytope?
- ▷ Are there in fact more simplicial 3-spheres than 4-polytopes?

We answer these questions in Chapters 8 and 9. For the first one, it turns out that in fact *all* of Kalai's 3-spheres are polytopal! We prove this in Theorem 8.1 by adapting yet again Billera and Lee's technique [8] (which had already inspired Kalai in the first place), to realize the 3-spheres in his family as boundary complexes of simplicial 4-polytopes. We then use the pictures constructed along the way to give a new and shorter proof for Hebble and Lee's result [35] that Kalai's 3-spheres are Hamiltonian, i.e., their dual skeleton admits a Hamiltonian path. These results were published in [74].

In our positive answer to the second question, we put together a classical construction by Heffter from 1898 [36], who introduced very special subdivisions of a surface of genus  $g$ , with a modern idea of Eppstein, Kuperberg & Ziegler [22] from 2002 for building interesting polytopes. Using these, we prove in Theorem 9.1 that on sufficiently many vertices, there *do* exist far more triangulated 3-spheres than simplicial 4-polytopes. This is joint work with Günter M. Ziegler, and finally settles the last case left open by Kalai in 1988.

Chapter 10 is devoted to a rather special kind of simplicial spheres, namely *centrally symmetric star-shaped* simplicial spheres. They generalize *centrally symmetric polytopes* (*cs-polytopes*), i.e., those polytopes  $P$  that satisfy  $P = -P$ . A *centrally symmetric simplicial sphere* (*cs-sphere*) is a simplicial sphere that admits an involution  $\varphi$  on its vertex set that does not fix any face. (In the case of cs-polytopes, this involution is induced by  $\mathbf{x} \mapsto -\mathbf{x}$ .) A cs-sphere is *star-shaped* if there exists a centrally symmetric simplicial fan (a *cs-fan*) with the same face lattice. In the simplicial case, we therefore have the following inclusions:

$$\{\text{cs-polytopes}\} \subsetneq \{\text{cs-fans}\} = \{\text{cs-star-shaped spheres}\} \subseteq \{\text{cs-spheres}\} \quad (1.2)$$

(We will see in Chapter 10 that the first inclusion is strict.) A cs-sphere  $\mathcal{S}$  is *k-neighborly centrally symmetric* [67] or *k-cs-neighborly* if every subset of  $k$  vertices of  $\mathcal{S}$  not containing two antipodal vertices is the vertex set of a  $(k-1)$ -simplex which is a face of  $\mathcal{S}$ . Equivalently,

$$f_i = \binom{n}{i+1} 2^{i+1} \quad \text{for all } 0 \leq i \leq k-1, \quad (1.3)$$

where  $f_i$  counts the number of  $i$ -dimensional faces of  $\mathcal{S}$ . A  $d$ -dimensional cs-sphere is *neighborly centrally symmetric* or *cs-neighborly* if (1.3) holds for  $k = \lfloor d/2 \rfloor$ .

The interest in cs-neighborly cs-spheres stems from Grünbaum's proof [31, Section 6.4] that there exist *no* 4-dimensional cs-neighborly cs-polytopes on more than 12 vertices.

In contrast, Jockusch [39] in 1995 gave an inductive construction of 3- and 4-dimensional cs-neighborly cs-spheres on  $n$  vertices for all even  $n \geq 8$  resp.  $n \geq 10$ , and Lutz [60] in 2002 provided an explicit construction for 3-dimensional cs-neighborly cs-spheres with a transitive cyclic group action on  $4m$  vertices, for all  $m \geq 2$ .

In Chapter 10, we investigate the middle set of (1.2) in the cs-neighborly case. We use the *cs-Gale transform* introduced by McMullen and Shephard [67] to prove in Theorem 10.1 that there exist no cs-neighborly centrally symmetric  $d$ -dimensional fans on  $2d+4$  rays for all even  $d \geq 4$  and odd  $d \geq 11$ .



## Chapter 2

### Definitions: Complexes, polytopes, spheres

Before we take off, a few words about terminology are in order. Much of the following material is taken from the handbook article [11].

An (abstract) *simplicial complex* on a finite *vertex set*  $V$  is an (of course finite) family  $\Delta$  of distinct nonempty subsets of  $V$ , called *simplices* or *faces*, such that for any  $\tau \subseteq \sigma \in \Delta$ , the set  $\tau$  is also in  $\Delta$ ; we require the empty set to be a face. The *dimension* of a face  $\sigma$  is  $\dim \sigma = |\sigma| - 1$  (where  $|\sigma|$  denotes the cardinality of  $\sigma$ ), and the *dimension* of  $\Delta$  is  $\dim \Delta = \max_{\sigma \in \Delta} \dim \sigma$ . Inclusion-maximal faces of  $\Delta$  are called *facets*, and  $\Delta$  is *pure* if all facets have the same dimension. The *face poset*  $P(\Delta) = (\Delta, \subseteq)$  of  $\Delta$  is the set of faces ordered by inclusion. The *face lattice* of  $\Delta$  is  $P(\Delta) \cup \{\hat{1}\}$ , where  $x \leq \hat{1}$  for all  $x \in P(\Delta)$ .

A *polytope*  $P \subset \mathbb{R}^k$  can be defined either as the convex hull of a finite set of points in  $\mathbb{R}^k$ , or equivalently [103, Theorem 1.1] as the (bounded) intersection of finitely many linear half-spaces  $H^{\leq 0} = \{\mathbf{x} \in \mathbb{R}^k : \mathbf{a}^T \mathbf{x} \leq a_0\}$ , where  $\mathbf{a} \in (\mathbb{R}^k)^*$  denotes a row vector of length  $k$ ,  $a_0 \in \mathbb{R}$ , and  $H$  denotes the hyperplane  $H = \{\mathbf{x} \in \mathbb{R}^k : \mathbf{a}^T \mathbf{x} = a_0\}$ . The *dimension* of a polytope  $P \subset \mathbb{R}^d$  is the dimension of its *affine span*

$$\text{aff}(P) = \left\{ \sum_{i=1}^n \lambda_i x_i : x_1, \dots, x_n \in P, \sum_{i=1}^n \lambda_i = 0 \right\}.$$

We refer to  $d$ -dimensional polytopes as *d-polytopes*. A linear inequality  $\mathbf{a}^T \mathbf{x} \leq a_0$  is *valid* for a polytope  $P$  if it satisfied for all points  $\mathbf{x} \in P$ . A *face*  $F$  of  $P$  is a subset of the form  $F = P \cap \{\mathbf{x} \in \mathbb{R}^d : \mathbf{a}^T \mathbf{x} \leq a_0\}$ , where  $\mathbf{a}^T \mathbf{x} \leq a_0$  is a valid inequality for  $P$ . Note that again, the empty set is a face of every polytope  $P$ , this time because the inequality  $\mathbf{0}^T \mathbf{x} \leq 1$  is valid for  $P$ . In addition,  $P$  is a face of itself because of the valid inequality  $\mathbf{0}^T \mathbf{x} \leq 0$ .

A *polytopal complex*  $\mathcal{P}$  in  $\mathbb{R}^d$  is a set of polytopes (called *faces* of  $\mathcal{P}$ ) that satisfies the *intersection property*: the intersection  $P \cap Q$  of any two polytopes  $P, Q \in \mathcal{P}$  is a face of both and contained in  $\mathcal{P}$ . Again, the *dimension* of  $\mathcal{P}$  is the maximal dimension of any face of  $\mathcal{P}$ .

A *geometric simplex* in  $\mathbb{R}^k$  is the convex hull of  $k+1$  affinely independent points  $\mathbf{v}_1, \mathbf{v}_2, \dots, \mathbf{v}_{k+1} \in \mathbb{R}^k$ . This means that in any equation  $\sum_{i=1}^{k+1} \lambda_i \mathbf{v}_i = \mathbf{0}$  with  $\sum_{i=1}^{k+1} \lambda_i = 0$ , there holds  $\lambda_i = 0$  for all  $i = 1, 2, \dots, k+1$ .

A *geometric simplicial complex*  $\Gamma$  is a polytopal complex all of whose faces are geometric simplices. The vertex sets of faces (in the polytopal sense) of faces (in the ‘complex’ sense) of  $\Gamma$  form an abstract finite simplicial complex  $\Delta(\Gamma)$ . Conversely, for any  $d$ -dimensional finite abstract simplicial complex  $\Delta \neq \emptyset$ , there exist geometric simplicial complexes  $\Gamma \subset \mathbb{R}^{2d+1}$  such that  $\Delta(\Gamma) \cong \Delta$ , in the sense that there is an inclusion-preserving bijection between the respective face sets. The *underlying space*  $\bigcup \Gamma = \bigcup_{\sigma \in \Gamma} \sigma$  is unique up to a piecewise linear

homeomorphism, and is called a *geometric realization*  $\|\Delta\|$  of  $\Delta$ . Conversely,  $\Delta$  is called a *triangulation* of the space  $\|\Delta\|$ , and of any space homeomorphic to it. Getting a *polyhedral embedding* (i.e., such that the image of any simplex is convex) of a  $d$ -simplicial complex on  $n$  vertices is easy: simply take an appropriate subset of the *d-skeleton* (the set of faces of dimension at most  $d$ ) of an  $(n - 1)$ -dimensional simplex.

The *boundary complex* of a  $d$ -dimensional polytope  $P$  is the polytopal complex  $\mathcal{P}$  of all *proper* (i.e., non-empty) faces of  $P$ . It is homeomorphic to the  $(d - 1)$ -dimensional sphere  $S^{d-1}$ . Just like for simplicial complexes, the top-dimensional faces of  $P$  are called *facets*, even though they are not necessarily geometric simplices. If this does happen, then  $P$  is called *simplicial*.

A *simplicial d-sphere* is a pure  $d$ -dimensional abstract simplicial complex  $\mathcal{S}$  whose underlying space  $\|\mathcal{S}\|$  is homeomorphic to the standard  $d$ -sphere  $S^d = \{\mathbf{x} \in \mathbb{R}^{d+1} : \sum_{i=1}^{d+1} x_i^2 = 1\}$ . Abusing the concept slightly, we say that a simplicial  $d$ -sphere is *realizable* or *polytopal* if there exists a convex  $(d + 1)$ -polytope whose boundary complex is isomorphic to  $S^d$ . The important point here as compared to realizations of arbitrary simplicial complexes is that we ask for a *convex geometric realization in one dimension higher*.

Note that a polytopal complex may have no convex realization at all, even allowing for embeddings into arbitrarily high-dimensional spaces: In [24, Chapter III.5], there is an example of a polyhedral 3-sphere on 8 vertices (!) which is not embeddable into *any*  $\mathbb{R}^k$ .

A *cellulation*  $\mathcal{C}$  of a manifold  $X$  is a finite CW complex whose underlying space is  $X$ .  $\mathcal{C}$  is *regular* if all closed cells are embedded, and *strongly regular* if in addition the intersection of any two cells is a cell. The *star* of a cell  $\sigma \in \mathcal{C}$  is the union of the closure of all cells containing  $\sigma$ , and the *link* of  $\sigma$  consists of all cells of star  $\sigma$  not incident to  $\sigma$ . The entry  $f_i$  of the *f-vector*  $f(\mathcal{C}) = (f_{-1}, f_0, f_1, \dots)$  of a cellulation counts the number of  $i$ -dimensional cells, and  $f_{-1} = 1$ . The  $d$ -dimensional cells are called the *facets*, and the  $(d - 1)$ -dimensional ones the *ridges*.

A  $d$ -dimensional *PL sphere* is a simplicial sphere that is piecewise linearly homeomorphic to the boundary of the  $(d + 1)$ -simplex. A *combinatorial manifold* (or *PL manifold*) is a triangulation of a topological manifold such that the link of every vertex is a PL sphere. We paraphrase [59]:

For  $d \neq 4$ , a triangulation of the  $d$ -sphere is a PL-sphere if and only if it is a PL-manifold. For  $d \leq 3$  this follows from the work of Kirby and Siebenmann; namely, there is a unique PL structure for spheres in these dimensions. For  $d = 4$  this question is not fully understood: Is a combinatorial manifold homeomorphic to the 4-sphere necessarily a PL sphere? Since in dimension 4 the category of PL manifolds is equivalent to the smooth category, the question is equivalent to: Does there exist an ‘exotic’ 4-sphere? (We are grateful to M. Kreck for clarifying this question.)

We write  $[n] := \{1, 2, \dots, n\}$  and  $[n]_0 := \{0, 1, \dots, n\}$ . For a finite subset  $V \subset \mathbb{R}^d$ , the *non-negative hull* of  $V$  is  $\text{cone}(V) = \{\sum_{v \in V} \lambda_v v : \lambda_v \geq 0 \text{ for all } v \in V\}$ , and  $\text{cone}(\emptyset) = \{0\}$ .

Finally, for real functions  $f, g : \mathbb{R} \rightarrow \mathbb{R}$ , we write

$$\begin{aligned} f &= \Omega(g) & \text{if } g &= O(f) \quad (\text{which is also expressed as } 'g \ll f') \\ f &= \Theta(g) & \text{if } f &= O(g) \quad \text{and} \quad g = O(f). \end{aligned}$$

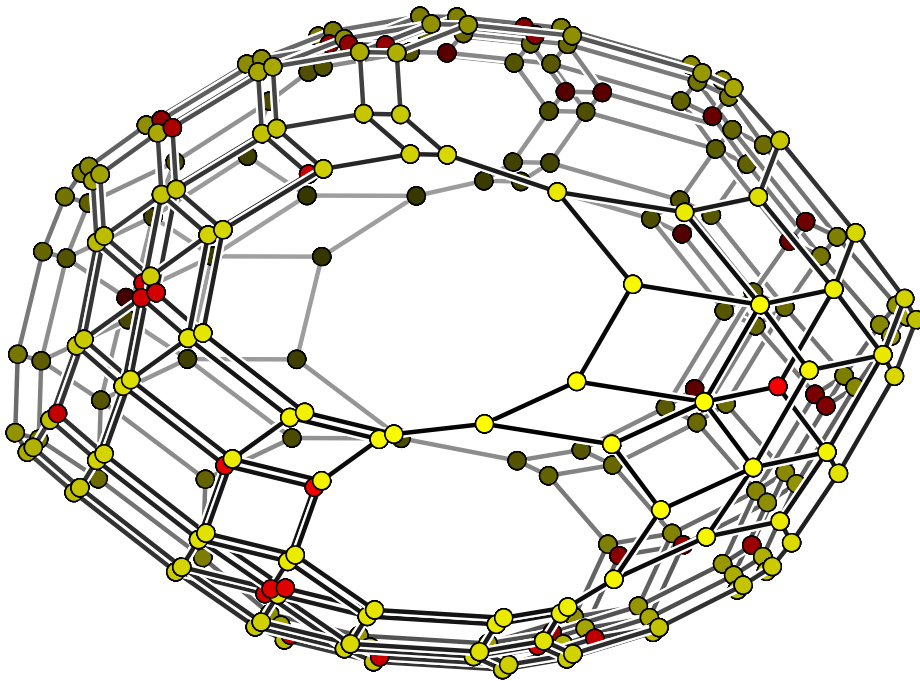






## Part I

# Polytopes





## Chapter 3

### The monotone upper bound problem: Overview

A big boost for polytope theory came from the development of linear optimization in the first half of the 20th century [88, p. 209ff]. Because of the huge success of the simplex algorithm for linear programming on real world problems (see [89] for an important historical instance and [10] for the state of the art in 2002), it was not fully realized that there could possibly be a problem until Klee and Minty in 1972 exhibited their by now classic examples [54]: For each dimension  $d$ , they produced a  $d$ -polytope (now called the *Klee-Minty cube*  $KM^d$ ) on which the classical Dantzig pivot rule as well as various lexicographic rules are fooled into exponential behavior. This polytope is combinatorially isomorphic to a  $d$ -dimensional cube, but realized in such a way that with respect to the linear functional  $\mathbf{x} \mapsto x_d$ , there exists a strictly ascending (i.e., *monotone*) path through all  $2^d$  vertices. Moreover, the simplex algorithm using Dantzig's pivot rule indeed follows this path.

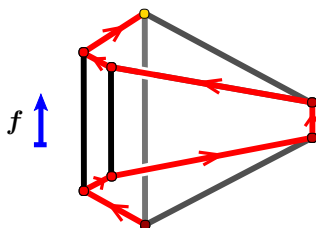


FIGURE 3.1: The 3-dimensional Klee-Minty cube  $KM^3$  with a linear objective function  $f$  that induces a monotone Hamiltonian path. This polytope is combinatorially but *not* projectively equivalent to a regular 3-cube (as claimed in [53]).

After this initial breakthrough, there came a whole flood (‘worstcasitis’ [70]) of additional examples for exponential behaviour of various pivot rules. These examples were subsequently unified via the *deformed product construction* by Amenta and Ziegler [3] in 1998.

As of this writing, it is still not clear whether this exponential behavior is merely produced by inadequate pivot rules, or whether it is intrinsic to the simplex algorithm: maybe we haven’t yet found or cannot adequately analyze the right pivot rule (see [53], [104] for the \$1000 reward offered by Zadeh for a proof of or a counterexample to the polynomiality of the LEAST\_ENTERED rule); or perhaps we shouldn’t be using the simplex algorithm at all. In fact, the following fundamental question is still not understood despite decades of effort:

**Problem 3.1** (Complexity of linear programming) *Is there a strongly polynomial (simplex) algorithm for linear programming?*

Currently, we know of *weakly polynomial* algorithms for linear programming (i.e., ones in which the number of arithmetic operations is bounded by a polynomial in the dimension  $d$ , the number  $n$  of inequalities, *and* the coding length  $L$  of the problem), namely the *ellipsoid method* by Khachiyan [50] from 1979 and the *interior point method* by Karmarkar [49] from 1984 (and variants of these). However, we are still not aware of a (provably) *strongly polynomial* algorithm, i.e., where the number of arithmetic operations is bounded by a polynomial *independent* of the size of the numbers involved in the problem statement. (We assume the *uniform time* model of computation, where each arithmetic operation can be executed in constant time.) The best combinatorial bounds known as of this writing are the following subexponential randomized running times for the simplex algorithm with a certain pivot rule, which were independently and almost simultaneously obtained by Kalai resp. Matoušek, Sharir and Welzl:

**Theorem 3.2** (Kalai [46] and Matoušek, Sharir and Welzl [63], 1992) *The running time of the simplex algorithm with the RANDOM\_FACET pivot rule has an expected sub-exponential (but not polynomial) upper bound of*

$$O\left(d^2n + c\sqrt{d\log d}\right),$$

where  $d$  is the ambient dimension,  $n$  the number of inequalities, and  $c > 1$  a real constant.

In this thesis, we focus on the following bound for the worst-case difficulty of solving a linear programming problem via a simplex algorithm, irrespectively of the pivot rule used:

**Definition 3.3** Let  $M(d, n)$  denote the maximal number of vertices on a monotone path on a  $d$ -dimensional polytope with  $n$  facets. (This quantity provides an upper bound for the running time of the simplex algorithm in the worst possible example, using the extremely stupid pivot rule SMALLEST\_INCREASE.)

**Problem 3.4** (Extremal path length problem, Klee 1965 [51]) *How large can  $M(d, n)$  be as a function of  $d$  and  $n$ ?*

To explain the progress we have been able to achieve on Problem 3.4, we need to first consider another classical extremal problem on polytopes posed earlier by Motzkin:

**Problem 3.5** (Upper bound problem, Motzkin 1957 [69]) *What is the maximal number of  $k$ -dimensional faces that a  $d$ -dimensional polytope on  $n$  vertices can have?*

Actually, Motzkin did not state this as a question, but in his abstract [69] claimed that this number is maximized by the cyclic polytope  $C_d(n)$ , and that moreover cyclic polytopes are unique with this property. The first statement was proved only in 1970 by McMullen [64]; see [103, Section 8.4] for some of the details of the long and involved history of the proof of what came to be known as the *upper bound theorem*. However, the second part of Motzkin's claim was disproved by Grünbaum and Sreedharan [32], who in 1967 discovered the first examples of non-cyclic neighborly polytopes; these will be important in the sequel.

**Theorem 3.6** (Upper bound theorem, McMullen 1970 [64]) *If  $P$  is a  $d$ -polytope with  $n$  vertices, then for every  $0 \leq k \leq d$  it has at most as many  $k$ -faces as a neighborly polytope with the same number of vertices. In particular, the number of facets of  $P$  is at most*

$$f_{d-1}(C_d(n)) = \binom{n - \lceil d/2 \rceil}{\lfloor d/2 \rfloor} + \binom{n - 1 - \lceil (d-1)/2 \rceil}{\lfloor (d-1)/2 \rfloor}.$$

(Polar dual version) *The maximal possible number of vertices that a  $d$ -dimensional polytope with  $n$  facets can have is  $M_{\text{ubt}}(d, n) = f_{d-1}(C_d(n))$ .*

The inequality

$$M(d, n) \leq M_{\text{ubt}}(d, n) \quad (3.1)$$

is clear by definition. To investigate its possible tightness, we tie together the two extremal problems 3.4 and 3.5 by formulating the following monotone analogue of Problem 3.5, which is central to Chapters 4 and 5 of this thesis:

**Problem 3.7** (Monotone upper bound problem) *Given integers  $n > d \geq 2$ , can the maximal possible number of vertices on a strictly ascending path on a  $d$ -dimensional polytope with  $n$  vertices be as large as  $M_{\text{ubt}}(d, n)$ ? In other words, do there exist*

- (1) *a realization of a (necessarily simple)  $d$ -polytope  $P \subset \mathbb{R}^d$  with  $n$  facets and  $M_{\text{ubt}}(d, n)$  vertices,*
- (2) *a linear objective function  $f \in (\mathbb{R}^d)^*$  in general position with respect to  $P$ ,*

*such that the orientation  $\mathcal{O}_f(G(P))$  induced by  $f$  on the graph  $G(P)$  of  $P$  admits a strictly ascending Hamiltonian path?*

Given the combinatorial type of a candidate polytope  $P$  with  $M_{\text{ubt}}(d, n)$  vertices and some candidate orientation  $\mathcal{O}$  of its graph (for example, one with a unique source and sink and a directed Hamiltonian path between the two), we can formulate the following problem:

**Problem 3.8** (Monotone realizability problem) *Given an orientation  $\mathcal{O}$  of the graph  $G(P)$  of a  $d$ -dimensional polytope  $P$ , do there exist a realization of  $P$  in  $\mathbb{R}^d$  and a linear function  $f \in (\mathbb{R}^d)^*$  such that  $\mathcal{O} = \mathcal{O}_f(G(P))$ ?*

However, even this restricted problem is far from being solved. In particular, it is in general still not clear what conditions an orientation  $\mathcal{O}$  must fulfill in order to allow a positive solution of Problem 3.8 (but see Theorems 3.13 and 3.15 in the next section). Related realizability questions have been studied before in polytope theory:

**Problem 3.9** (Combinatorial realizability or Steinitz problem) *Given some lattice, is it isomorphic to the face lattice of a polytope?*

**Problem 3.10** (Complexity of the combinatorial realization space) *How complicated is the realization space of a given polytope?* (A loose description of the *realization space* of a polytope  $P$  is ‘the set of all coordinatizations of  $P$  modulo affine coordinate transformations’. See [82] for a precise definition.)

### 3.1 Solution status of the problems

#### 3.1.1 The combinatorial realizability problem

In dimension 3, Steinitz' famous theorem completely solves Problems 3.9 and 3.10 by characterizing the graphs (and therefore the face lattices) and realization spaces of 3-polytopes:

**Theorem 3.11** (Steinitz and Rademacher, 1934 [98])

- (a) *For every 3-dimensional polytope  $P$ , the graph  $G(P)$  is a simple, planar 3-connected graph. Conversely, for every simple, planar 3-connected graph  $G$ , there is a unique combinatorial type of 3-polytope  $P$  whose graph  $G(P)$  is isomorphic to  $G$ .*
- (b) *The realization space  $\mathcal{R}(P)$  of the combinatorial type of a 3-polytope  $P$  is homeomorphic to  $\mathbb{R}^{f_1(P)-6}$ , and contains rational points. In particular,  $\mathcal{R}(P)$  is connected, i.e. any two realizations of  $P$  can be continuously deformed into each other while maintaining the same combinatorial type throughout.*  $\square$

In higher dimensions, reconstructing a (non-simple [45]) polytope from its graph alone is of course out of the question: For  $n \geq 5$ , already the complete graph  $K_n$  is the graph of *any* neighborly  $d$ -polytope with  $d < n$ , for example the  $(n-1)$ -simplex or the cyclic  $d$ -polytope on  $n$  vertices. For more on *dimensional ambiguity*, consult (the recent second edition of) Grünbaum's classic [31].

By a result of Richter-Gebert from 1996, already for dimension  $d = 4$  the nice characterization of Theorem 3.11 fails spectacularly—the realization space of a 4-polytope can be ‘arbitrarily complicated’ (see [82] and [6] for definitions of the terms not explained here):

**Theorem 3.12** (Universality theorem for 4-polytopes; Richter-Gebert, 1996 [82]) *For every basic semi-algebraic set  $S$  defined over  $\mathbb{Z}$ , there is a 4-polytope  $P_S$  whose realization space is stably equivalent to  $S$ . Furthermore, for every fixed  $d \geq 4$ , the Steinitz problem for  $d$ -dimensional polytopes is at least as hard as the existential theory of the reals (ETR-hard), with respect to polynomial-time reductions.*  $\square$

In particular, the Steinitz problem in fixed dimension is NP-hard. It is not yet known whether the problem is in NP; but see [43, Problem 29] for the latest news!

#### 3.1.2 The monotone realizability problem

Since Problems 3.7 and 3.8 ask for a realization of *two* objects, a polytope and a linear function, we would expect them to be more difficult than Problems 3.9 and 3.10. Indeed, even the 3-dimensional case of Problem 3.8 has been solved only quite recently:

**Theorem 3.13** (Mihalisin and Klee, 2000 [68]) *Let  $\mathcal{O}$  be an orientation of the graph of a 3-dimensional polytope  $P$ . There exists a realization of  $P$  such that  $\mathcal{O}$  is induced by a linear objective function if and only if  $\mathcal{O}$  satisfies the following conditions:*

- ▷  $\mathcal{O}$  is acyclic with a unique source and a unique sink,
- ▷ it has a unique local sink in every face cycle (the non-separating induced cycles), and
- ▷ it admits three directed paths from its source to its sink with disjoint sets of interior nodes.

□

We conclude from Theorem 3.13 that Problem 3.7 has a positive solution in dimension  $d = 3$  for all  $n \geq 4$ :

**Corollary 3.14** For any  $n \geq 4$ , there exists a (simple) 3-dimensional polytope with  $n$  facets that admits a realization with an ascending Hamiltonian path along edges.

*Proof.* Orient the 1-skeleton of the polar  $C_3(n)^\Delta$  of the 3-dimensional cyclic polytope  $C_3(n)$  with  $n$  vertices as in Figure 3.2. This orientation satisfies the three criteria of Theorem 3.13 and admits a Hamiltonian path from source to sink along edges.

□

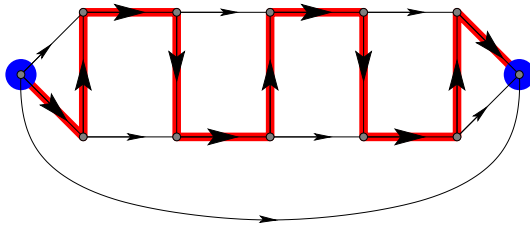


FIGURE 3.2: An orientation of the graph of the 3-dimensional polytope  $C_3(8)^\Delta$  with 8 facets and 12 vertices (see also Figure 1.2) that satisfies the conditions of Theorem 3.13, and admits a Hamiltonian path from source to sink along edges (thick lines).

For general dimension  $d$ , Holt and Klee proved the necessity of the following condition analogous to the statement of Theorem 3.13:

**Theorem 3.15** (Holt and Klee, 1999 [37]) *In any orientation induced on the graph of a  $d$ -dimensional polytope by a linear objective function in general position (i.e., the function values at vertices are distinct), there are  $d$  vertex-disjoint monotone paths from the (unique) source to the (unique) sink.*

□

Theorems 3.13 and 3.15 motivate the following definitions.

**Definition 3.16** Let  $\mathcal{O}$  be an acyclic orientation of the graph  $G_P$  of a  $d$ -dimensional polytope  $P$  that has a unique source and sink.

- (a) If  $\mathcal{O}$  has a unique sink in each non-empty face of  $P$ , it is called an *AOF-orientation* of  $P$ , and  $\mathcal{O}$  is said to satisfy the *AOF condition*. Any linear extension of an AOF-orientation is called an *abstract objective function* on  $\text{vert } P$ . (In particular, any orientation of  $G_P$  induced by a linear objective function on  $\mathbb{R}^d$  is an AOF orientation.)
- (b)  $\mathcal{O}$  is a *Holt-Klee orientation* if it admits  $d$  independent monotone paths between the global source and the global sink. (cf. Theorem 3.15.)

- (c)  $\mathcal{O}$  is an *AOF Holt-Klee orientation* if it satisfies (a) and (b), and a *Hamiltonian AOF Holt-Klee orientation* if it additionally admits a directed Hamiltonian path from source to sink.

Another case in which Problem 3.7 has recently been found to have a positive solution is for  $n = d + 2$  and  $d \geq 2$  (the case  $d = 2$  is of course trivial).

**Theorem 3.17** (Amenta & Ziegler, 1998 [3]; Gärtner, Solymosi, Tschirschnitz, Valtr & Welzl, 2001 [27]) *For all  $d \geq 2$ , the (combinatorially unique and simple)  $d$ -polytope  $P \cong \Delta_{\lfloor d/2 \rfloor} \times \Delta_{\lceil d/2 \rceil}$  with  $n = d + 2$  facets and  $M_{\text{ubt}}(d, d + 2)$  vertices admits a geometric realization together with a linear objective function that induces an ascending Hamiltonian path along edges.*  $\square$

### 3.2 New results in this thesis

To recapitulate, Problem 3.7 was known to have a positive solution in dimension 3, where an  $n$ -facet polytope can have at most  $M_{\text{ubt}}(3, n) = 2n - 4$  vertices, and for  $d$ -polytopes with  $n = d + 2$  facets and  $M_{\text{ubt}}(d, d + 2) = (\lfloor \frac{d}{2} \rfloor + 1)(\lceil \frac{d}{2} \rceil + 1)$  many vertices.

In Chapter 4 of this thesis, we completely analyze the first interesting case of Problem 3.7 after Corollary 3.14 and Theorem 3.17, namely the case  $d = 4$  and  $n = 7$ .

**Theorem 3.18** ([31, Theorem 6.2.3]) *For all  $d \geq 4$ , the combinatorial type of a  $d$ -dimensional polytope with  $d + 3$  facets and  $M_{\text{ubt}}(d, d + 3)$  vertices is uniquely that of the polar  $C_d(d + 3)^\Delta$  of the cyclic  $d$ -polytope on  $d + 3$  vertices.*

We combine *combinatorial enumeration*, the *Gale $^\Delta$ -transform* [27] and (an oriented matroid version of) the *Farkas Lemma* to prove the following theorem (Theorem 4.1):

**Theorem** *There exist 7 combinatorial equivalence classes with respect to graph isomorphism of Hamiltonian AOF Holt-Klee orientations of the graph of  $C_4(7)^\Delta$ . Of these, exactly 4 equivalence classes are realizable. In particular,  $M(4, 7) = M_{\text{ubt}}(4, 7) = 14$ .*

For even  $d \geq 2$  and all  $n \geq d + 3$ , the symmetry group of  $C_d(n)^\Delta$  is the dihedral group of order  $2n$ . In particular,  $|\text{Sym}(C_4(7)^\Delta)| = 14$ .

Chapter 5 completely solves Problem 3.7 *positively* in the case  $d = 4$ . More precisely, for each  $m \geq 0$  we realize a 4-dimensional polytope  $Q_m$  with  $n = m + 5$  facets and  $M_{\text{ubt}}(4, n)$  vertices such that  $Q_m$  admits an ascending Hamiltonian path (Theorem 5.1):

**Theorem** *For  $d = 4$ , the bound given by Theorem 3.6 is sharp for monotone paths: The maximal number  $M(4, n)$  of vertices on a strictly ascending path in the 1-skeleton of a simple 4-polytope  $P$  with  $n$  facets equals the maximal number of vertices that  $P$  can have according to the (combinatorial) upper bound theorem. That is,*

$$M(4, n) = M_{\text{ubt}}(4, n) = \frac{n(n - 3)}{2}.$$



**Remark 3.19** Two noteworthy features of our construction are the following:

- (a) Our polytopes are *not* deformed products in the sense of Amenta and Ziegler [3].
- (b) Our polytopes are polars of neighborly ones, but they are *not* polar to cyclic polytopes.

**Corollary 3.20** The 4-dimensional Klee-Minty cube  $KM^4$  is not extremal for Problem 3.4.

*Proof.* The 4-cube has 8 facets but only 16 vertices, while  $f_0(Q_3) = M_{\text{ubt}}(4, 8) = 20$ .  $\square$

We summarize the known status of Problem 3.7 in Figure 3.3.

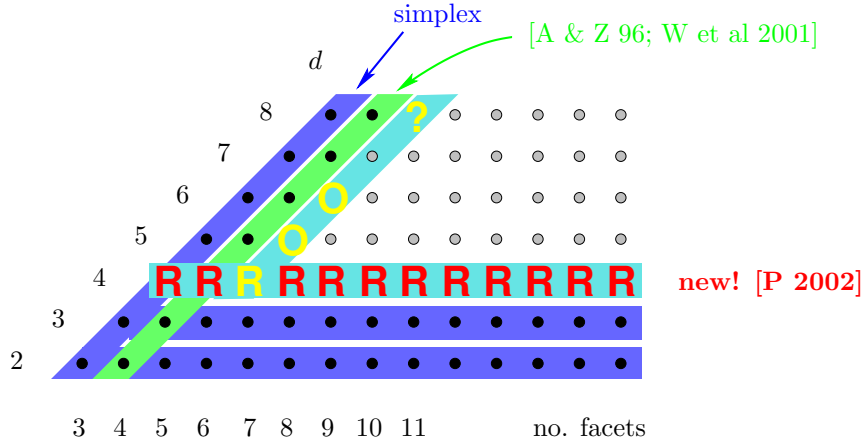


FIGURE 3.3: Progress on the monotone upper bound problem. The case  $n = d + 2$  is covered by Theorem 3.17, while the realizations in dimension 4 are new in this thesis. For  $(d, n) = (5, 8)$  and  $(d, n) = (6, 9)$  (marked with an ‘O’), we found Hamiltonian AOF Holt-Klee orientations on simple polar-to-neighborly polytopes with these parameters (for  $(d, n) = (6, 9)$  this polytope is unique); the question mark indicates a still open but hopefully accessible instance.

Theorems 4.10 and 4.22 together give the following result for  $d = 4$  and  $n = 7, 8$ :

**Theorem** (a) *There exist realizations of the equivalence classes  $R_1$ – $R_4$  of Hamiltonian AOF Holt-Klee orientations of the graph of  $C_4(7)^\Delta$  listed in Theorem 4.1.*  
 (b) *The Hamiltonian AOF Holt-Klee orientations  $NR_1$ – $NR_3$  of  $C_4(7)^\Delta$  are not realizable.*  
 (c) *There does not exist any Hamiltonian AOF Holt-Klee orientation of the graph of  $C_4(8)^\Delta$ .*  
 (d) *There exist realizations of several equivalence classes of Hamiltonian AOF Holt-Klee orientations of the graph of the two other combinatorial types  $N'_4(8)$ ,  $N''_4(8)$  of polar-to-neighborly 4-polytopes with 8 facets [31, Section 7.2.4].*

**Corollary 3.21** The result of Mihalisin & Klee (Theorem 3.13) does not hold in any dimension greater than three: For all  $d \geq 4$ , there are nonrealizable AOF Holt-Klee orientations of the graph of a  $d$ -dimensional simple polytope.

*Proof.* For  $d = 4$ , this follows from Theorem 4.1. For  $d > 4$ , inductively take the prism  $\Pi(P)$  over a  $(d - 1)$ -dimensional polytope  $P$  that admits a non-realizable AOF Holt-Klee orientation  $\mathcal{O}_P$ . Put  $\mathcal{O}_P$  resp. its reorientation  $-\mathcal{O}_P$  on the bottom resp. top facet of  $\Pi(P)$ ,

and orient all ‘new’ edges of  $\Pi(P)$  from bottom to top. Any realization of  $\Pi(P)$  with this orientation induces realizations of  $\mathcal{O}_P$  resp.  $-\mathcal{O}_P$  on the bottom resp. top facets of  $\Pi(P)$ .  $\square$

For finding Hamiltonian HK AOF orientations of the graph of  $C_6(9)^\Delta$ , straightforward enumeration is hopeless because there are too many orientations to check. We therefore adopt the strategy of Algorithm 1 to restrict the search, and prove the following theorem:

**Theorem 3.22** *There are exactly six equivalence classes of Hamiltonian AOF Holt-Klee orientations (with respect to graph isomorphism and reorientation) on  $C_6(9)^\Delta$ ; cf. Figure 3.4.*

---

**Algorithm 1** Enumerating all Hamiltonian AOF Holt-Klee orientations on a simple polytope by using the induced orientations on smaller-dimensional faces as templates

---

**Input:** A  $d$ -dimensional simple polytope  $Q$ , represented by a `polymake` file

A collection  $\mathcal{F}$  of faces of  $Q$

**Output:** All Hamiltonian AOF HK orientations of  $G(Q)$

- 1: Generate the collection  $\overline{\mathcal{F}}$  of equivalence classes (with respect to graph isomorphism) of the faces in  $\mathcal{F}$
  - 2: Create one file for each  $\overline{F} \in \overline{\mathcal{F}}$ , along with the isomorphism map  $\mu_F : \text{vert } F \rightarrow \text{vert } \overline{F}$  between each  $F \in \mathcal{F}$  and its representative  $\overline{F} \in \overline{\mathcal{F}}$
  - 3: Enumerate *all* AOF HK orientations of each  $\overline{F} \in \overline{\mathcal{F}}$  (not just the Hamiltonian ones)
  - 4: Make one object **Face** for *each*  $F \in \mathcal{F}$  of  $Q$  (not just one per representative)
  - 5: Make one object **Edge** for each edge of  $Q$
  - 6: Enumerate all Hamiltonian paths  $\pi$  in  $G(Q)$  in the following way:
  - 7: **for all** new edges  $e$  to be added to  $\pi$  **do**
  - 8:   check in all **Faces**  $F \in \mathcal{F}$  containing **Edge**( $e$ ) if there is still some AOF HK orientation of  $F$  compatible with this orientation of  $e$
  - 9:   check if the orientation induced on  $Q$  so far by  $\pi$  is still AOF
- 

### 3.3 Open problems

**Conjecture 3.23** For all  $n \geq 8$ , the graph of the polar  $C_4(n)^\Delta$  of the cyclic 4-polytope on  $n$  vertices does not admit a Hamiltonian AOF Holt-Klee orientation.

**Question 3.24** Are any of the six equivalence classes of Hamiltonian AOF Holt-Klee orientations of  $C_6(9)^\Delta$  realizable?

**Question 3.25** Does the graph of the polar  $C_8(11)^\Delta$  of the cyclic 8-polytope on 11 vertices admit a Hamiltonian AOF Holt-Klee orientation? We ran our program for two weeks—in fact, using one computer for each equivalence class of edges of  $C_8(11)^\Delta$  under its symmetry group (see Figure 3.5)—but the problem is still too large.

	$d = 3:$	#	$f_0$	# HK-AOFs	
		0	8	448	$C_3(8)^\Delta$
N_VERTICES		1	4	24	$\Delta_3$
30		2	6	120	$\Pi(\Delta_2)$
F_VECTOR		3	8	656	$C^3$
30 90 117 84 36 9					
	$d = 4:$	#	$f_0$	# HK-AOFs	
N_ISOMORPHIC_3_FACES		0	14	71652	$C_4(7)^\Delta$
(0 54) (1 9) (2 18) (3 3)		1	11	21264	
N_ISOMORPHIC_4_FACES		2	13	61064	
(0 9) (1 9) (2 9) (3 9)		3	12	32128	
	$d = 5:$	0	20	>450M data	$C_5(8)^\Delta$
HAM_HK_AOF_ORIENTATION_CLASSES					
0 1 2 7 8 6 3 4 5 19 16 21 25 22 24 23 12 14 15 13 9 11 10 27 29 28 26 17 18 20					
4 2 17 26 23 22 24 12 8 14 19 5 16 21 25 11 13 9 10 27 28 29 20 0 3 1 18 15 7 6					
4 2 26 25 21 27 28 10 11 13 9 6 7 8 14 15 17 16 18 1 3 0 29 20 24 12 23 22 19 5					
4 2 26 25 21 27 28 10 11 13 9 7 6 8 14 15 17 16 18 1 3 0 29 20 24 12 23 22 19 5					
4 3 1 18 28 27 29 0 20 24 22 23 12 14 19 5 16 21 25 26 11 10 13 9 8 6 7 15 17 2					
5 3 0 1 18 16 15 7 6 4 2 17 23 22 24 12 8 14 19 20 29 28 26 25 11 9 10 13 21 27					

FIGURE 3.4: A partial **polymake** [40] description for  $C_6(9)^\Delta$ . *Left:* the line following the entry ‘N\_ISOMORPHIC\_3\_FACES’ means that there are 54 representatives of the 3-face called ‘0’ under graph isomorphism, 9 representatives of the 3-face ‘1’, etc. *Right:* The number of vertices, the total number of HK AOF orientations, and in some cases the combinatorial type ( $\Pi$  stands for ‘prism’,  $C^3$  for the 3-cube) of the equivalence classes of 3- and 4-dimensional faces of  $C_6(9)^\Delta$ . *Bottom:* the vertex labels in the six classes of Hamiltonian paths that induce HK AOF orientations on  $C_6(9)^\Delta$ .

	$d = 3:$	#	$f_0$	# HK-AOFs	
		0	8	448	$C_3(8)^\Delta$
N_VERTICES		1	4	24	$\Delta_3$
55		2	6	120	$\Pi(\Delta_2)$
F_VECTOR		3	8	656	$C^3$
55 220 407 451 330 165 55 11					
	$d = 4:$	#	$f_0$	# HK-AOFs	
N_ISOMORPHIC_3_FACES		0	14	71652	$C_4(7)^\Delta$
(0 231) (1 66) (2 132) (3 22)		1	11	21264	
N_ISOMORPHIC_4_FACES		2	13	61064	
(0 44) (1 77) (2 77) (3 77)		3	12	32128	
(4 11) (5 22) (6 11) (7 11)		4	5	120	$\Delta_4$
SYMMETRY_CLASSES_OF_EDGES		5	8	1920	
(1 0) (2 1) (3 0) (3 1)		6	9	3132	
(6 0) (7 2) (7 6) (8 5)		7	12	60216	
(8 6) (9 6) (9 7) (9 8) (11 9)					

FIGURE 3.5: A partial **polymake** [40] description of  $C_8(11)^\Delta$ ; cf. Figure 3.4.



## Chapter 4

### An exhaustive analysis of a small polytope

This chapter focuses on the first interesting case for the monotone upper bound problem in dimension 4. Namely, we study the smallest 4-dimensional polytope that is not a priori known to admit an ascending Hamiltonian path along edges, but has the maximal possible number of vertices given its number of facets.

Of course, the 4-polytope with 5 facets (i.e., the 4-simplex) admits a realization with an ascending Hamiltonian path. We saw in Theorem 3.17 that the same is true for the 4-polytope  $C_4(6)^\Delta$  with 6 facets (and 9 vertices), which is combinatorially unique by [31, Section 6.1]. The first interesting case is therefore the polytope  $C_4(7)^\Delta$  with 7 facets and the maximal number 14 of vertices, which is also combinatorially unique by Theorem 3.18.

**Theorem 4.1** *There are exactly four realizable equivalence classes (with respect to graph isomorphism) of AOF Holt-Klee orientations of the graph of  $C_4(7)^\Delta$  that admit a monotone Hamiltonian path; see Figure 4.1.*

Our proof of Theorem 4.1 uses three nontrivial ingredients. The first is the following result of *combinatorial enumeration* first achieved by Schultz, which was independently re-implemented and verified:

**Theorem 4.2** (Schultz, 2001 [90]) *Exactly seven equivalence classes of AOF Holt-Klee orientations of the graph of  $C_4(7)^\Delta$  admit a monotone Hamiltonian path.*

For deciding realizability, we additionally use Welzl's [27] geometric *Gale $^\Delta$ -transform* (Algorithm 4.2) and (an oriented matroid version of) the *Farkas Lemma* [88] (Theorem 4.19).

#### 4.1 A very brief introduction to the Gale transform

The Gale transform in the setting of polytope theory is due to Perles (around 1965) and was first published in [31]. It is a powerful method for visualizing high-dimensional point configurations, such as the vertex sets of convex polytopes, whose cardinality is only slightly larger than the dimension of the affine span of the points. Typically, it is used for visualizing point configurations in  $\mathbb{R}^d$  that consist of not more than  $d + 5$  points.

The basic idea is that (the combinatorics of) a point configuration is determined by the signs of its affine dependencies. If the configuration consists only of few points compared to the dimension of the ambient space, the affine space of affine dependencies will be low-dimensional. See [103, Chapter 6] and [62, Section 5.6] for more detailed expositions, and [21] for insights into the algebro-geometric aspects of the Gale transform.

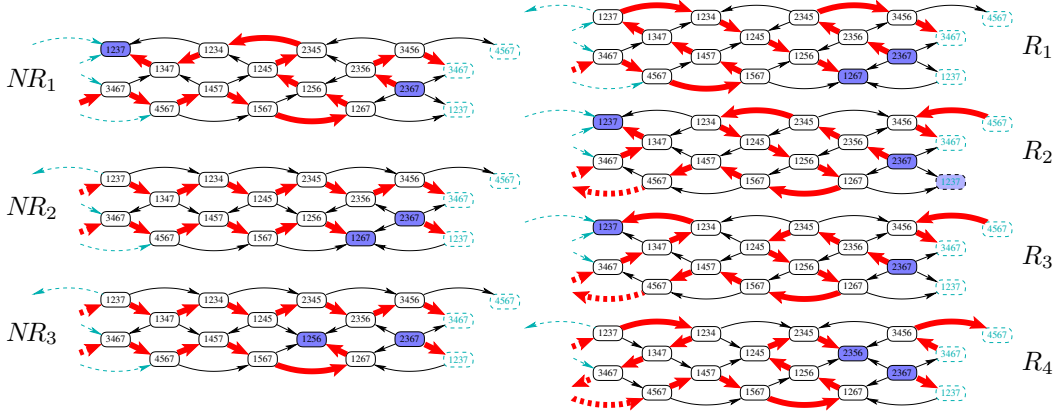


FIGURE 4.1: The seven Hamiltonian Holt-Klee AOF orientations of the graph  $G$  of  $C_4(7)^\Delta$ . ( $G$  can be embedded on a Möbius strip, cf. e.g. [33]). Each vertex is labeled with its incident facets; each label thus corresponds to a facet of  $C_4(7)$ . The bold lines indicate Hamiltonian paths connecting source and sink of each orientation. An arrow  $v \rightarrow w$  means that the vertex  $v$  should lie lower than  $w$ ; in particular, e.g. the orientation  $NR_1$  corresponds to the following sequence of heights:

$$2367 < 2356 < 3456 < 3467 < 4567 < 1457 < 1245 < 2345 < 1234 < 1347 < 1237.$$

The version of the Gale transform considered in this thesis converts an (affinely spanning) sequence of  $n$  points in  $\mathbb{R}^d$  into a (linearly spanning) sequence of  $n$  vectors in  $\mathbb{R}^{n-d-1}$ .

---

**Algorithm 2** The Gale transformation

---

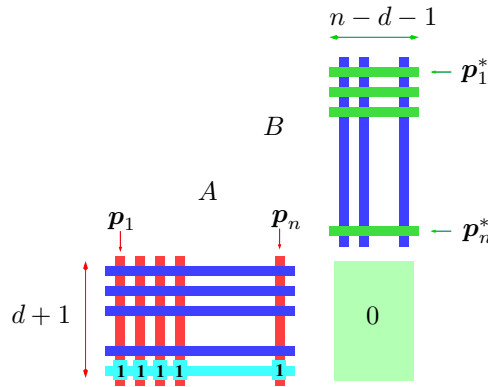
**Input:** An affinely spanning sequence  $\mathcal{A} = (\mathbf{p}_1, \mathbf{p}_2, \dots, \mathbf{p}_n) \subset \mathbb{R}^d$  of  $n$  points.

**Output:** A linearly spanning sequence  $\mathcal{A}^* = (\mathbf{p}_1^*, \mathbf{p}_2^*, \dots, \mathbf{p}_n^*) \subset \mathbb{R}^{n-d-1}$  of  $n$  vectors.

- 1: Form the  $(d+1) \times n$ -matrix  $A$  by appending a row of ‘1’s to the column vectors  $\mathbf{p}_i$ .
  - 2: Choose a basis for  $\ker A$ , i.e., an  $n \times (n-d-1)$ -matrix  $B$  such that  $AB = 0$ .
  - 3: The output configuration  $(\mathbf{p}_1^*, \mathbf{p}_2^*, \dots, \mathbf{p}_n^*)$  is the sequence of rows of  $B$ , see Figure 4.2.
- 

**Definition 4.3** Let  $\mathcal{A} = (\mathbf{p}_1, \mathbf{p}_2, \dots, \mathbf{p}_n)$  resp.  $\mathcal{B} = (\mathbf{v}_1, \mathbf{v}_2, \dots, \mathbf{v}_n)$  be sequences of  $n$  points in  $\mathbb{R}^d$  resp.  $n$  vectors in  $\mathbb{R}^e$  with  $\dim \text{aff}\{\mathbf{p}_1, \mathbf{p}_2, \dots, \mathbf{p}_n\} = d$  and  $\dim \text{lin}\{\mathbf{v}_1, \mathbf{v}_2, \dots, \mathbf{v}_n\} = e$ .

- (a) A *cocircuit* of the point configuration  $\mathcal{A}$  is a partition  $\mathcal{C}^* : [n] = (\mathcal{C}^*)^+ \cup (\mathcal{C}^*)^- \cup (\mathcal{C}^*)^0$  such that there is an affine functional  $f : \mathbb{R}^d \rightarrow \mathbb{R}$  where  $(\mathcal{C}^*)^+ = \{i \in [n] : f(\mathbf{p}_i) > 0\}$ ,  $(\mathcal{C}^*)^- = \{i \in [n] : f(\mathbf{p}_i) < 0\}$ ,  $(\mathcal{C}^*)^0 = \{i \in [n] : f(\mathbf{p}_i) = 0\} \subsetneq [n]$ , and  $(\mathcal{C}^*)^+ \cup (\mathcal{C}^*)^-$  is minimal with respect to inclusion. The *values* of  $\mathcal{C}^*$  are  $\{f(\mathbf{p}_i) : i \in [n]\}$ .
- (b) A *circuit* or *minimal linear dependency* of the vector configuration  $\mathcal{B}$  is a partition  $\mathcal{C} : [n] = \mathcal{C}^+ \cup \mathcal{C}^- \cup \mathcal{C}^0$  of  $[n]$ , such that  $\mathcal{C}^+ \cup \mathcal{C}^- \neq \emptyset$  is inclusion-minimal with the property that there is a linear dependency  $\sum_{i \in \mathcal{C}^+ \cup \mathcal{C}^-} \lambda_i \mathbf{v}_i = 0$ , where  $\mathcal{C}^+ = \{i \in [n] : \lambda_i > 0\}$  and  $\mathcal{C}^- = \{i \in [n] : \lambda_i < 0\}$ . The *values* of  $\mathcal{C}$  are  $\{\lambda_i : i \in [n]\}$ .

FIGURE 4.2: Calculating the Gale transform means fixing a basis of  $\ker A$ .

**Remark 4.4** The cocircuits of  $\mathcal{A}$  with nonnegative values (the *nonnegative cocircuits*) determine the facets of  $\text{conv } \mathcal{A}$ , and the nonnegative circuits of  $\mathcal{B}$  determine minimal sets of vectors in  $\mathcal{B}$  that contain  $\mathbf{0}$  in their positive span.

**Proposition 4.5** [103, Corollary 6.15] If  $\mathcal{A}^*$  is a Gale transform of the point configuration  $\mathcal{A}$ , then  $\mathcal{C}$  is a cocircuit of  $\mathcal{A}$  if and only if  $\mathcal{C}$  is a circuit of  $\mathcal{A}^*$ . (The dual statement also holds.) In particular, the vertex sets of facets of  $\text{conv } \mathcal{A}$  exactly correspond to the complements of minimal sets of vectors in the Gale transform that contain  $\mathbf{0}$  inside their convex hull.

**Observation 4.6** If  $\mathcal{A} = \{p_1, p_2, \dots, p_n\}$  is an affine point configuration in  $\mathbb{R}^d$  and  $p_n$  lies in the relative interior of  $\text{conv } \mathcal{A}$ , then  $n \in (C^*)^+$  for any nonnegative cocircuit  $C^*$  of  $\mathcal{A}$ . Equivalently, by Proposition 4.5, we get  $n \in C^+$  for any nonnegative circuit  $C$  of  $\mathcal{A}^*$ .

## 4.2 The polar-Gale transform

Welzl's *Gale $^\Delta$ -transformation* [27] takes a sequence  $(w_1, w_2, \dots, w_m, g)$  of points in  $\mathbb{R}^d$  and produces a sequence  $(w_1^*, w_2^*, \dots, w_m^*, \tilde{g}^*)$  of vectors in  $\mathbb{R}^{m-d}$ . In the standard interpretation, the  $w_i$ 's represent the  $m$  facet-defining hyperplanes  $W_i = \{x \in \mathbb{R}^d : w_i^T x = 1\}$ ,  $i \in [m]$ , of a full-dimensional polytope  $P \subset \mathbb{R}^d$  such that  $\mathbf{0} \in \text{int } P$ , and  $g \in \mathbb{R}^d$  encodes a linear objective function  $g^T \in (\mathbb{R}^d)^*$ . Note that  $m$  counts the number of *facets* of  $P$ , and *not* the number of vertices as in the usual Gale transform! With this interpretation of the input, the Gale $^\Delta$ -transform produces  $m+1$  labelled vectors in  $\mathbb{R}^{m-d}$  that encode both the face lattice of  $P$  and the orientation  $\mathcal{O}_g$  of the 1-skeleton of  $P$  induced by  $g^T$ .

Let  $v_1, v_2, \dots, v_n$  be the vertices of  $P$ , and label them in such a way that

$$g^T v_1 \leq g^T v_2 \leq \dots \leq g^T v_k < 0 < g^T v_{k+1} \leq \dots \leq g^T v_n \quad (4.1)$$

holds for some  $k \in \mathbb{N}$  with  $1 < k < n$ , where we may assume that  $g^T v_i \neq 0$  for all  $i$ .

**Algorithm 3** The Gale $^\Delta$ -transformation

**Input:** A sequence  $(\mathbf{w}_1, \mathbf{w}_2, \dots, \mathbf{w}_m, \mathbf{g} =: \mathbf{w}_0)$  of points in  $\mathbb{R}^d$  such that  $P = \{\mathbf{x} \in \mathbb{R}^d : \mathbf{w}_i^T \mathbf{x} \leq 1, i \in [m]\}$  is bounded, i.e., a polytope, and the  $\mathbf{w}_i$  define *facets* of  $P$ . (This implies that  $\dim P = d$  and  $\mathbf{0} \in \text{int } P$ .)

**Output:** A sequence  $(\mathbf{w}_1^*, \mathbf{w}_2^*, \dots, \mathbf{w}_m^*, \tilde{\mathbf{g}}^* =: \mathbf{w}_0^*)$  of vectors in  $\mathbb{R}^{m-d}$ .

- 1: Replace  $\mathbf{g}$  by some positive scalar multiple  $\tilde{\mathbf{g}} = c\mathbf{g}$  such that  $\tilde{\mathbf{g}} \in \text{int } P^\Delta$ , where  $P^\Delta = \text{conv}\{\mathbf{w}_1, \mathbf{w}_2, \dots, \mathbf{w}_m\}$  is  $P$ 's polar dual.
- 2: Output the Gale transform  $\text{Gale}^\Delta(P, \tilde{\mathbf{g}}) := (\mathbf{w}_1^*, \mathbf{w}_2^*, \dots, \mathbf{w}_m^*, \tilde{\mathbf{g}}^*)$  of the point sequence  $(\mathbf{w}_1, \mathbf{w}_2, \dots, \mathbf{w}_m, \tilde{\mathbf{g}})$ .

The point  $\mathbf{t}_i$  of intersection between the line  $g = \mathbb{R}\mathbf{g}$  and the  $i$ -th facet  $V_i = \{\mathbf{x} \in \mathbb{R}^d : \mathbf{v}_i^T \mathbf{x} = 1\}$  of  $P^\Delta$  is given by  $\mathbf{t}_i = (1/\mathbf{g}^T \mathbf{v}_i)\mathbf{g}$ . Thus, the ordering of the vertices of  $P$  by  $\mathbf{g}^T$  induces an ordering of the facets of  $P^\Delta$  by  $g$  via

$$\mathbf{t}_k \leq \mathbf{t}_{k-1} \leq \dots \leq \mathbf{t}_1 < 0 < \mathbf{t}_n \leq \mathbf{t}_{n-1} \leq \dots \leq \mathbf{t}_{k+1}. \quad (4.2)$$

If  $\mathbf{g}$  is in *general position* with respect to  $P$ , which for our purposes means that the values  $\{\mathbf{g}^T \mathbf{v} : \mathbf{v} \in \text{vert } P\}$  are all distinct, we have strict inequalities in (4.1) and (4.2), and the ordering (4.2) is a Bruggesser-Mani *line shelling* [14], [103, Section 8.2] of the facets of  $P^\Delta$ . Conversely, every line shelling of the boundary of  $P^\Delta$  gives rise to a linear objective function in general position on  $P$ . See also [103, Exercise 8.10].

Step 1 of Algorithm 4.2 works because by construction the origin  $\mathbf{0}$  is contained in the interior of  $P^\Delta$ . In Step 2, having chosen  $\tilde{\mathbf{g}}$  in the interior of  $P^\Delta$  implies by Observation 4.6 that for any facet  $F$  of  $P^\Delta$ , the set  $C = \{i \in [m] : \mathbf{w}_i \notin F\} \cup \{0\}$  is a *positive cocircuit* of  $P^\Delta$ . (This means that there is a nonnegative cocircuit  $C^*$  of  $P^\Delta$  such that  $C = (C^*)^+$ .) By Proposition 4.5,  $C$  indexes a positive linear combination of  $\{\mathbf{w}_1^*, \mathbf{w}_2^*, \dots, \mathbf{w}_n^*, \tilde{\mathbf{g}}^* = \mathbf{w}_0^*\}$  summing to zero, so we conclude that  $\text{conv}\{\mathbf{w}_i^* : \mathbf{w}_i \notin F\} \cap \mathbb{R}\tilde{\mathbf{g}}^* \neq \emptyset$ .

**Definition 4.7** Let  $\mathcal{A}_{\mathbf{g}}^* = (\mathbf{w}_1^*, \mathbf{w}_2^*, \dots, \mathbf{w}_m^*, \tilde{\mathbf{g}}^*) \subset \mathbb{R}^{m-d}$  be the Gale $^\Delta$ -transform of a point sequence  $\mathcal{A}_{\mathbf{g}} = (\mathbf{w}_1, \mathbf{w}_2, \dots, \mathbf{w}_m, \mathbf{g}) \subset \mathbb{R}^d$ , let  $p$  be a vertex of  $P = \{\mathbf{x} \in \mathbb{R}^d : \mathbf{w}_i \mathbf{x} \leq 1\}$ , and let  $I_p \subset [m]$  index the  $\mathbf{w}_i$  that correspond to the facets of  $P$  intersecting in  $p$ . The *intersection height*  $z_p$  of  $p$  is  $z_p = -(\tilde{\mathbf{g}}^*)^T \mathbf{z}_p$ , where  $\mathbf{z}_p = \mathbb{R}\tilde{\mathbf{g}}^* \cap \text{conv}\{\mathbf{w}_i^* : i \notin I_p\}$  is the intersection point of the line  $\mathbb{R}\tilde{\mathbf{g}}^*$  with the convex hull of the  $\mathbf{w}_i^*$ 's indexed by the complement of  $I_p$ . (See Figure 4.3.)

**Example 4.8** Let  $P$  be a triangular prism in  $\mathbb{R}^3$  (see Figure 4.3, left); in particular, the number of facets of  $P$  is  $m = 5$ , and the number of vertices is  $n = 6$ . The polar  $P^\Delta$  is the polytope of Figure 4.3 (middle) with  $n = 6$  facets and  $m = 5$  vertices, and the Gale transform of  $P^\Delta$  (the Gale $^\Delta$ -transform of  $P$ ) consists of  $m = 5$  points in  $\mathbb{R}^{5-3-1} = \mathbb{R}^1$  (Figure 4.3, right, horizontal line). If we additionally encode a linear objective function  $\mathbf{g}$  by a point in the relative interior of  $P$  and  $P^\Delta$ , the dimension of the Gale $^\Delta$ -transform increases by 1, and Proposition 4.9 below tells us that the intersection points of affine spans of complements of facets of  $P^\Delta$  encode the values of the objective function.



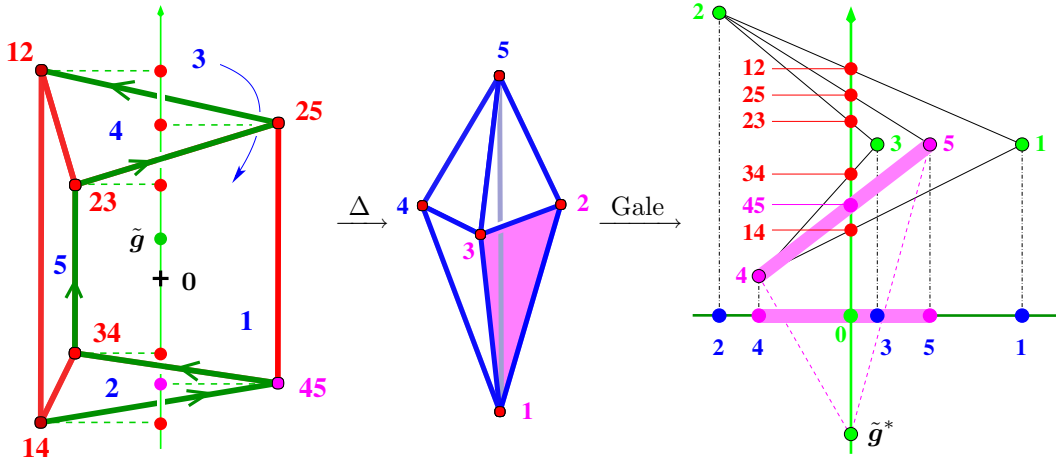


FIGURE 4.3: An instance of the  $\text{Gale}^\Delta$ -transform: “ $\text{Gale}^\Delta(P, \tilde{g}) = \text{Gale}(P^\Delta, \tilde{g})$ ”. *Left*: A simple polytope  $P$  whose vertices are labeled with the facets they are *not* incident to, and the ordering of the vertices induced by the linear objective function  $\tilde{g}$ . *Middle*: The simplicial polar polytope  $P^\Delta$ , whose vertices are labeled like the corresponding facets of  $P$ . *Right*: On the bottom line, a Gale transform of the vertices of  $P^\Delta$ . As in Proposition 4.5, complements of facets of  $P^\Delta$  correspond to positive circuits (minimal linear dependencies) in  $(\text{vert } P^\Delta)^*$ . Taking into account  $\tilde{g}$  results in a lifting of the Gale transform such that the sequence of intersection heights of facet complements encodes the ordering of the vertices of the original polytope by the objective function.

**Proposition 4.9** We have  $p, q \in \text{vert } P$  with  $\mathbf{g}^T \mathbf{p} < \mathbf{g}^T \mathbf{q}$ , if and only if  $z_p < z_q$ .

*Proof.* Let  $F_p = \{\mathbf{x} \in \mathbb{R}^d : \mathbf{p}^T \mathbf{x} = 1\}$  resp.  $F_q = \{\mathbf{x} \in \mathbb{R}^d : \mathbf{q}^T \mathbf{x} = 1\}$  be the supporting hyperplanes of the facets of  $P^\Delta = \text{conv}\{\mathbf{w}_i : i \in [m]\}$  corresponding to  $p$  resp.  $q$ , and let  $\mathbf{w}_0 := \tilde{\mathbf{g}} = c\mathbf{g} \in \text{int } P^\Delta$  for  $c > 0$ . For  $i, j \in [m]_0$ , set  $\lambda_i = \mathbf{p}^T \mathbf{w}_i - 1 \geq 0$  and  $\mu_j = \mathbf{q}^T \mathbf{w}_j - 1 \geq 0$ . Then  $\lambda_i > 0$  resp.  $\mu_j > 0$  if and only if  $i \in [m]_0 \setminus I_p$  resp.  $j \in [m]_0 \setminus I_q$ , where  $I_p$  resp.  $I_q$  index the vertices of  $P^\Delta$  in  $F_p$  resp.  $F_q$ . By Proposition 4.5, in the  $\text{Gale}^\Delta$ -transform there holds

$$\sum_{i \in [m]_0 \setminus I_p} \lambda_i \mathbf{w}_i^* = 0 \quad \text{and} \quad \sum_{j \in [m]_0 \setminus I_q} \mu_j \mathbf{w}_j^* = 0,$$

so that

$$\sum_{i \in [m] \setminus I_p} \lambda_i \mathbf{w}_i^* = -\lambda_0 \tilde{\mathbf{g}}^* \quad \text{and} \quad \sum_{j \in [m] \setminus I_q} \mu_j \mathbf{w}_j^* = -\mu_0 \tilde{\mathbf{g}}^*, \quad (4.3)$$

and therefore  $\mathbf{z}_p = -\lambda_0 \tilde{\mathbf{g}}^*$  and  $\mathbf{z}_q = -\mu_0 \tilde{\mathbf{g}}^*$ . Since by assumption  $\lambda_0 = \mathbf{p}^T \mathbf{w}_0 - 1 = \mathbf{g}^T \mathbf{p} - 1 < \mathbf{g}^T \mathbf{q} - 1 = \mu_0$ , so that  $\lambda_0 < \mu_0$ , and on the other hand  $\mathbf{z}_p = -(\tilde{\mathbf{g}}^*)^T \mathbf{z}_p = \lambda_0 \|\tilde{\mathbf{g}}^*\|^2$  and  $\mathbf{z}_q = \mu_0 \|\tilde{\mathbf{g}}^*\|^2$ , the claim follows.  $\square$

### 4.3 Three nonrealizable Hamiltonian AOF Holt-Klee orientations

**Theorem 4.10** *The three Hamiltonian AOF Holt-Klee orientations  $NR_1, NR_2, NR_3$  of the graph of  $C_4(7)^\Delta$  in Figure 4.1 are not realizable.*

Before proving Theorem 4.10, we assemble some notation for vector configurations in  $\mathbb{R}^2$ .

**Convention 4.11** For  $i \in [7]$ , we will write  $\mathbf{i}$  for a vector  $(x_i, y_i)^T \in \mathbb{R}^2$ , and  $\mathbf{i}^\perp$  for the vector  $(y_i, -x_i)^T$  orthogonal to  $\mathbf{i}$  that is obtained by rotating  $\mathbf{i}$  in the clockwise direction. With this convention, the following relations hold for the scalar product of two vectors:

$$\mathbf{i}\mathbf{j}^\perp = x_i y_j - x_j y_i = \det(\mathbf{i}\mathbf{j}) = -\det(\mathbf{j}\mathbf{i}) = -\mathbf{j}\mathbf{i}^\perp = -\mathbf{i}^\perp \mathbf{j}. \quad (4.4)$$

We further abbreviate

$$\mathbf{i}\mathbf{j}^\perp := \text{sign}(\mathbf{i}\mathbf{j}^\perp), \quad [\mathbf{i}\mathbf{j}\mathbf{k}] := \det \begin{pmatrix} \mathbf{i} & \mathbf{j} & \mathbf{k} \\ 1 & 1 & 1 \end{pmatrix}, \quad [\mathbf{i}\mathbf{j}\mathbf{k}] := \text{sign}([\mathbf{i}\mathbf{j}\mathbf{k}]), \quad (4.5)$$

so that  $[\mathbf{i}\mathbf{j}\mathbf{k}] = +$  if and only if  $\mathbf{i}, \mathbf{j}, \mathbf{k}$  come in anti-clockwise order around 0.

**Lemma 4.12** (a) If  $\mathbf{i}, \mathbf{i} + \mathbf{j}, \mathbf{j} \in \mathbb{R}^2$  come in anti-clockwise order around 0, then  $\mathbf{i}\mathbf{j}^\perp = +$ .  
 (b) If in a configuration of 4 vectors  $\mathbf{i}, \mathbf{j}, \mathbf{k}, \ell \in \mathbb{R}^2 \setminus \{0\}$  the vectors  $\mathbf{i}, \mathbf{j}, \mathbf{k}$  are ordered clockwise around 0,  $\mathbf{j} \in \text{relint cone}(\mathbf{i}, \mathbf{k})$ ,  $[\mathbf{i}\mathbf{j}\mathbf{k}] = +$ , and  $\ell \in \text{relint cone}(-\mathbf{i}, -\mathbf{k})$ , then  $[\mathbf{i}\ell\mathbf{j}] = [\mathbf{j}\ell\mathbf{k}] = +$ .

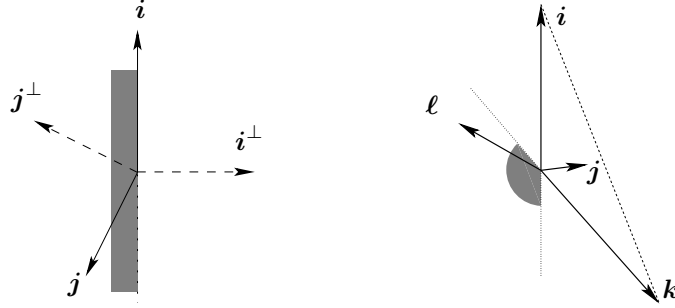


FIGURE 4.4: Deducing sign patterns. *Left:* If  $\mathbf{i}, \mathbf{j} \in \mathbb{R}^2$  come in clockwise order around 0, then  $\mathbf{i}\mathbf{j}^\perp = +$ . *Right:* If  $[\mathbf{i}\mathbf{j}\mathbf{k}] = +$ , then  $[\mathbf{i}\ell\mathbf{j}] = [\mathbf{j}\ell\mathbf{k}] = +$ .

*Proof.* (a) The first condition is equivalent to  $\mathbf{i}^\perp \mathbf{j} < 0$  by Figure 4.4 (left), and to  $\mathbf{i}\mathbf{j}^\perp > 0$  by (4.4). For (b), the affine point  $\ell$  lies to the right of the directed affine lines  $\mathbf{i}\mathbf{j}$  and  $\mathbf{j}\mathbf{k}$ , so the triangles  $\mathbf{i}\ell\mathbf{j}$  and  $\mathbf{j}\ell\mathbf{k}$  are positively oriented. The statement follows.  $\square$

Our strategy for proving Theorem 4.10 is the following. For each of the three orientations  $NR_1, NR_2, NR_3$ , we assume a realization of  $P = C_4(7)^\Delta$  and a corresponding objective function  $\mathbf{g}$  in  $\mathbb{R}^4$ . Applying the Gale $^\Delta$ -transformation yields a configuration of 8 vectors

$\mathbf{w}_1^*, \mathbf{w}_2^*, \dots, \mathbf{w}_7^*, \mathbf{w}_8^* = \tilde{\mathbf{g}}^*$  in  $\mathbb{R}^{8-4-1} = \mathbb{R}^3$  with  $\mathbf{w}_i^* = (\mathbf{i}^T, h_i)^T = (x_i, y_i, h_i)^T$  for  $i \in [8]$ . We then use a Farkas Lemma argument to show that assuming certain signs  $[ijk]$  to be positive resp. negative leads to a contradiction to realizability, but that choosing all signs in a locally consistent way also leads to a contradiction.

**Observation 4.13** [31, Exercise 7.3.7] Any Gale transform of  $C_4(7)$  is *balanced*: exactly 3 vectors lie on each side of the linear span of any one; cf. Figure 4.5.  $\square$

**Convention 4.14** We label the vertices  $v = v_I$  of  $C_4(7)^\Delta$  with the 4-element sets  $I$  of (indices of) the vertices whose convex hull is the facet of  $C_4(7)$  polar to  $v$ . In the same way, the affine hyperplanes  $\pi_{\bar{I}} = \text{aff}\{\mathbf{w}_j^* : j \notin I\}$  in  $\mathbb{R}^{7-4} = \mathbb{R}^3$  spanned by points corresponding to complements of facets of  $C_4(7)$  receive the 3-element labels  $\bar{I} = [7] \setminus I$ . Furthermore, we assume the Gale transform of  $C_4(7)^\Delta$  labeled in such a way that (cf. Figure 4.5)

$$1, 3, 5, 7, 2, 4, 6 \text{ come in clockwise order around the origin.} \quad (4.6)$$

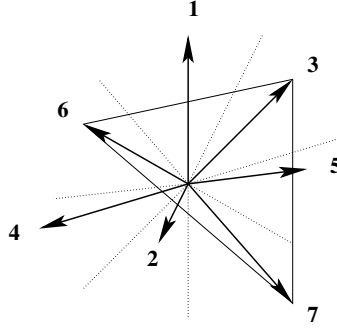


FIGURE 4.5: How to label a Gale transform of  $C_4(7)$ . With this labeling, the natural ordering of the complement of a facet of  $C_4(7)$  induces the anti-clockwise orientation of some triangle enclosing the origin: for example, the complement of the facet  $\{1, 2, 4, 5\}$  of  $C_4(7)$  is  $\{3, 6, 7\}$ , and  $3 < 6 < 7$  is an anti-clockwise orientation.

**Observation 4.15** For any facet  $F_p$  of  $P^\Delta$ , we may assume via an affine transformation that  $\tilde{\mathbf{g}}^* = (0, 0, \dots, 0, -\tilde{g}_{n-d}^*)$  with  $\tilde{g}_{n-d}^* > 0$ , and that  $(\mathbf{w}_i^*)_{n-d} = z_p$  for all  $i \in \bar{I}_p = [n] \setminus I_p$ , where  $I_p$  indexes  $F_p$  (cf. Definition 4.7).

*Proof.* We will find an orientation-preserving linear transformation of  $\mathbb{R}^{n-d}$  such that

- (a) The ‘ $\tilde{\mathbf{g}}^*$ -coordinates’ of the transform of  $F_p$  are all equal:  $(\tilde{\mathbf{g}}^*)^T \mathbf{w}_i^* = z_p$  for all  $i \in \bar{I}_p$ ,
- (b)  $\tilde{\mathbf{g}}^* = (0, 0, \dots, 0, -\tilde{g}_{n-d}^*)$ .

Indeed, the positive cocircuit corresponding to  $F_p$  yields a circuit as in (4.3), so that  $\dim \text{aff}\langle \mathbf{w}_i^* : i \in \bar{I}_p \rangle = n - d - 1$ . Now we can achieve (a) by appropriately choosing  $n - d - 1$  vectors of a linear basis of  $\mathbb{R}^{n-d}$ , leaving one degree of freedom for choosing  $\mathbf{g}^*$ .  $\square$

**Remark 4.16** After applying Observation 4.15 and a translation  $\mathbf{x} \mapsto \mathbf{x} - c(0, 0, 1)^T$ , we may assume in any Gale transform of  $(C_4(7), \mathbf{g})$  that  $h_i = h_j = h_k = 0$  for some facet

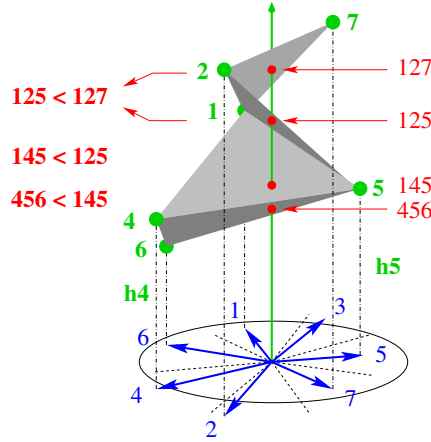


FIGURE 4.6: Intersection heights encode values of the objective function. Suppose that the objective function  $\tilde{g}$  orders four vertices of  $C_4(7)$  as follows:  $1237 < 2367 < 3456 < 3456$  (we assume the labeling of Convention 4.14). Then the intersection points between  $\mathbb{R}\tilde{g}^*$  and the lifted triangles corresponding to the complements of these labels are ordered  $z_{456} < z_{145} < z_{125} < z_{127}$ .

complement  $\{i, j, k\}$ . The resulting configuration is not a  $\text{Gale}^\Delta$ -transform of  $C_4(7)^\Delta$  and an objective function, but projecting along the 3-axis does yield a Gale-transform of  $C_4(7)$ .

**Lemma 4.17** The intersection height  $z_p = z_{\{i,j,k\}}$  where the line  $g = \{(0, 0, h)^T : h \in \mathbb{R}\}$  meets the affine plane  $\pi_{\{i,j,k\}}$  through the points  $w_i^*, w_j^*, w_k^* \in \mathbb{R}^3$  (corresponding to the vertex  $p = [7] \setminus \{i, j, k\}$  of  $P$ ) is given by

$$z_{\{i,j,k\}} = \frac{\mathbf{i}\mathbf{j}^\perp h_k + \mathbf{k}\mathbf{i}^\perp h_j + \mathbf{j}\mathbf{k}^\perp h_i}{[\mathbf{i}\mathbf{j}\mathbf{k}]} \quad (4.7)$$

As a consistency check, note that (4.7) is symmetric under any permutation of the indices.

*Proof.* Expand the third row of the determinant in the equation

$$\begin{vmatrix} 0 & x_i & x_j & x_k \\ 0 & y_i & y_j & y_k \\ z_{\{i,j,k\}} & h_i & h_j & h_k \\ 1 & 1 & 1 & 1 \end{vmatrix} = 0. \quad \square$$

By Proposition 4.9, the total ordering of the vertices  $v_I$  of  $C_4(7)^\Delta$  induced by the linear objective function  $\mathbf{g}$  induces a total ordering of the intersection heights  $z_{\bar{I}}$  of the affine hyperplanes  $H_{\bar{I}}$  in  $\mathbb{R}^3$  with the 3-axis. If two vertices of  $C_4(7)^\Delta$  span an edge, then the corresponding facets of  $C_4(7)$  share a ridge, which in turn means that the complementary affine hyperplanes have two points  $w_i^*, w_j^*$  in common. This permits us to relate the intersection heights of two adjacent vertices in the graph of  $C_4(7)^\Delta$  in the following way:

**Lemma 4.18** For any  $\{i, j, k, \ell\} \in \binom{[7]}{4}$ , we have the following relation between intersection heights of adjacent vertices of  $C_4(7)^\Delta$ :

$$z_{\{i,j,k\}} - z_{\{i,j,\ell\}} = \frac{(ij^\perp)[jkl]}{[ijk][ij\ell]} h_i + \frac{(ij^\perp)[kil]}{[ijk][ij\ell]} h_j + \frac{ij^\perp}{[ijk]} h_k + \frac{-ij^\perp}{[ij\ell]} h_\ell. \quad (4.8)$$

If  $[ijk] = [ij\ell]$ , then the signs of the coefficients of the  $h$ 's are, in this order,

$$(ij^\perp)[jkl], \quad (ij^\perp)[kil], \quad +, \quad -. \quad (4.9)$$

*Proof.* From Equation (4.7), we obtain

$$\begin{aligned} z_{\{i,j,k\}} - z_{\{i,j,\ell\}} &= \frac{ij^\perp h_k + ki^\perp h_j + jk^\perp h_i}{[ijk]} - \frac{ij^\perp h_\ell + \ell i^\perp h_j + j\ell^\perp h_i}{[ij\ell]} \\ &= h_i \left( \frac{jk^\perp}{[ijk]} - \frac{j\ell^\perp}{[ij\ell]} \right) + h_j \left( \frac{ki^\perp}{[ijk]} - \frac{\ell i^\perp}{[ij\ell]} \right) + h_k \frac{ij^\perp}{[ijk]} - h_\ell \frac{ij^\perp}{[ij\ell]}, \end{aligned}$$

so that it only remains to evaluate the numerators  $N_i$  and  $N_j$  of the coefficients of  $h_i$  and  $h_j$ . Now

$$\begin{aligned} N_i &= (jk^\perp)[ij\ell] - (j\ell^\perp)[ijk] \\ &= (jk^\perp)(ij^\perp + j\ell^\perp + \ell i^\perp) - (j\ell^\perp)(ij^\perp + jk^\perp + ki^\perp) \\ &= (jk^\perp)(ij^\perp) + (jk^\perp)(\ell i^\perp) - (j\ell^\perp)(ij^\perp) - (j\ell^\perp)(ki^\perp), \end{aligned}$$

while the straightforward identity

$$(ij^\perp)(k\ell^\perp) = (\ell i^\perp)(jk^\perp) + (j\ell^\perp)(ik^\perp)$$

tells us that we can expand the second term in the preceding expression to

$$(jk^\perp)(\ell i^\perp) = (ij^\perp)(k\ell^\perp) + (ki^\perp)(j\ell^\perp),$$

arriving at

$$N_i = (ij^\perp)(jk^\perp + k\ell^\perp + \ell j^\perp) = (ij^\perp)[jkl].$$

The coefficient of  $h_j$  is calculated in a similar way. The statement about the signs of the coefficients follows from Convention 4.14 and Lemma 4.12.  $\square$

Our strategy for proving nonrealizability of a certain orientation of  $C_4(7)^\Delta$  is to consider certain relations between intersection heights that are induced by this orientation, and to show that assuming certain signs to be positive resp. negative forces a contradiction by a Farkas Lemma. Specifically, we will write the sign pattern of the coefficients of  $h_i, h_j, h_k, h_\ell$  in the inequality  $z_{\{i,j,k\}} < z_{\{i,j,\ell\}}$  in the form

$$\left( (ij^\perp)[jkl], \quad (ij^\perp)[kil], \quad +, \quad - \right) \begin{pmatrix} h_i \\ h_j \\ h_k \\ h_\ell \end{pmatrix} < 0, \quad (4.10)$$

and use the following version of the Farkas Lemma to show infeasibility:

**Theorem 4.19** cf. [88, Section 7.8] *For  $A \in \mathbb{R}^{m \times d}$ , exactly one of the following is true:*

- ▷ *There exists an  $\mathbf{h} \in \mathbb{R}^d$  such that  $A\mathbf{h} < \mathbf{0}$ .*
- ▷ *There exists a row vector  $\mathbf{c} \in (\mathbb{R}^m)^*$  such that  $\mathbf{c} \geq \mathbf{0}$ ,  $\mathbf{c}A = \mathbf{0}$ , and  $\mathbf{c} \neq \mathbf{0}$ .* □

However, the only information about our assumed realization we can use are sign patterns of determinants. Therefore, in order to show that a system of inequalities  $A\mathbf{h} < \mathbf{0}$  is infeasible, we must produce a Farkas certificate  $\mathbf{c}$  that shows already at the level of signs that some positive combination of the rows of  $A$  sums to zero. Stated in the language of oriented matroids, we must prove infeasibility of the OM program  $A\mathbf{h} < \mathbf{0}$  using only partial knowledge of the circuits; in particular, we can in general perform no circuit elimination, and by extension, no general pivoting.

Nevertheless, for each of the orientations  $NR_1, NR_2, NR_3$  we will find enough linear inequalities to conclude via Theorem 4.19 that the system  $A\mathbf{h} < \mathbf{0}$  is infeasible in *any* realization of  $C_4(7)^\Delta$  and  $\mathbf{g}$  giving rise to these orientations. Theorem 4.10 follows from Propositions 4.20 and 4.21 below.

**Proposition 4.20** The orientation

$$\begin{aligned} NR_1 : \quad z_{145} &< z_{147} < z_{127} < z_{125} < z_{123} < z_{236} < z_{234} \\ &< z_{345} < z_{347} < z_{367} < z_{167} < z_{567} < z_{256} < z_{456} \end{aligned}$$

is not realizable.

*Proof.* We abbreviate ' $z_{\{i,j,k\}} < z_{\{i,j,\ell\}}$ ' by ' $ijk < ij\ell$ '.

**Step 1.** Assume that  $[726] = +$  in a realization of  $NR_1$  labeled as in Convention 4.14. By Lemma 4.12 (b), we also know that  $[752] = +$ . Lemma 4.18 tells us the sign patterns of the coefficients of the  $h$ 's in the following inequalities:

	$h_1$	$h_2$	$h_3$	$h_4$	$h_5$	$h_6$	$h_7$	$i \ j \ k \ \ell$
$567 < 562:$	0	−	0	0	$[726]$	$-[572]$	+	5 6 7 2
$127 < 125:$	$-[572]$	$[157]$	0	0	−	0	+	1 2 7 5
$172 < 176:$	$-[726]$	+	0	0	0	−	$[126]$	1 7 2 6

By setting  $h_1 = h_2 = h_7 = 0$  via Remark 4.16, we obtain the sign pattern

	$h_3$	$h_4$	$h_5$	$h_6$
$567 < 562:$	0	0	$[726] = +$	$-[572] = +$
$127 < 125:$	0	0	−	0
$172 < 176:$	0	0	0	−

which contradicts realizability by Theorem 4.19: regardless of the actual values of the entries in this matrix, we can find a positive combination of the rows that sums to zero. Therefore, in any realization of  $NR_1$ , we have  $[726] = -$ .

**Step 2.** Let us suppose that  $[157] = +$ . However, the inequalities

	$h_1$	$h_2$	$h_3$	$h_4$	$h_5$	$h_6$	$h_7$	$i \ j \ k \ \ell$
$145 < 147$ :	[574]	0	0	-[157]	+	0	-	1 4 5 7
$154 < 152$ :	[524]	-	0	+	-[124]	0	0	1 5 4 2
$127 < 125$ :	-[572]	[157]	0	0	-	0	+	1 2 7 5

prove that  $[157] = -$ , if we specialize to  $h_1 = h_2 = h_5 = 0$ :

	$h_3$	$h_4$	$h_6$	$h_7$
$145 < 147$ :	0	-[157] = -	0	-
$154 < 152$ :	0	+	0	0
$127 < 125$ :	0	0	0	+

**Step 3.** Consider the inequalities

	$h_1$	$h_2$	$h_3$	$h_4$	$h_5$	$h_6$	$h_7$	$i \ j \ k \ \ell$
$127 < 125$ :	-[572]	[157]	0	0	-	0	+	1 2 7 5
$451 < 453$ :	+	0	-	[135]	-[134]	0	0	4 5 1 3
$342 < 345$ :	0	+	-[524]	[352]	-	0	0	3 4 2 5
$345 < 347$ :	0	0	[574]	-[357]	+	0	-	3 4 5 7 ,

and specialize to  $h_3 = h_4 = h_5 = 0$ :

	$h_1$	$h_2$	$h_6$	$h_7$
$127 < 125$ :	-[572]	[157] = -	0	+
$451 < 453$ :	+	0	0	0
$342 < 345$ :	0	+	0	0
$345 < 347$ :	0	0	0	-

If  $[572] = +$ , we have a contradiction; therefore  $[572] = -$ . But now consider

	$h_1$	$h_2$	$h_3$	$h_4$	$h_5$	$h_6$	$h_7$	$i \ j \ k \ \ell$
$567 < 562$ :	0	-	0	0	[726]	-[572]	+	5 6 7 2
$342 < 347$ :	0	+	-[724]	[372]	0	0	-	3 4 2 7
$345 < 347$ :	0	0	[574]	-[357]	+	0	-	3 4 5 7
$374 < 376$ :	0	0	-[746]	+	0	-	[346]	3 7 4 6

under  $h_3 = h_4 = h_7 = 0$ :

	$h_1$	$h_2$	$h_5$	$h_6$
$567 < 562$ :	0	-	[726] = -	-[572] = +
$342 < 347$ :	0	+	0	0
$345 < 347$ :	0	0	+	0
$374 < 376$ :	0	0	0	-

which finally contradicts the realizability of  $NR_1$ .  $\square$

**Proposition 4.21** The Hamiltonian Holt-Klee AOF orientations  $NR_2$  and  $NR_3$  are not realizable.

*Proof.* We prove the nonrealizability of  $NR_2$  in the following way.

**Step 1.** Suppose that in a realization of  $NR_2$ , there holds  $[137] = +$ . By Lemma 4.12 (b), this implies  $[163] = +$ , and we are led to consider the following table of signs:

	$h_1$	$h_2$	$h_3$	$h_4$	$h_5$	$h_6$	$h_7$	$i \ j \ k \ \ell$
763 < 761:	−	0	+	0	0	−[137]	[136]	7 6 3 1
125 < 123:	−[352]	[135]	−	0	+	0	0	1 2 5 3
256 < 251:	−	[156]	0	0	−[126]	+	0	2 5 6 1
127 < 125:	−[572]	[157]	0	0	−	0	+	1 2 7 5 ,

which using  $h_1 = h_2 = h_5 = 0$  becomes

	$h_3$	$h_4$	$h_6$	$h_7$
763 < 761:	+	0	−[137] = −	[136] = −
125 < 123:	−	0	0	0
256 < 251:	0	0	+	0
127 < 125:	0	0	0	+

and thus proves that  $[137] = −$ .

**Step 2.** The inequalities

	$h_1$	$h_2$	$h_3$	$h_4$	$h_5$	$h_6$	$h_7$	$i \ j \ k \ \ell$
763 < 761:	−	0	+	0	0	−[137]	[136]	7 6 3 1
231 < 236:	+	−[136]	[126]	0	0	−	0	2 3 1 6
127 < 123:	−[372]	[137]	−	0	0	0	+	1 2 7 3

with the choice of  $h_1 = h_2 = h_3 = 0$  become

	$h_4$	$h_5$	$h_6$	$h_7$
763 < 761:	0	0	−[137] = +	[136]
231 < 236:	0	0	−	0
127 < 123:	0	0	0	+

If  $[136] = −$ , we arrive at a contradiction; therefore,  $[136] = +$ .

**Step 3.** Finally, consider

	$h_1$	$h_2$	$h_3$	$h_4$	$h_5$	$h_6$	$h_7$	$i \ j \ k \ \ell$
763 < 761:	−	0	+	0	0	−[137]	[136]	7 6 3 1
451 < 453:	+	0	−	[135]	−[134]	0	0	4 5 1 3
451 < 456:	+	0	0	−[156]	[146]	−	0	4 5 1 6
145 < 147:	[574]	0	0	−[157]	+	0	−	1 4 5 7



and set  $h_1 = h_4 = h_5 = 0$ , to obtain

	$h_2$	$h_3$	$h_6$	$h_7$
$763 < 761$ :	0	+	$-[137] = +$	$[136] = +$
$145 < 345$ :	0	−	0	0
$451 < 456$ :	0	0	−	0
$145 < 147$ :	0	0	0	−

and a proof of the nonrealizability of  $NR_2$ .

The same argument proves that  $NR_3$  is nonrealizable. The only difference between this orientation and  $NR_2$  is that  $345 < 347$  in  $NR_3$ , whereas  $347 < 345$  in  $NR_2$ , but the proof of the nonrealizability of  $NR_2$  did not use this inequality.  $\square$

The proof of Theorem 4.10 is now complete.  $\square$

#### 4.4 Realizing ascending Hamiltonian paths

Using the techniques of Section 4.3, we prove the following theorem.

**Theorem 4.22** (a) *There exist realizations of the equivalence classes  $R_1$ – $R_4$  of Hamiltonian AOF Holt-Klee orientations of the graph of  $C_4(7)^\Delta$  listed in Theorem 4.1.*  
 (b) *There does not exist any Hamiltonian AOF Holt-Klee orientation of the graph of  $C_4(8)^\Delta$ .*  
 (c) *There exist realizations of several equivalence classes of Hamiltonian AOF Holt-Klee orientations of the graph of the two other combinatorial types  $N'_4(8)$ ,  $N''_4(8)$  of polar-to-neighborly 4-polytopes with 8 facets [31, Section 7.2.4].*

Our strategy for proving Theorem 4.22 (and therefore completing the proof of Theorem 4.1) is summarized in the following pseudo-code.

- 1: Enumerate (all or all equivalence classes of) Hamiltonian AOF Holt-Klee orientations of the graph of  $P$ , where  $P$  is one of the polytopes of Theorem 4.22. In the case  $P = C_4(8)^\Delta$ , this step already shows that no such orientations exist.
- 2: Using Figure 4.7 below, create ‘random’ instances  $G$  of a Gale diagram of  $P$  using (exact) rational arithmetic and the CGAL library [16]. (The distribution from which they were drawn is not at all uniform.)
- 3: For each Hamiltonian AOF Holt-Klee orientation  $\mathcal{O}$  of the graph of  $P$ , determine if there exists a lifting  $\tilde{G}$  of  $G$  compatible with  $\mathcal{O}$ . This is done by generating one instance of the linear inequality (4.10) for each edge of the Hamiltonian path in  $\mathcal{O}$ , and checking the resulting system for feasibility in (approximate) real arithmetic using CPLEX [18]. In case CPLEX returns a solution, this is checked in rational arithmetic using the PTL library [40]. Repeat this step until a solution is found or too many attempts were made.
- 4: Using rational arithmetic and the PTL library, calculate the Gale diagram  $\tilde{G}^*$  of the found realization, check that the convex hull of  $\tilde{G}^*$  contains exactly one point in its interior, and output the polar polytope  $(\tilde{G}^*)^\Delta$ .

**Remark 4.23** For Step 2 of the preceding pseudo-code, the combinatorial type of a Gale diagram of  $C_4(7)^\Delta$  is given by Figure 4.5, and (affine) Gale diagrams of the three polytopes  $C_4(8)^\Delta$ ,  $N_4'(8)$  and  $N_4''(8)$  are given in Figure 4.7 below.

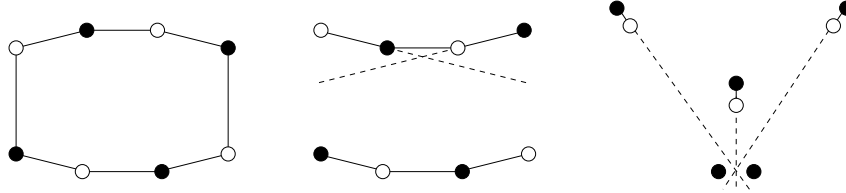


FIGURE 4.7: Affine Gale diagrams of the three combinatorial types of polar-to-neighborly 4-polytopes on 8 vertices. That these Gale diagrams represent different polytopes follows because their *inseparability graphs* (join two vertices by an edge if none or all lines through different vertices separate them [12, Section 7.8]) are non-isomorphic (solid lines). By [32], there are only three combinatorial types of (polar-to-)neighborly 4-polytopes with 8 vertices. See [55] for generalizations of the third diagram.

In the near future, source code and data files for these polytopes will be made available.





## Chapter 5

# Long ascending paths in dimension 4

### 5.1 Introduction

For each integer  $m \geq 0$ , we construct a simple polar-to-neighborly 4-dimensional polytope  $Q_m$  with  $n = m + 5$  facets and a linear objective function  $f \in (\mathbb{R}^4)^*$ , such that the orientation induced by  $f$  on the 1-skeleton of  $Q_m$  admits an ascending Hamiltonian path.

Arguably, the best-known polar-to-neighborly polytopes are the polars  $C_d(n)^\Delta$  of *cyclic polytopes*  $C_d(n)$ , which will also make an appearance in Chapter 8. (Here,  $d$  denotes the dimension and  $n$  the number of vertices of  $C_d(n)$ , hence  $n$  counts the number of facets of  $C_d(n)^\Delta$ ). However, exhaustive enumeration shows that already  $C_4(8)^\Delta$  does not admit a Hamiltonian AOF Holt-Klee orientation, even at the combinatorial level. We are quite convinced that the same is true for  $C_4(n)^\Delta$  for all  $n \geq 8$ , but as yet have no proof.

Our family  $\{Q_m = \tilde{Q}_m^4 : m \geq 0\}$  is a special case of a family  $\{\tilde{Q}_m^d : d = 2k \geq 4, m \geq 0\}$  (cf. Section 5.2), and a slight variation of polar-to-cyclic polytopes. The polytopes  $Q_m$  have  $n = m + d + 1$  facets and *do* allow at least one Hamiltonian AOF Holt-Klee orientation (Corollary 5.14). Section 5.4 is devoted to realizing this orientation in  $\mathbb{R}^4$ .

To build the  $Q_m$ 's, we make explicit a special case of Barnette's technique of *facet splitting* [5]. We start with the 4-simplex  $Q_0$ , and for  $m \geq 0$  intersect the polytope  $Q_m$  with a suitable affine half-space  $H_{m+1}^{\geq 0}$  in general position with respect to the vertices of  $Q_m$  such that the resulting polytope is also polar-to-neighborly. For this,  $Q_m \cap H_{m+1}^{\geq 0}$  has to have maximally many vertices, so we must maximize  $|\{\text{intersected edges}\}| - |\{\text{removed vertices}\}|$ .

As an aside, Barnette's facet splitting is a special case of Shemer's *sewing* construction [91]. To locate the new half-space, Barnette uses a flag of faces with exactly one face of each dimension, while Shemer's flags may be more sparse. This additional freedom allows Shemer to construct the asymptotically optimal number (in fixed dimension  $d$ ) of  $2^{\Omega(n \log n)}$  neighborly  $d$ -dimensional polytopes on  $n$  vertices, for fixed  $d \geq 4$ .

In Corollary 5.8, we give an explicit description of the combinatorial structure of the  $Q_m$ 's reminiscent of Gale's Evenness Criterion for (polar-to-)cyclic polytopes, and use it to specify a Hamiltonian path on each  $Q_m$  (Proposition 5.9). In Section 5.4, we then apply a projective transformation  $\psi$  to  $\mathbb{R}^4$  such that the image of this path on  $Q_{m+1} := \psi(Q_m \cap H_{m+1}^{\geq 0})$  is strictly ascending with respect to the objective function  $f : \mathbb{R}^4 \rightarrow \mathbb{R}$ ,  $\mathbf{x} \mapsto x_4$ :

**Theorem 5.1** For  $d = 4$ , the (combinatorial) upper bound theorem is sharp for monotone paths: *The maximal number  $M(4, n)$  of vertices on a strictly ascending path in the 1-skeleton of a 4-polytope  $P$  with  $n$  facets equals the maximal number of vertices that such a polytope can have according to Theorem 3.6. That is,  $M(4, n) = M_{\text{ubt}}(4, n) = n(n - 3)/2$ .*

## 5.2 A family of polar-to-neighborly $d$ -polytopes

For even  $d \geq 4$ , we follow Barnette [5] and equip the  $d$ -simplex  $\Delta^d = \tilde{Q}_0^d$  on the vertex set  $\{v_1, v_2, \dots, v_{d+1}\}$  with an ascending flag  $\mathcal{F}_0 : \emptyset = F_0^{-1} \subset F_0^0 \subset F_0^1 \subset \dots \subset F_0^d = \tilde{Q}_0^d$  of faces such that  $\dim F_0^i = i$  for  $i = 0, 1, \dots, d$ . This flag is defined by setting, for  $i = 0, 1, \dots, d$ ,

$$F_0^i := \text{conv}\{v_1, v_2, \dots, v_{i+1}\} \quad \text{and} \quad T_0^i := \text{vert}(F_0^i) \setminus \text{vert}(F_0^{i-1}) = \{v_{i+1}\}. \quad (5.1)$$

Algorithm 4 below inductively produces for each  $m > 0$  a simple polar-to-neighborly  $d$ -dimensional polytope  $\tilde{Q}_m^d$  with  $m + d + 1$  facets that comes equipped with an ascending flag  $\mathcal{F}_m : \emptyset = F_m^{-1} \subset F_m^0 \subset F_m^1 \subset \dots \subset F_m^d = \tilde{Q}_m^d$  of faces of  $\tilde{Q}_m^d$ . For each  $m > 0$ , this is done by using  $\mathcal{F}_m$  to find a ‘good’ oriented hyperplane  $H_{m+1}$  in general position with respect to the vertices of  $\tilde{Q}_m^d$ , and setting  $\tilde{Q}_{m+1}^d = \tilde{Q}_m^d \cap H_{m+1}^{\geq 0}$ .

**Definition 5.2** For  $i = 0, 1, \dots, d$  and  $m \geq 0$ , we partition the vertex set of the facet  $F_m^i$  along the flag  $\mathcal{F}_m$  by setting  $T_m^i = \text{vert } F_m^i \setminus \text{vert } F_m^{i-1}$ , the  $i$ -th *tip* of the flag  $\mathcal{F}_m$ . We say that the tip  $T_m^i$  is *even* resp. *odd* according to the parity of  $i$ . Moreover, for  $0 \leq k \leq d$  we set

$$T_m^{\text{even}}(k) = \bigcup_{\substack{0 \leq e \leq k \\ e \text{ even}}} T_m^e \quad \text{and} \quad T_m^{\text{odd}}(k) = \bigcup_{\substack{1 \leq o \leq k \\ o \text{ odd}}} T_m^o.$$

---

**Algorithm 4** A special procedure for facet splitting

---

**Input:** An even integer  $d \geq 4$ , a pair  $(\tilde{Q}_m^d, \mathcal{F}_m)$  consisting of a simple polar-to-neighborly  $d$ -dimensional polytope  $\tilde{Q}_m^d$  with  $m + d + 1$  facets, and a flag  $\mathcal{F}_m : \emptyset = F_m^{-1} \subset F_m^0 \subset F_m^1 \subset \dots \subset F_m^d = \tilde{Q}_m^d$  of faces of  $\tilde{Q}_m^d$ .

**Output:** A pair  $(\tilde{Q}_{m+1}^d, \mathcal{F}_{m+1})$ , consisting of a simple polar-to-neighborly  $d$ -dimensional polytope  $\tilde{Q}_{m+1}^d$  with  $m + d + 2$  facets and a flag  $\mathcal{F}_{m+1}$  of faces of  $\tilde{Q}_{m+1}^d$ .

- 1: Use Proposition 5.4(a) below to find an oriented hyperplane  $H_{m+1}$  in general position with respect to  $\tilde{Q}_m^d$ , such that the vertices of  $\tilde{Q}_m^d$  contained in odd resp. even tips lie in  $H_{m+1}^-$  resp.  $H_{m+1}^+$ .
- 2: Set  $\tilde{Q}_{m+1}^d = \tilde{Q}_m^d \cap H_{m+1}^{\geq 0}$ .
- 3: Choose the new tips in the following way, cf. Figure 5.1:

$$T_{m+1}^j = \text{vert} \begin{cases} \text{conv} \bigcup_{0 \leq k \leq d/2} T_m^{2k} & \text{for } j = d \\ \text{conv} \left( T_m^{j+1} \cup \bigcup_{\substack{0 \leq k < j \\ k+j \equiv 0 \pmod{2}}} T_m^k \right) \cap H_{m+1} & \text{for } j = 2, 3, \dots, d-1, \\ \text{conv}(T_m^0 \cup T_m^1) \cap H_{m+1} & \text{for } j = 1, \\ \text{conv}(T_m^1 \cup T_m^2) \cap H_{m+1} & \text{for } j = 0. \end{cases} \quad (5.2)$$


---

**Remark 5.3** (1) The polytopes  $C_d(n)^\Delta$  arise by exchanging  $T_{m+1}^0$  and  $T_{m+1}^1$  in (5.2).

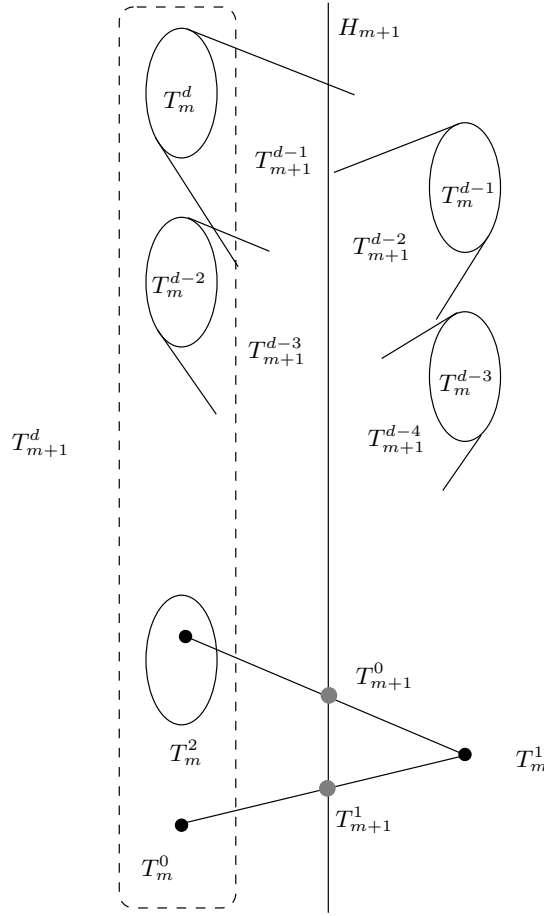


FIGURE 5.1: New tips.

- (2) General position of  $H_{m+1}$  implies that  $\tilde{Q}_{m+1}^d$  is a simple  $d$ -polytope with  $n = m + d + 1$  facets. All new vertices arise as the intersection of  $H_{m+1}$  with some edge  $\text{conv}\{v, w\}$  of  $\tilde{Q}_m^d$ , where  $v$  and  $w$  lie in tips of different parity. Furthermore, all vertices of  $\tilde{Q}_m^d$  belonging to even tips are also vertices of  $\tilde{Q}_{m+1}^d$ , and vertices in odd tips disappear.

**Proposition 5.4** For each  $m \geq 0$ , the following statements hold for the polytope  $\tilde{Q}_m^d$ :

- (a) There exists an affine oriented hyperplane  $H_{m+1}$  in general position with respect to  $\tilde{Q}_m^d$  such that the vertices in odd resp. even tips lie in  $H_{m+1}^-$  resp.  $H_{m+1}^+$ .
- (b) For all  $i, j \in \mathbb{N}$  with  $0 \leq i < j \leq d$  and  $i + j = 1 \pmod{2}$  and all  $v \in T_m^i$ , there is exactly one  $w \in T_m^j$  such that  $\text{conv}\{v, w\} \in \text{sk}^1(\tilde{Q}_m^d)$ . This gives rise to bijections  $T_m^{\text{even}}(k) \cong T_{m+1}^k$  for odd  $0 < k < d$  resp.  $T_m^{\text{odd}}(k) \cong T_{m+1}^k$  for even  $0 \leq k \leq d$ .
- (c)  $|T_m^e| = |T_{m+1}^{e+1}| = \binom{e/2+m}{m}$  for  $e = 0, 2, \dots, d-2$ , and  $|T_m^d| = \binom{d/2+m}{m}$ . In particular,  $\tilde{Q}_m^d$  is polar-to-neighborly.

*Proof.* (a) Pick an oriented point  $v = H^0 \in \text{relint } F_m^1$  such that  $T_m^0 \in (H^0)^+$ . Inductively, for  $1 \leq k \leq d-1$ , if we have already chosen an oriented  $(k-1)$ -dimensional affine subspace  $H^{k-1}$  in  $\text{aff } F_m^k$  such that

$$T_m^{\text{odd}}(k-1) \subset (H^{k-1})^- \quad \text{and} \quad T_m^{\text{even}}(k-1) \subset (H^{k-1})^+, \quad (*)$$

we construct a  $k$ -plane  $H^k$  that initially coincides with  $\text{aff } F_m^k$ , and rotate it slightly around  $H^{k-1}$  such that  $T_m^{\text{even}}(k) \subset (H^k)^+$ . We do this until  $H^k$  separates  $T_m^{\text{even}}(k) \cup T^{k+1}$  from  $T_m^{\text{odd}}(k)$  if  $k+1$  is even, resp.  $T_m^{\text{even}}(k)$  from  $T_m^{\text{odd}}(k) \cup T^{k+1}$  if  $k+1$  is odd. Then  $(*)$  even holds with  $k$  replaced by  $k+1$ . By construction,  $H_{m+1} = H^{d-1}$  is in general position with respect to  $\tilde{Q}_m^d$ .

(b) This follows because  $v$  lies in  $F_m^{j-1} = \bigcup_{i=0}^{j-1} T_m^i$ , and  $\text{conv}(F_m^{j-1})$  is a  $(j-1)$ -dimensional face of the simple polytope  $\text{conv}(F_m^j) = \text{conv}(F_m^{j-1} \cup T_m^j)$ .

(c) We proceed by induction, and can assume that the assertion holds for  $m \geq 0$ . From the bijections in part (b), we conclude for all even  $0 \leq e \leq d-2$  that

$$|T_{m+1}^{e+1}| = |T_{m+1}^e| = \sum_{\substack{i=0 \\ i \text{ even}}}^e |T_m^i| = \sum_{k=0}^{e/2} |T_m^{2k}| = \sum_{k=0}^{e/2} \binom{k+m}{m} = \binom{e/2+m+1}{m+1}.$$

Here we used the identity  $\sum_{k \leq r} \binom{k+m}{m} = \binom{r+m+1}{m+1}$ . For  $|T_{m+1}^d|$ , a similar calculation holds. The fact that  $\tilde{Q}_m^d$  is polar-to-neighborly follows, since

$$\begin{aligned} f_0(\tilde{Q}_m^d) &= \sum_{k=0}^{d/2} \binom{k+m}{m} + \sum_{k=0}^{\lfloor (d-1)/2 \rfloor} \binom{k+m}{m} \\ &= \binom{m+d/2+1}{d/2} + \binom{m+\lfloor (d-1)/2 \rfloor + 1}{\lfloor (d-1)/2 \rfloor} \\ &= \binom{n-d/2}{d/2} + \binom{n-\lceil (d-1)/2 \rceil - 1}{\lfloor (d-1)/2 \rfloor} \\ &= f_0(N_d(n)^\Delta), \end{aligned}$$

where  $n = m + d + 1$  and  $f_0(N_d(n)^\Delta)$  denotes the number of vertices of a simple polar-to-neighborly  $d$ -dimensional polytope with  $n$  facets and even  $d$ ; by [103, Chapter 8], *any* polytope with that many vertices is polar-to-neighborly.  $\square$

We introduce labelings to make explicit the combinatorics of these polytopes:

- Convention 5.5** (a) Let the facets of a simple  $d$ -polytope  $P$  be labeled in some way with labels in  $[n]$ , and let  $\lambda : \text{vert } P \rightarrow \binom{[n]}{d}$  assign to each vertex  $v$  of  $P$  the set of labels of all facets that  $v$  is incident to. We identify a vertex  $v$  with its label  $\lambda(v)$ .
- (b) The facets of the  $d$ -simplex  $\tilde{Q}_0^d$  on the vertex set  $\{v_1, v_2, \dots, v_{d+1}\}$  are labeled in such a way that  $v_1 \equiv \lambda(v_1) = [d+1] \setminus \{2\}$ ,  $v_2 = [d+1] \setminus \{1\}$ , and  $v_j = [d+1] \setminus \{j\}$  for  $j = 3, 4, \dots, d+1$  (cf. Figure 5.2).
- (c) The ‘new’ facet  $\tilde{Q}_m^d \cap H_{m+1} \subset \tilde{Q}_{m+1}^d$  is labelled  $m + d + 2$ .



$$\begin{array}{llll}
T_0^6 & 2b & 12|34|56 & \\
\{v_5\} = T_0^4 & 2b & 12|34|67 & 123|45|7 \quad 2a \quad T_0^5 \\
\{v_3\} = T_0^2 & 2b & 12|45|67 & 123|56|7 \quad 2a \quad T_0^3 = \{v_4\} \\
\{v_1\} = T_0^0 & 1 & 13|45|67 & 234|56|7 \quad 2a \quad T_0^1 = \{v_2\}
\end{array}$$

FIGURE 5.2: The labeling of the vertices of the 6-simplex  $\tilde{Q}_0^6$  according to Convention 5.5(b). Also shown is the classification of the vertices into types 1, 2a, 2b as in Proposition 5.6.

**Proposition 5.6** Let  $m \geq 0$  and  $n = m + d + 1$ . (a) A vertex  $v$  of  $\tilde{Q}_m^d$  lies in  $T_m^i$  exactly if

$$\max_n \bar{v} := \max \{[n] \setminus v\} = \begin{cases} m+2 & \text{for } i=0, \\ m+1 & \text{for } i=1, \\ m+i+1 & \text{for } 2 \leq i \leq d. \end{cases}$$

(b) Moreover, the vertices of  $\tilde{Q}_m^d$  are all  $d$ -subsets of the following types (cf. Convention 5.5):

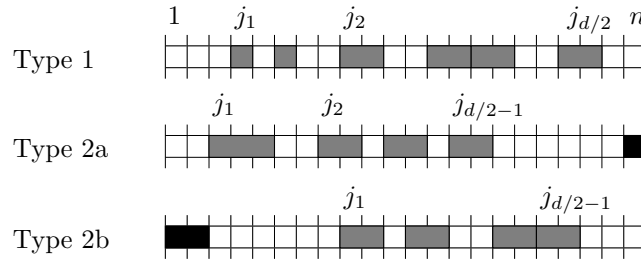


FIGURE 5.3: The vertex-facet incidences of the polytopes  $\tilde{Q}_m^d$  are obtained from these patterns by fixing the dark boxes, and sliding the lighter boxes between 1 and  $n$  without overlap. For Type 1, the box  $\{j_1, j_1 + 2\}$  must be regarded as one rigid unit.

▷ *Type 1.* The union of one ‘triplet with a hole’ and  $d/2 - 1$  pairs of indices

$$\{j_1, j_1 + 2\} \cup \{j_2, j_2 + 1\} \cup \cdots \cup \{j_{d/2}, j_{d/2} + 1\},$$

where  $1 \leq j_1 < n - d + 1$ ,  $j_1 + 3 \leq j_2$ ,  $j_k + 2 \leq j_{k+1}$  for  $2 \leq k \leq d/2 - 1$ , and  $j_{d/2} < n$ .

▷ *Type 2a.* The union of one triplet, the singleton  $\{n\}$ , and  $d/2 - 2$  pairs of indices

$$\{j_1, j_1 + 1, j_1 + 2\} \cup \{j_2, j_2 + 1\} \cup \cdots \cup \{j_{d/2-1}, j_{d/2-1} + 1\} \cup \{n\},$$

where  $1 \leq j_1 < n - d + 1$ ,  $j_1 + 3 \leq j_2$ ,  $j_k + 2 \leq j_{k+1}$  for  $2 \leq k \leq d/2 - 2$ , and  $j_{d/2-1} < n - 1$ .

▷ *Type 2b.* The union of  $d/2$  pairs of indices

$$\{1, 2\} \cup \{j_1, j_1 + 1\} \cup \cdots \cup \{j_{d/2-1}, j_{d/2-1} + 1\},$$

where  $3 \leq j_1$ ,  $j_k + 2 \leq j_{k+1}$  for  $2 \leq k \leq d/2 - 2$ , and  $j_{d/2-1} < n$ .

More specifically, all vertices of  $T_m^{\text{even}}(d)$  are of type 1 or 2b, and  $T_m^{\text{odd}}(d-1)$  is made up entirely of vertices of type 2a, cf. Figure 5.4.

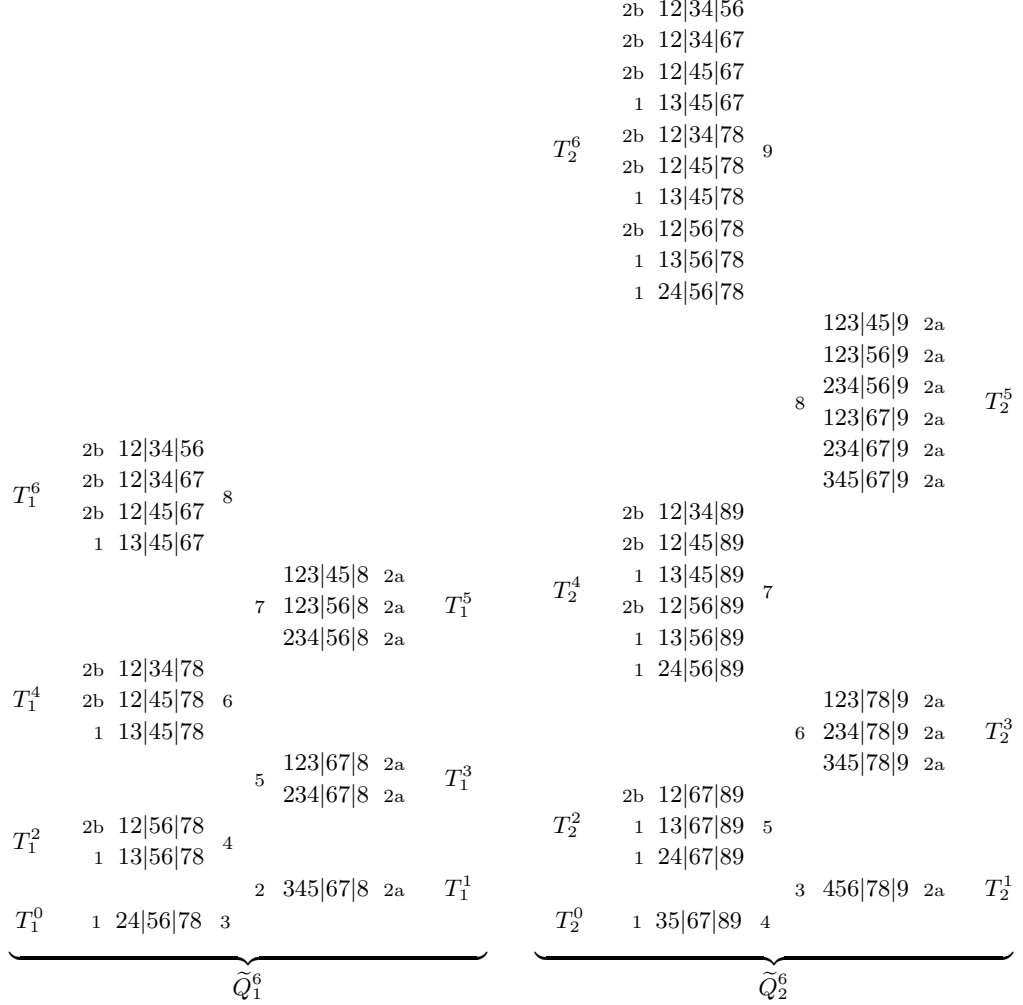


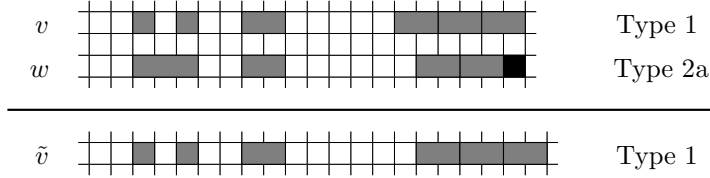
FIGURE 5.4: Vertex labels in the polytopes  $\tilde{Q}_1^6$  (left) and  $\tilde{Q}_2^6$  (right). Also shown are the type (outside) of each vertex  $v$  and the value of  $\max_n \bar{v}$  (inside).

*Proof.* (a) This is true for  $m = 0$  by (5.1) and Convention 5.5, see also Figure 5.2. For  $m > 0$  and  $2 \leq i < d$ , the statement follows because any vertex  $\tilde{v} \in T_m^i$  is of the form  $\tilde{v} = \text{conv}\{v, w\} \cap H_m \equiv (v \cap w) \cup \{n\}$  for some  $v \in T_{m-1}^k$  and  $w \in T_{m-1}^{i+1}$  with  $k \leq i$ . But then by induction,

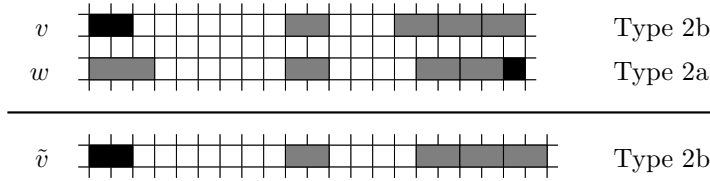
$$\max_{n-1} \bar{v} < \max_{n-1} \bar{w} = (m-1) + (i+1) + 1 = m + i + 1,$$

so  $\max \{[n] \setminus \tilde{v}\} = m + i + 1$  as required. The case  $i = d$  follows directly from Algorithm 4, and  $i = 0, 1$  are checked similarly.

(b) The last statement is checked to hold for  $m = 0$  and by induction for  $m > 0$  and  $T_m^d$ . We first show that all vertices of  $T_m^{\text{even}}(d)$  are of type 1 or 2b. For  $2 \leq e \leq d - 2$ , all vertices  $\tilde{v}$  of  $T_m^e(d)$  are of the form  $\tilde{v} = (v \cap w) \cup \{n\}$ , for some  $v \in T_{m-1}^{e'}$ ,  $w \in T_{m-1}^{e'+1}$ , and even  $0 \leq e' \leq e$ . By (a), we know that  $\max_{n-1} \bar{v} < \max_{n-1} \bar{w}$ , so by induction, we need to check what happens if  $\max_{n-1} \bar{v} < \max_{n-1} \bar{w}$ ,  $w$  is of type 2a, and  $v$  of type 1 or 2b. If  $v$  is of type 1, then  $\tilde{v}$  is also of type 1:



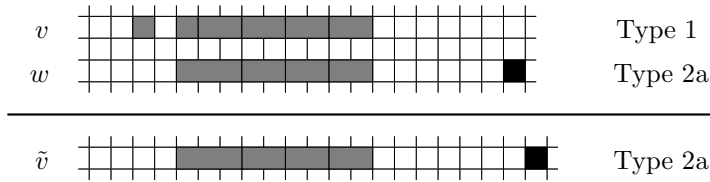
If  $v$  is of type 2b, then again because  $\max_{n-1} \bar{v} < \max_{n-1} \bar{w}$ , the new vertex  $\tilde{v}$  is of type 2b:



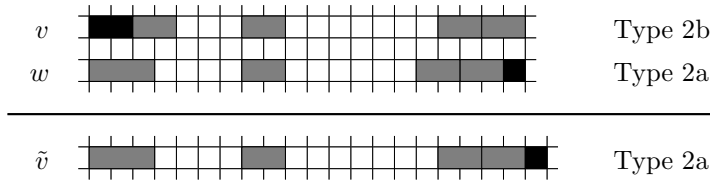
For  $e = e' = 0$ , i.e.,  $\{v\} = T_{m-1}^0$  and  $\{w\} = T_{m-1}^1$ , we have  $\{\tilde{v}\} = T_m^1$  by (5.2) and  $\max_{n-1} \bar{v} > \max_{n-1} \bar{w}$  by (a), so  $\tilde{v}$  is of type 2a.

Finally, we prove that all remaining vertices  $\tilde{v} \in T_m^{\text{odd}}(d-1)$  are of type 2a. For  $3 \leq o \leq d-1$ , a vertex  $\tilde{v} \in T_m^o$  is of the form  $\tilde{v} = (v \cap w) \cup \{n\}$  for some  $v \in T_{m-1}^{o+1}$ ,  $w \in T_{m-1}^{o'}$ , and odd  $1 \leq o' \leq o$ . By (a), we have  $\max_{n-1} \bar{v} > \max_{n-1} \bar{w}$ , and by induction,  $w$  is of type 2a.

If  $v$  is of type 1, then necessarily  $\max_{n-1} \bar{v} = \max_{n-1} \bar{w} + 1$ , and there are two cases:  $\max_{n-1} \bar{v}$  could attain the minimal possible value  $(m-1) + 2$ ; but then  $\{v\} = T_{m-1}^0$  and  $o = -1$ , a contradiction. The other possibility is that  $\tilde{v}$  is again of type 1:



If on the other hand  $v$  is of type 2b, we again obtain a vertex of type 2a:







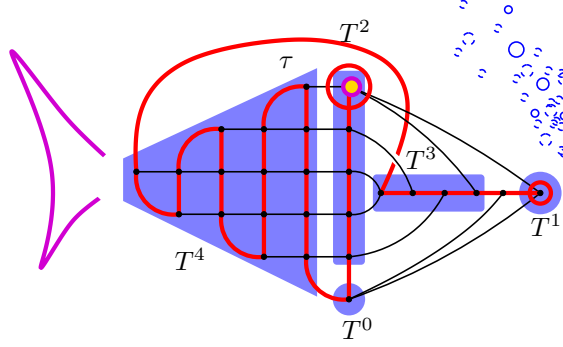


FIGURE 5.7: Another representation of  $\tilde{Q}_4^4$  and  $\tilde{\pi}_4$ . Not all edges are drawn!

Let  $P$  be a simple  $d$ -polytope, and recall from Definition 3.16 the concepts of *AOF-orientation* and *abstract objective function* on  $P$ . For every  $0 \leq k \leq d$ , let  $h_k(\mathcal{O})$  denote the number of vertices in the graph of  $P$  of in-degree  $k$  with respect to an orientation  $\mathcal{O}$ .

**Proposition 5.13** (see e.g. [103, Chap. 8.3] and [42]) An acyclic orientation  $\mathcal{O}$  of the graph of a simple  $d$ -polytope  $P$  is an AOF-orientation if and only if the  $h$ -vector of  $P$  coincides with the vector  $(h_0(\mathcal{O}), h_1(\mathcal{O}), \dots, h_d(\mathcal{O}))$ .  $\square$

**Corollary 5.14** The orientation induced on the 1-skeleton of  $\tilde{Q}_m^4$  by the Hamiltonian path  $\tilde{\pi}_m$  is an AOF-orientation.

*Proof.* The  $h$ -vector of a simple polar-to-neighborly  $d$ -polytope with  $n = m + d + 1$  facets is given by  $h_k = \binom{n-d-1+k}{k} = \binom{m+k}{k}$  for  $k = 0, 1, \dots, d$ . Proposition 5.4 therefore tells us that

$$(|T_m^1|, |T_m^3|, |T_m^4|, |T_m^2|, |T_m^0|) = (h_0, h_1, h_2, h_3, h_4).$$

By Proposition 5.13, it suffices to check using Figure 5.6 that if the orientation of each edge of the graph of  $\tilde{Q}_m^4$  is consistent with the total ordering induced by  $\tilde{\pi}_m$ , then the vertices of  $T^1$ ,  $T^3$ , resp.  $T^4$  all have in-degree 0, 1 resp. 2, furthermore  $T^0$  and all but one vertex of  $T^2$  have in-degree 3, and this vertex, the sink, has in-degree 4.  $\square$

## 5.4 Realizing the ascending Hamiltonian paths

The following theorem implies Theorem 5.1.

**Theorem 5.15** For all  $m \geq 0$ , there exists a special realization of a simple, polar-to-neighborly 4-polytope  $Q_m$  with  $n = m + 5$  facets and the same combinatorial type as  $\tilde{Q}_m^4$  (via an isomorphism  $\varphi : \mathcal{F}(\tilde{Q}_m^4) \rightarrow \mathcal{F}(Q_m)$  of face lattices). In this realization, the Hamiltonian path  $\pi_m := \varphi(\tilde{\pi}_m)$  visits the vertices of  $Q_m$  in the order given by the  $x_4$ -coordinate.

Moreover, the family  $\{Q_m : m \geq 0\}$  may be realized inductively starting from the 4-simplex  $Q_0$  in such a way that for all  $m \geq 0$ , a realization of  $Q_{m+1}$  with an ascending Hamiltonian path  $\pi_{m+1}$  may be obtained from any realization of  $Q_m$  with such a path  $\pi_m$ .

Our strategy for proving Theorem 5.15 exploits the fact (Remark 5.10) that the Hamiltonian path  $\pi_m$  begins in the facet  $F_m^3$ , traverses the rest of the polytope  $Q_m$ , and then returns to  $F_m^3$ , as in Figures 5.6 and 5.7. We call  $T_m^{\text{odd}}(3) = T_m^1 \cup T_m^3$  the *odd* part, and the remaining vertices the *even* part of  $\pi_m$ .

#### 5.4.1 Outline of the inductive construction

For all  $m \geq 0$ , we first find an oriented hyperplane  $H_{m+1}$  that separates the odd and even parts of the path. We then create an intermediate pair  $(Q'_{m+1}, \mathcal{F}'_{m+1})$  as in Proposition 5.4:  $Q'_{m+1} = Q_m \cap H_{m+1}^{\geq 0}$  is a simple polar-to-neighborly polytope of the same combinatorial type as  $\tilde{Q}_{m+1}^4$ , and the flag  $\mathcal{F}'_{m+1}$  of faces is defined by  $F_{m+1}^i = \text{conv} \bigcup_{k=0}^i T_{m+1}^k$  for  $i = 0, 1, \dots, 4$ , where we find the new tips as follows:

$$\begin{aligned} T_{m+1}^4 &= T_m^0 \cup T_m^2 \cup T_m^4, \\ T_{m+1}^3 &= \text{vert} \left( \text{conv} \{ T_m^4 \cup T_m^1 \cup T_m^3 \} \cap H_{m+1} \right), \\ T_{m+1}^2 &= \text{vert} \left( \text{conv} \{ T_m^3 \cup T_m^0 \cup T_m^2 \} \cap H_{m+1} \right), \\ T_{m+1}^1 &= \text{vert} \left( \text{conv} \{ T_m^0 \cup T_m^1 \} \cap H_{m+1} \right), \\ T_{m+1}^0 &= \text{vert} \left( \text{conv} \{ T_m^1 \cup T_m^2 \} \cap H_{m+1} \right). \end{aligned}$$

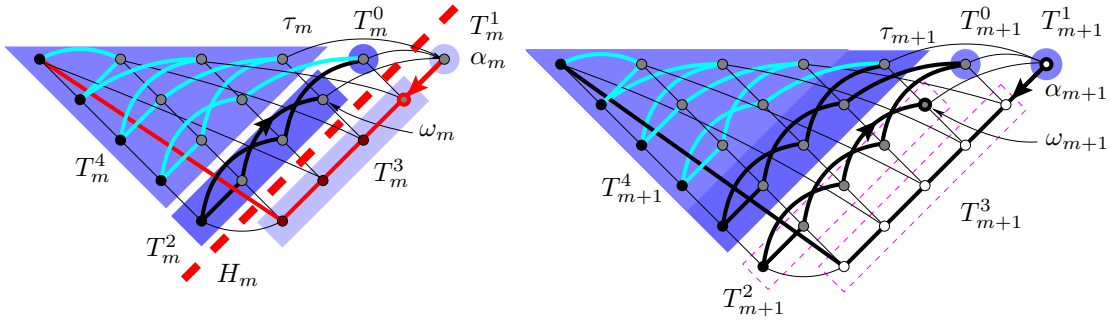


FIGURE 5.8: Passing from  $\tilde{\pi}_m$  to  $\tilde{\pi}_{m+1}$  (in the case  $m = 3$ ). Note that in the left picture, the hyperplane  $H_m$  (dashed) cuts through 12 edges. Each intersection corresponds to a new vertex.

Our combinatorial model  $\tilde{Q}_{m+1}^4$  provides us with a Hamiltonian path  $\pi_{m+1} = \varphi(\tilde{\pi}_{m+1})$  on  $Q'_{m+1}$ , which is not yet ascending with respect to the objective function  $f : \mathbf{x} \mapsto x_4$ . However, we will choose  $H_{m+1}$  in such a way that there exists a family  $\mathcal{H} = \{H_t : t \in \mathbb{P}^1(\mathbb{R})\}$  of hyperplanes in  $\mathbb{R}^4$  that ‘sorts the vertices of  $Q'_{m+1}$  correctly’: If  $p, q$  are vertices of  $Q'_{m+1}$  that lie in  $H_r$  resp.  $H_s$  with  $r, s \neq \infty$  and  $p$  precedes  $q$  in  $\pi_{m+1}$ , then  $r < s$  (here we abuse notation and write  $\mathbb{P}^1(\mathbb{R}) = \mathbb{R} \cup \{\infty\}$ ). Additionally, all planes in  $\mathcal{H}$  will intersect in a common 2-flat  $R = \bigcap_{t \in \mathbb{P}^1(\mathbb{R})} H_t$ , the *axis* of  $\mathcal{H}$ .

We then apply a projective transformation  $\psi$  that sends  $H_\infty$  to infinity. Because the common intersection  $R$  of the  $H_t$ ’s is also mapped to infinity, the images  $\{\psi(H_t) : t \in \mathbb{R}\}$  form a

family of parallel affine hyperplanes, the level planes of a new objective function  $f_{m+1}$ . The fact that the original  $H_t$ 's sorted the vertices of  $Q'_{m+1}$  'angle-wise' in the order given by  $\pi_{m+1}$  implies that the Hamiltonian path  $\psi(\pi_{m+1})$  on  $Q_{m+1} = \psi(Q'_{m+1})$  is strictly ascending with respect to  $f_{m+1}$ .

#### 5.4.2 Properties of the family of polytopes

**Proposition 5.16** *(Some aspects of the combinatorics of the  $Q_m$ 's)*

- (a) The induced subgraph of  $sk^1(Q_m)$  on  $T_m^1 \cup T_m^3$  is a path of length  $m+1$  on the  $m+2$  vertices  $v_0^m = \alpha_m, v_1^m, \dots, v_{m+1}^m$ , and the induced subgraph on  $T_m^2$  is a path  $w_1^m, w_2^m, \dots, w_{m+1}^m$ .
- (b) For  $0 \leq i \leq m$ , the edge  $e_i = \text{conv}\{v_i^m, v_{i+1}^m\}$  in  $T_m^3$  is incident to a 2-face  $G_i$  of  $Q_m$  such that the vertices of  $G_i \setminus e_i$  are consecutive in  $\pi_m \cap T_m^4$ .
- (c) For  $1 \leq i \leq m$ , the edge  $f_i$  of  $Q_m$  that connects  $w_i^m$  and  $w_{i+1}^m$  in  $T_m^2 \cap \pi_m$  is incident to a quadrilateral  $R_i$  whose other two vertices are consecutive in  $T_m^4 \cap \pi_m$ .
- (d) Set  $G(m) = \text{vert} \bigcup_{i=0}^m G_i \setminus e_i$  and  $R(m) = \text{vert} \bigcup_{i=1}^m R_i \setminus f_i$ . Then  $G(m) \cup R(m) = T_m^4$ , and  $G(m) \cap R(m) = \tau$ .

*Proof.* (a) All vertices of  $T_m^3$  are of the form  $\{i, i+1, i+2, n\}$  for  $1 \leq i \leq n-3$  and the only way for two such vertices  $v_i^m$  and  $v_j^m$  to be adjacent for  $i < j$  is to have  $j = i+1$ . The statement about the  $w_i^m$  follows in a similar way. (b) For  $1 \leq i \leq m+1$ , the 2-face incident to  $v_{m+2-i} = \{i, i+1, i+2, n\}$  and  $v_{m+1-i} = \{i+1, i+2, i+3, n\}$  that is the intersection of the facets  $i+1$  and  $i+2$  consists of the vertices of Figure 5.9. The claim (b) follows because these vertices form a contiguous segment of  $\pi_m$ , and (c) and (d) from Figure 5.10 (left).  $\square$

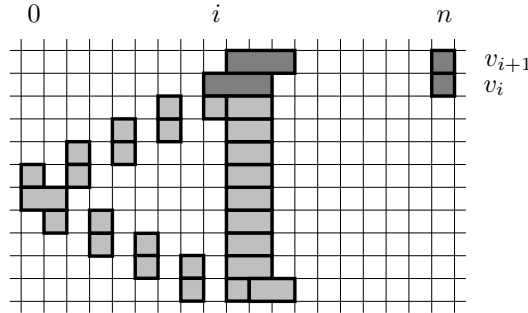


FIGURE 5.9: Vertices of a 2-face incident to  $v_i = \{i, i+1, i+2, n\}$  and  $v_{i+1} = \{i+1, i+2, i+3, n\}$  (dark) in  $T_m^1 \cup T_m^3$ . The light vertices lie in  $T_m^4$  and form a subpath of  $\pi_m$ .

**Observation 5.17** The new start vertex  $\alpha_{m+1}$  of  $\tilde{\pi}_{m+1}$  lies on  $\text{conv}\{\alpha_m, \beta_m\}$ , the new end vertex  $\omega_{m+1}$  on  $\text{conv}\{v_1^m, \beta_m\}$ , and  $\beta_{m+1}$  on  $\text{conv}\{\alpha_m, \omega_m\}$ ; see Figure 5.10 (right).



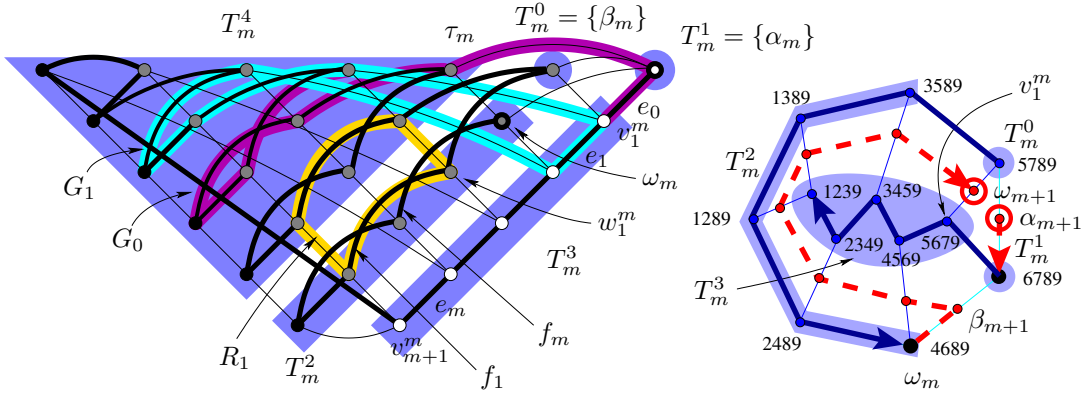


FIGURE 5.10: *Left:* More details about the graph of  $Q_m$ . We have highlighted the graphs of the 2-faces  $G_0$  and  $G_1$  that correspond to the edges  $e_0$  and  $e_1$  by Proposition 5.16 (b), and the 2-face  $R_1$  that corresponds to the edge  $f_1$  according to Proposition 5.16 (c). *Right:* The portion of the new Hamiltonian path  $\tilde{\pi}_{m+1}$  in the facet  $F_m^3$ .

#### 5.4.3 Start of the induction and inductive invariant

We work in  $\mathbb{R}^4$  with standard coordinate vectors  $e_1, e_2, e_3, e_4$ , and abbreviate a linear subspace  $\mathbb{R}\langle e_i : i \in I \rangle$  by  $\langle i : i \in I \rangle$  for all  $I \subset \{1, 2, 3, 4\}$ . An essential tool will be *shear transformations*: these are linear maps  $\sigma_{i,j}^a : \mathbb{R}^4 \rightarrow \mathbb{R}^4$  for  $i \neq j \in \{1, 2, 3, 4\}$  and  $a \in \mathbb{R}$  whose matrix is  $I_4 + a\delta_{i,j}$  with respect to the standard basis of  $\mathbb{R}^4$ . Here  $I_4$  is the  $4 \times 4$  unit matrix and  $\delta_{i,j}$  is the  $4 \times 4$  matrix whose only nonzero entry is a 1 in position  $(i, j)$ . In particular,  $\sigma_{i,j}^a$  maps  $e_i$  to  $e_i + ae_j$ , and the standard basis vectors  $e_k$ ,  $k \neq i$ , to themselves.

The start of the induction is the pair  $(Q_0, \mathcal{F}_0)$ , where  $Q_0$  is the 4-simplex whose vertices  $v_1, v_2, v_3, v_4, v_5$  are given by the columns of the matrix

$$\begin{pmatrix} 0 & 0 & 1 & 0 & 0 \\ 0 & 1 & 0 & 0 & 0 \\ -3 & -1 & 3 & 2 & 1 \\ -2 & -1/2 & 0 & 1/4 & 2 \end{pmatrix}, \quad (5.3)$$

and  $\mathcal{F}$  is the ascending flag  $\mathcal{F}_0 : F_0^0 \subset F_0^1 \subset \dots \subset F_0^4 = Q_0^4$  of faces labeled as in Algorithm 4. In particular, the vertices  $v_i$  lie in the following tips,

$$\begin{array}{c|c|c|c|c} v_1 & v_2 & v_3 & v_4 & v_5 \\ \hline T_0^1 & T_0^3 & T_0^4 & T_0^0 & T_0^2 \end{array},$$

$F_0^2 = \text{conv}\{v_1, v_4, v_5\}$ ,  $F_0^3 = \text{conv}\{v_1, v_2, v_4, v_5\}$ , and  $\pi_0 = (v_1, v_2, v_3, v_4, v_5)$ . For all  $m \geq 0$  our polytopes  $Q_m$  will maintain the following property:

- (1) The Hamiltonian path  $\pi_m$  in the 1-skeleton of  $Q_m$  is strictly ascending with respect to the objective function  $f : \mathbb{R}^4 \rightarrow \mathbb{R}$ ,  $\mathbf{x} \mapsto x_4$ .

## 5.4.4 Induction step I: Positioning the polytope

In this and the following section, we will position our polytope  $Q_m$  in such a way that the coordinate subspaces of  $\mathbb{R}^4$  are compatible with the flag  $\mathcal{F}_m$ . More precisely,

- ▷  $F_m^3 = Q_m \cap \{\mathbf{x} \in \mathbb{R}^4 : x_1 = 0\}$ , and  $T_m^4 \subset \{\mathbf{x} \in \mathbb{R}^4 : x_1 > 0\}$ ; and
- ▷ the hyperplane  $H_S = \{\mathbf{x} \in \mathbb{R}^4 : x_3 = 0\}$  will separate the even from the odd part of  $\mathcal{F}_m$ .

**Lemma 5.18** Let  $\pi$  be the linear projection  $\pi : \mathbb{R}^4 \rightarrow \langle 3, 4 \rangle$ , and use the notation of Convention 5.12 and Proposition 5.16 (a). There exists a non-singular affine transformation  $\sigma$  of  $\mathbb{R}^4$  such that the image of  $Q_m$  under  $\sigma$  meets the following additional requirements, while  $\pi_m$  still satisfies (1), i.e., it is strictly ascending with respect to the  $x_4$ -coordinate:

- (2)  $F_m^2 \subset \{\mathbf{x} \in \mathbb{R}^4 : x_1 = 0\}$ .
- (3)  $\text{aff } F_m^3 = \{\mathbf{x} \in \mathbb{R}^4 : x_1 = 0\}$  and  $Q_m \subset \{\mathbf{x} \in \mathbb{R}^4 : x_1 \geq 0\}$ .
- (4)  $(\alpha_m)_2 = 0$ ,  $q_2 < 0$  for all  $q \in F_m^2 \setminus \{\alpha_m\}$ , and  $(\beta_m)_2 < (v_1^m)_2$ .
- (5) The image of  $F_m^2$  under  $\pi$  is full-dimensional:  $\dim \text{aff } (\pi(F_m^2)) = 2$ .
- (6) The 3-flat  $H_S = \{\mathbf{x} \in \mathbb{R}^4 : x_3 = 0\}$  strictly separates the odd from the even part of  $\pi_m$  (i.e., the vertices in odd resp. even tips). Moreover, we may choose the point of  $H_S \cap F_m^3$  of lowest 4-coordinate to be  $\alpha_{m+1} = \text{conv}\{\alpha_m, \beta_m\} \cap H_S$ , where  $(\alpha_{m+1})_4 = \tau_4$ .

*Proof.* Properties (2) and (3) are a matter of trivial affine transforms that can be chosen to leave the 4-coordinate values invariant, thereby maintaining (1), and property (4) can be achieved via a translation and a shear  $\sigma_{2,4}^a : x_2 \mapsto x_2 + ax_4$ .

For (5), choose  $t \in F_m^2$  with  $t_4 = q_4$  for some  $q \in T_m^3$ ; such a point exists, since  $\alpha_m \in F_m^2$ , and by (1) and Remark 5.10 there holds  $(\alpha_m)_4 < q'_4 < \max\{s_4 : s \in F_m^2\}$  for all  $q' \in T_m^3$ . Translate  $t$  to the origin of  $\mathbb{R}^4$ , and apply a shear transform  $\sigma_{3,2}^b : x_3 \mapsto x_3 + bx_2$  to  $\mathbb{R}^4$ , where  $b \in \mathbb{R}$  is chosen such that  $\pi(\sigma_{3,2}^b(q)) = \pi(\sigma_{3,2}^b(t))$ . This can be done because  $\pi(t) - \pi(q) \in \mathbb{R}e_3$ . Then (5) is fulfilled because  $\dim \text{aff } F_m^3 = 3$ : supposing that  $\dim \text{aff } (\pi(F_m^2)) = 1$  would imply via  $t \in F_m^2$  and  $q \in F_m^3$  that  $q \in \text{aff } F_m^2$ ; however, this is absurd by the choice  $q \in T_m^3$ . Note that none of the translations we used affects properties (2) and (3).

For (6), define  $\tilde{b}$  to be the point of greatest 3-coordinate of  $F_m^2 \cap \{\mathbf{x} \in \mathbb{R}^4 : x_4 = \tau_4\}$ . In particular,  $\tilde{b}_4 > \max_{z \in T^3} z_4$ , and  $\tilde{b}$  lies either on the edge  $\text{conv}\{\alpha_m, \beta_m\}$  or on the edge  $\text{conv}\{\alpha_m, \omega_m\}$  of  $F_m^2 \subset Q_m$  (cf. Figure 5.11).

Possibly using the transform  $x_3 \mapsto -x_3$ , we can achieve  $\tilde{b} = \alpha_{m+1} \in \text{conv}\{\alpha_m, \beta_m\}$ . Now choose a non-horizontal line  $\ell$  through  $\alpha_{m+1}$  such that  $\pi(\ell)$  separates  $\pi(T_m^1 \cup T_m^3)$  from  $\pi(F_m^2 \setminus T_m^1)$  (for example, perturb  $\ell = \alpha_{m+1} + \mathbb{R}e_3$ ), translate  $Q_m$  again such that  $\alpha_{m+1} = 0$ , and apply a shear  $\sigma_{3,4}^c : x_3 \mapsto x_3 + cx_4$  to  $\mathbb{R}^4$  such that  $\ell' := \sigma_{3,4}^c(\ell) = \{\mathbf{x} \in \mathbb{R}^4 : x_1 = x_3 = 0\} \cap \text{aff } F_m^2$  is vertical, and  $y_3 > 0 > x_3$  for all  $y \in F_m^2 \setminus T_m^1$  and  $x \in T_m^1 \cup T_m^3$  (cf. Figure 5.11). If the hyperplane  $\pi^{-1}(\pi(\ell'))$  does not yet separate  $T_m^1$  from  $T_m^4$ , apply another shear  $\sigma_{3,1}^d : x_3 \mapsto x_3 + dx_1$  with  $d > 0$  until it does (note that (3) already holds), and then define  $H_S := \pi^{-1}(\pi(\ell'))$ . This hyperplane then separates the odd and even parts of  $\pi_m$  by construction, and  $(\alpha_{m+1})_4 = \tau_4$  also by construction and because the shears  $\sigma_{3,4}^c$  and  $\sigma_{3,1}^d$  do not affect 4-coordinates. Neither do they affect conditions (1)–(5), so we can define the transform  $\sigma$  as the composition of all these maps.  $\square$

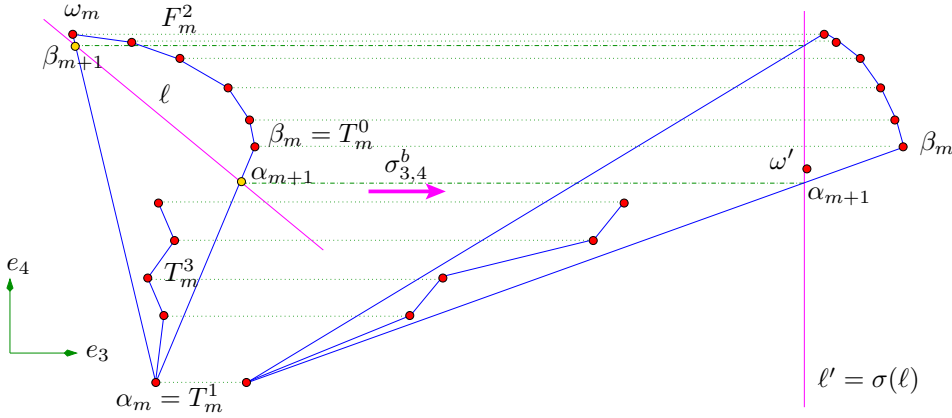


FIGURE 5.11: Positioning the polytope, step (6). The map  $\sigma_{3,4}^b$  shears the polytope until (the preimage under  $\pi$  of) a vertical line  $\ell'$  separates the odd from the even tips. On the right, you can see the approximate position of  $\omega'$ ; this point will become important shortly.

**Remark 5.19** The conditions (1)–(6) are satisfied by the coordinates (5.3) for  $Q_0$ .

#### 5.4.5 Induction step II: Finding the cutting plane

In this section, we find a hyperplane  $H_{m+1}$  giving rise to a polytope  $Q'_{m+1} = Q_m \cap H_{m+1}^{\geq 0}$  of the same combinatorial type as  $\tilde{Q}_{m+1}^4$ . Namely, assume that the conditions (1)–(6) hold, define  $H_{m+1} = \{\mathbf{x} \in \mathbb{R}^4 : \mathbf{n}^T \mathbf{x} = 0\}$  with  $\mathbf{n} = (0, -\delta, 1, \varepsilon)^T$  for some small  $\varepsilon \gg \delta > 0$ , and assign the label  $n+1 = m+d+2$  to  $H_{m+1}$ . Note that  $H_{m+1}$  converges to  $H_S$  for  $\varepsilon, \delta \rightarrow 0$ .

**Convention 5.20** We retain the names  $\alpha_{m+1}, \beta_{m+1}, \omega_{m+1}$  for points of intersection of  $Q_m$  and  $H_S$ , and additionally define  $\alpha' := \alpha'_{m+1} = \text{conv}\{\alpha_m, \beta_m\} \cap H_{m+1}$  and  $\omega' := \omega'_{m+1} = \text{conv}\{\beta_m, v_1^m\} \cap H_{m+1}$ ; see Figure 5.10 (right). We also use the abbreviations  $v := v_1^m$ ,  $u := (v_1^{m+1})' = \text{conv}\{\alpha_m, \tau_m\} \cap H_{m+1}$  and  $\tau := \tau_m$ . In this way, we can use e.g.  $\alpha'_3$  to refer to the 3-coordinate of  $\alpha'_{m+1}$ .

Up to now, we have put the facet  $F_m^3$  of  $Q_m$  into its own 3-plane  $\{\mathbf{x} \in \mathbb{R}^4 : x_1 = 0\}$  and the tip  $T^4$  into the half-space  $\{\mathbf{x} \in \mathbb{R}^4 : x_1 > 0\}$ . This allows us to move *almost all* of the vertices of the Hamiltonian path (namely, the portion inside  $T_m^4$ ) ‘out of the way’, via a shear  $\sigma_{3,1}^a$  that only affects 3-coordinates. These ‘old’ vertices will then be dealt with in Lemma 5.22 below.

We still need to arrange for the first and last part of  $\pi_{m+1}$  to be traversed in the right order. We achieve this by adjusting the position of  $H_{m+1}$  via the parameters  $\varepsilon$  and  $\delta$  in the definition of  $\mathbf{n}$  (note that we chose  $n_1 = 0$ , because we are already done with  $T_m^4$ ). If  $\delta = 0$ , then  $\pi(H_{m+1})$  is a line whose slope is determined by  $\varepsilon$ . We choose  $\varepsilon > 0$  to ‘push out’ the first part  $T_{m+1}^1 \cup T_{m+1}^3$  of the new path  $\pi_{m+1}$ . However, if we left  $\delta = 0$  we would not appropriately sweep the last portion  $T_{m+1}^0 \cup T_{m+1}^2$ . Items (8)–(10) of the following Lemma 5.21 guarantee that by appropriately choosing  $0 < \delta \ll \varepsilon$ , the sweep of Lemma 5.22 will proceed smoothly.

**Lemma 5.21** Assume conditions (1)–(6) and  $(\alpha_{m+1})_3 = (\alpha_{m+1})_4 = 0$ , and fix vertices  $q \in T_m^{\text{odd}}$  and  $s \in T_m^{\text{even}}$ . Let  $q' = \text{conv}\{q, s\} \cap H_{m+1}$  be the intersection with  $H_{m+1}$  of the line through  $q$  and  $s$  (which is not necessarily an edge of  $Q_m$ ). Then, if  $a > 0$  is sufficiently large and  $0 < \delta \ll \varepsilon$  are sufficiently small, the image  $\sigma_{3,1}^a(Q_m)$  of  $Q_m$  under the shear  $\sigma_{3,1}^a$  satisfies the conditions (7)–(10) on the next page (cf. also Figure 5.13).

- (7)  $q'_3 > 0$  for  $0 < \delta \ll \varepsilon$ , and  $q'_3 \rightarrow 0$  as  $\delta, \varepsilon \rightarrow 0$ . In other words, all points in  $\sigma_{3,1}^a(Q_m) \cap H_{m+1}$  can be chosen to have positive 3-coordinate, but to lie arbitrarily close to  $H_S$ .
- (8) The image  $\pi(\text{aff}\{u, q'\}) \subset \langle 3, 4 \rangle$  of the line through  $u$  and  $q'$  under  $\pi$  comes arbitrarily close to being vertical as  $a \rightarrow \infty$  and  $\varepsilon, \delta \rightarrow 0$ .
- (9) If  $q, \bar{q} \in T_m^3$  and  $q_4 < \bar{q}_4$ , then the slope of the line  $\pi(\text{aff}\{\alpha', \bar{q}'\})$  is greater than that of the line  $\pi(\text{aff}\{\alpha', q'\})$ .
- (10) The slope  $\sigma_{\omega'\alpha'}$  of  $\pi(\text{aff}\{\omega', \alpha'\})$  is less than the slope  $\sigma_{\omega'u}$  of  $\pi(\text{aff}\{\omega', u\})$ .

*Proof.* We abbreviate  $\sigma = \sigma_{3,1}^a$ . For (7), we have  $\text{conv}\{q, s\} \cap H_{m+1} \neq \emptyset$  since  $q$  and  $s$  are separated by  $H_{m+1}$  for small enough  $\delta, \varepsilon$ . We calculate the intersection point  $q' = \text{conv}\{q, s\} \cap H_{m+1}$  by solving  $\mathbf{n}^T \mathbf{q} + \mu \mathbf{n}^T (\mathbf{s} - \mathbf{q}) = 0$  for  $\mu$ , obtaining

$$\mathbf{q}' = \mathbf{q} + \frac{\mathbf{n}^T \mathbf{q}}{\mathbf{n}^T (\mathbf{q} - \mathbf{s})} (\mathbf{s} - \mathbf{q}).$$

By (2), the map  $\sigma$  leaves the points  $\alpha', q$ , and  $\omega'$  invariant, and maps  $\mathbf{s}$  to  $\sigma(\mathbf{s}) = \mathbf{s} + a s_1 \mathbf{e}_3$ ; as a consequence,  $\mathbf{n}^T \sigma(\mathbf{s}) = \mathbf{n}^T \mathbf{s} + a s_1$ . Using  $\mathbf{n}^T \mathbf{q} = -\delta q_2 + q_3 + \varepsilon q_4$ , we obtain

$$\begin{aligned} \sigma(\mathbf{q}') &= \mathbf{q} + \frac{\mathbf{n}^T \mathbf{q}}{\mathbf{n}^T (\mathbf{q} - \mathbf{s}) - a s_1} (\mathbf{s} - \mathbf{q} + a s_1 \mathbf{e}_3) \\ &\xrightarrow{a \rightarrow \infty} \mathbf{q} + (0, 0, -\mathbf{n}^T \mathbf{q}, 0)^T = (0, q_2, \delta q_2 - \varepsilon q_4, q_4)^T. \end{aligned} \quad (5.4)$$

Because  $q_4 < (\alpha_{m+1})_4 = 0$  and  $\varepsilon, \delta > 0$ , we can choose  $\delta \ll \varepsilon$  so small that  $\sigma(\mathbf{q}')_3 > 0$  (note that by (4), there holds  $q_2 \leq 0$ ). In particular, we obtain  $\sigma(\mathbf{q}')_3 \rightarrow 0$  as  $\varepsilon, \delta \rightarrow 0$ .

Statement (8) follows from (5.4) and the fact that

$$\lim_{a \rightarrow \infty} \frac{\sigma(\mathbf{q}')_4 - \sigma(\mathbf{u})_4}{\sigma(\mathbf{q}')_3 - \sigma(\mathbf{u})_3} = \frac{q_4 - u_4}{\delta(q_2 - u_2) - \varepsilon(q_4 - u_4)}.$$

For (9), note that

$$\frac{\sigma(\mathbf{q}')_4 - \alpha'_4}{\sigma(\mathbf{q}')_3 - \alpha'_3} \xrightarrow{a \rightarrow \infty} \frac{q_4 - \alpha'_4}{\delta q_2 - \alpha'_3 - \varepsilon q_4} \xrightarrow{\varepsilon, \delta \rightarrow 0} -\frac{q_4 - \alpha'_4}{\alpha'_3},$$

and similarly for  $\bar{q}$ ; the statement now follows from  $q_4 < \bar{q}_4$ .

To prove part (10), set  $\alpha := \alpha_m$  and  $\beta := \beta_m$ . Then by Convention 5.20,  $u = \text{conv}\{\alpha, \tau\} \cap H_{m+1}$ ,  $\alpha' = \text{conv}\{\alpha, \beta\} \cap H_{m+1}$ , and  $\omega' = \text{conv}\{v, \beta\} \cap H_{m+1}$ . We need to verify that

$$\sigma_{\omega'\alpha'} := \frac{\alpha'_4 - \omega'_4}{\alpha'_3 - \omega'_3} < \frac{u_4 - \omega'_4}{u_3 - \omega'_3} =: \sigma_{\omega'u}.$$

From equation (5.4) and condition (4), we deduce that  $\lim_{a \rightarrow \infty} u = (0, 0, -\varepsilon\alpha_4, \alpha_4)^T$ . For  $\alpha'$  and  $\omega'$  we get the following expressions:

$$\begin{aligned}\alpha' &= \alpha + \frac{n^T \alpha}{n^T(\alpha - \beta)}(\beta - \alpha) = \begin{pmatrix} 0 \\ 0 \\ \alpha_3 \\ \alpha_4 \end{pmatrix} + \frac{\alpha_3 + \varepsilon\alpha_4}{\delta\beta_2 + \alpha_3 - \beta_3 + \varepsilon(\alpha_4 - \beta_4)} \begin{pmatrix} 0 \\ \beta_2 \\ \beta_3 - \alpha_3 \\ \beta_4 - \alpha_4 \end{pmatrix}, \\ \omega' &= v + \frac{n^T v}{n^T(v - \beta)}(\beta - v) = \begin{pmatrix} 0 \\ v_2 \\ v_3 \\ v_4 \end{pmatrix} + \frac{-\delta v_2 + v_3 + \varepsilon v_4}{-\delta(v_2 - \beta_2) + v_3 - \beta_3 + \varepsilon(v_4 - \beta_4)} \begin{pmatrix} 0 \\ \beta_2 - v_2 \\ \beta_3 - v_3 \\ \beta_4 - v_4 \end{pmatrix}.\end{aligned}$$

For convenience, we will verify that  $1/\sigma_{\omega'\alpha'} > 1/\sigma_{\omega'u}$ . Indeed, expanding these expressions in terms of  $\delta, \varepsilon$ , we obtain

$$\begin{aligned}\frac{1}{\sigma_{\omega'\alpha'}} &= \frac{\beta_3 v_2 - \beta_2 v_3 + \overbrace{\alpha_3(\beta_2 - v_2)}^{t_1}}{v_3(\alpha_4 - \beta_4) + \beta_3(v_4 - \alpha_4) + \underbrace{\alpha_3(\beta_4 - v_4)}_{t_2}} \delta - \varepsilon + p_1(\delta, \varepsilon), \\ \frac{1}{\sigma_{\omega'u}} &= \frac{\beta_3 v_2 - \beta_2 v_3}{v_3(\alpha_4 - \beta_4) + \beta_3(v_4 - \alpha_4)} \delta - \varepsilon + p_2(\delta, \varepsilon),\end{aligned}$$

where  $p_1$  and  $p_2$  are power series in  $\delta, \varepsilon$  with min-degree at least 2. Notice that up to terms of degree at least 2 in  $\delta, \varepsilon$ , the two formulas are equal except for the expressions  $t_1$  resp.  $t_2$  in the numerator resp. denominator of  $1/\sigma_{\omega'\alpha'}$ . Therefore, we can write the difference between the inverses of the slopes as

$$\frac{1}{\sigma_{\omega'\alpha'}} - \frac{1}{\sigma_{\omega'u}} = \left( \frac{A + t_1}{B + t_2} - \frac{A}{B} \right) \delta + p_3(\delta, \varepsilon).$$

Since  $\alpha_3 < (\alpha_{m+1})_3 < 0$  by assumption and  $\beta_2 < v_2$  by (4), we obtain  $t_1 > 0$ ; and the inductive assumption (1) implies that  $\beta_4 > v_4$  and therefore  $t_2 < 0$ . The claim follows.  $\square$

#### 5.4.6 Induction step III: The projective transformation

Finally, we construct a 1-parameter family  $\mathcal{H} = \{H_t : t \in \mathbb{P}^1(\mathbb{R})\}$  of hyperplanes that contains a 2-plane  $R$  as their common ‘axis’. The family  $\mathcal{H}$  will sort the vertices of  $Q'_{m+1}$  in the order given by  $\pi_{m+1} = \varphi(\tilde{\pi}_{m+1})$ , in the following sense: If  $p, q$  are vertices of  $Q'_{m+1}$  that lie in  $H_r$  resp.  $H_s$  with  $r, s \neq \infty$  and  $p$  precedes  $q$  in  $\pi_{m+1}$ , then  $r < s$ . (Recall our abuse of notation in writing  $\mathbb{P}^1(\mathbb{R}) = \mathbb{R} \cup \{\infty\}$ .) Let  $O = \pi(b + \varepsilon_1(\omega - \alpha) - \varepsilon_3 e_3)$  for some small  $\varepsilon_1, \varepsilon_3 > 0$ , so that  $O$  lies outside but very close to the edge  $\text{conv}\{\alpha, \omega\}$  of  $\pi(F_{m+1}^2)$ , and define the 2-plane  $R \subset \mathbb{R}^4$  to be  $R = \pi^{-1}(O)$ .

**Lemma 5.22** Define  $\mathcal{H}$  as the pencil of hyperplanes in  $\mathbb{R}^4$  sharing the 2-plane  $R$ , and such that  $\pi(H_\infty)$  is the line through  $O$  parallel to  $\text{conv}\{\alpha, \omega\}$ , and the slope of  $\pi(H_r)$  is smaller than the slope of  $\pi(H_s)$  exactly if  $r < s$ . Then  $\mathcal{H}$  sorts the vertices of  $Q_{m+1}$  in the order given by  $\tilde{\pi}_{m+1}$ .

*Proof.* We examine the pieces of  $\pi_{m+1}$  in order; cf. Figure 5.13.

- ▷  $T_{m+1}^1 = \{\alpha\}$  is the start of  $\pi_{m+1}$ : This follows for small enough  $\varepsilon_3$  by (10).
- ▷  $T_{m+1}^3$  is traversed next, in the right order, and before  $T_{m+1}^4$ : The first two statements follow from (7), (8) and (9), and the last one because  $z_3 \rightarrow \infty$  as  $a \rightarrow \infty$  for any  $z \in T_m^4$ , while the 3-coordinates of  $T_{m+1}^3$  remain bounded by (7).
- ▷ The correct order in  $T_m^4 \subset T_{m+1}^4$ . By Proposition 5.16(b), each edge  $e_i = \text{conv}\{v_i^m, v_{i+1}^m\}$ ,  $0 \leq i \leq m$  of  $T_m^1 \cup T_m^3$  is incident to an  $(m+1)$ -gonal 2-face  $G_i$  (see Figure 5.10), and the edges  $E_i$  of  $G_i$  not incident to  $e_i$  form a monotone subpath of  $\pi_{m+1}$ . This implies that for each  $e_i \in T_m^3$ , the slopes of the projection of each  $E_i$  to  $\langle 3, 4 \rangle$  are strictly positive (and, by convexity, monotonically decreasing; see Figure 5.12). Therefore,  $\pi(\bigcup_{i=0}^m E_i)$  is a strictly increasing chain of edges, and this remains true after applying the linear map  $\sigma = \sigma_{3,1}^a$  by invariance of the  $e_i$ 's and all 4-coordinates under  $\sigma$ , and the convexity of the projections of 2-faces. The correct order up to  $\tau$  in  $T_m^4 \subset T_{m+1}^4$  follows from condition (6):  $\alpha_4 \geq s_4$  for all  $s \in \bigcup_{i=0}^m \text{vert } G_i \setminus \text{vert } e_i$ . Similarly, the 4-gonal 2-faces incident to  $T_m^2$  of Proposition 5.16(c) enforce the right order between  $\tau$  and  $T_m^0$ .

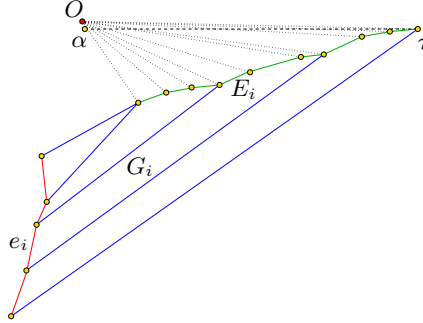


FIGURE 5.12: Convexity of the  $(m+1)$ -gonal faces enforces the correct order in  $T_m^4 \subset T_{m+1}^4$ .

- ▷  $T_{m+1}^2$  is traversed after  $T_{m+1}^4$ : Since  $\beta$ , the first vertex of  $\pi_{m+1}$  to come after  $T_{m+1}^4$ , lies on  $\text{conv}\{\alpha_m, \omega_m\}$ , this can be achieved by choosing  $\varepsilon$  and  $\varepsilon_1$  suitably small.
- ▷ Correct order in  $T_{m+1}^2$  and  $T_{m+1}^0$ . This follows because the convex polygon  $\pi(F_{m+1}^2)$  is star-shaped with respect to any point on its boundary, and the choice of  $O$  close to an edge of  $\pi(F_{m+1}^2)$ .

This concludes the proof of Lemma 5.22.  $\square$

Finally, we apply the projective transform  $\psi : \mathbb{R}^4 \rightarrow \mathbb{R}^4$ ,  $\mathbf{x} \mapsto \mathbf{x}/(\mathbf{a}\mathbf{x} - a_0)$  that sends the 3-plane  $\mathcal{H}_\infty = \{\mathbf{x} \in \mathbb{R}^4 : \mathbf{a}\mathbf{x} = a_0\}$  to infinity, and set  $Q_{m+1} = \psi(Q'_{m+1})$ . Lemma 5.22 then implies the inductive condition (1), namely that  $Q_{m+1}$  admits an ascending Hamiltonian path  $\pi_{m+1}$ . The proof of Theorem 5.15, and so of Theorem 5.1, is concluded.  $\square$

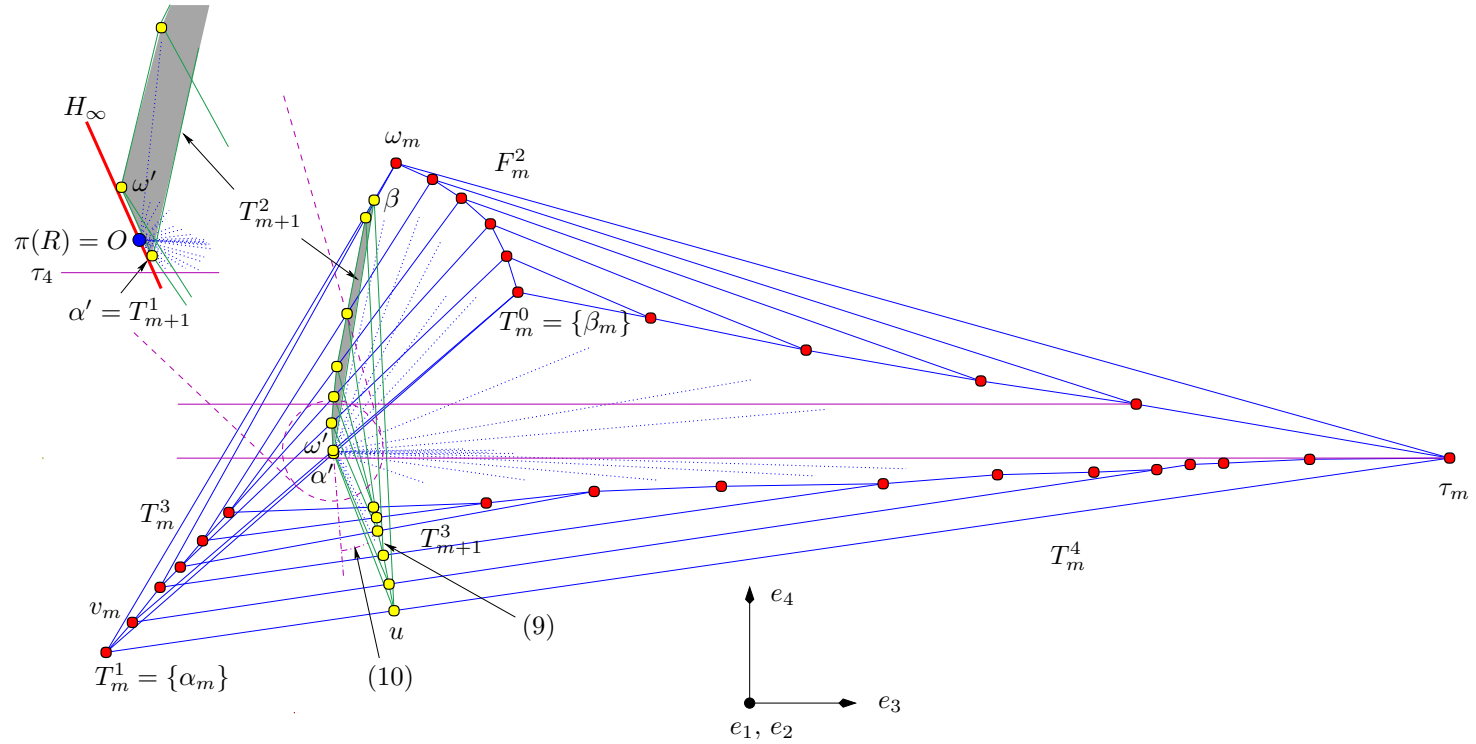


FIGURE 5.13: *The inductive step:* We show the projection of the polytope  $Q_4$  to the  $\langle 3, 4 \rangle$ -plane, and the vertices obtained by intersecting  $Q_4$  with  $H_5$ . The arrows next to the labels (9) and (10) point to the lines about whose slope the corresponding condition in Lemma 5.21 makes an assertion. The line through  $O$  is the projection of the 3-plane  $H_\infty$ . A sweep around  $O$  encounters all vertices of  $Q_m \cap H_{m+1}$  in the correct order  $\pi_m$  prescribed by  $\tilde{\pi}_{m+1}$ .





## Chapter 6

### Secondary Polytopes: An Invitation

This chapter [75] does not contain any new research results; instead, its excuse for being included in this thesis are the pictures you find at the end, and the perhaps surprisingly large variety of different flavors of mathematics tied together by the concept of ‘secondary polytopes’. The pace will accordingly be somewhat faster than in other chapters of this thesis, and we will not always pause to rigorously define every concept.

We will speak chiefly about *triangulations of point sets* and *flips*—the best known way of passing from one triangulation to another. Just in case you have never seen a flip before, here is one between two triangulations of a 3-dimensional point set:

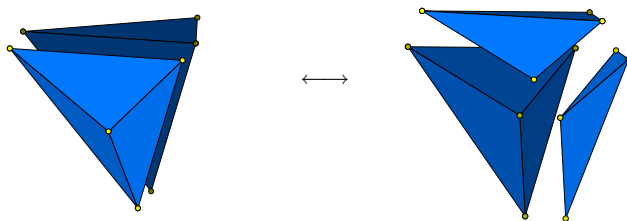


FIGURE 6.1: A flip between two triangulations of a point set in  $\mathbb{R}^3$ . Note that the number of tetrahedra is different in the two triangulations (unlike in the 2-dimensional case).

To define flips more rigorously, we need some definitions. Let  $\mathcal{A} = \{a_1, a_2, \dots, a_n\}$  be a configuration of  $n$  points in  $\mathbb{R}^d$ , which affinely spans  $\mathbb{R}^d$ . A *triangulation* of  $\mathcal{A}$  is a simplicial complex  $\mathcal{T}$  on the index set  $[n]$  such that  $\tilde{\mathcal{T}} = \{\{a_i : i \in \sigma\} : \sigma \in \mathcal{T}\}$  is a geometric simplicial complex (see Chapter 2) on the vertex set  $\mathcal{A}$  with the property that  $\|\mathcal{T}\| = \text{conv } \mathcal{A}$ . Let  $C = C^+ \cup C^- \subseteq [n]$  index a non-trivial *minimal affine dependency* on  $\mathcal{A}$ . This means that for each  $i \in C^+$  and  $j \in C^-$ , there exist  $\lambda_i > 0$  and  $\mu_j > 0$  such that  $\sum_{i \in C^+} \lambda_i a_i = \sum_{j \in C^-} \mu_j a_j$ ,  $\sum_{i \in C^+} \lambda_i = \sum_{j \in C^-} \mu_j$ , and  $C^+$ ,  $C^-$  are minimal with respect to inclusion, as long as  $C \neq \emptyset$ . Then there are exactly two triangulations of  $\{a_i : i \in C\}$ , namely

$$\begin{aligned} \mathcal{T}^+(C) &= \{C \setminus \{c_-\} : c_- \in C^-\}, \\ \mathcal{T}^-(C) &= \{C \setminus \{c_+\} : c_+ \in C^+\}. \end{aligned}$$

In Figure 6.1, one could e.g. choose  $C^+$  to index the vertices of the base triangle and  $C^-$  to index the apexes of the bipyramid. The left triangulation would then correspond to  $\mathcal{T}^+(C)$ , and the right one to  $\mathcal{T}^-(C)$ .

We will build on this concept to present one of the most striking and beautiful constructions of the theory of polyhedral subdivisions, which shows that the regular triangulations (see below) of a point configuration carry quite a lot of structure. Namely, we outline the construction of the *secondary polytope* of a point configuration, briefly sketch one situation where it can be useful, and calculate some examples obtained by integrating TOPCOM [77], [79] into the POLYMAKE [40], [41] framework.

### 6.1 The convex hull of triangulations: Secondary polytopes

It is known that any point configuration  $\mathcal{A}$  in  $\mathbb{R}^d$  can be triangulated, for example via a *placing triangulation* [57]. A triangulation of  $\mathcal{A}$  is *regular* or *coherent* if it arises by projecting the ‘lower’ facets (with respect to some fixed direction) of a  $(d+1)$ -dimensional polytope  $\tilde{P}$  to  $\mathbb{R}^d$ , in such a way that the ‘lower’ vertices of  $\tilde{P}$  project exactly to the points in  $\mathcal{A}$ . Another way of stating this condition is to ask for a convex lifting function from  $\mathbb{R}^d$  to  $\mathbb{R}^{d+1}$  that is linear on the simplices of the triangulation. More generally, we will also consider *regular subdivisions* of  $\mathcal{A}$ , i.e., polytopal complexes whose underlying space subdivides  $\text{conv } \mathcal{A}$  and that satisfy the regularity property. See Figure 6.2 for an example.

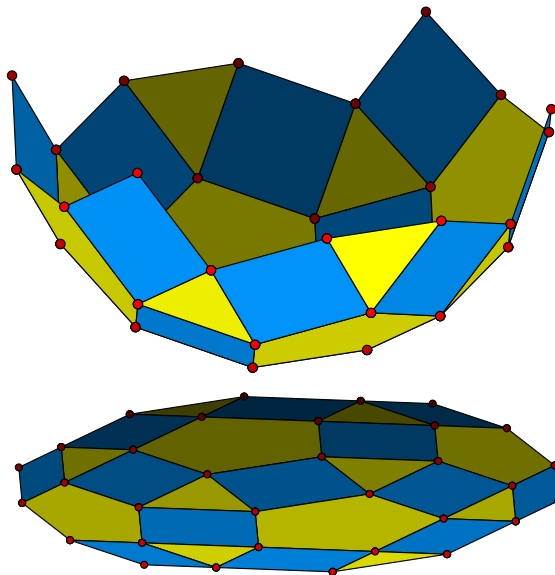
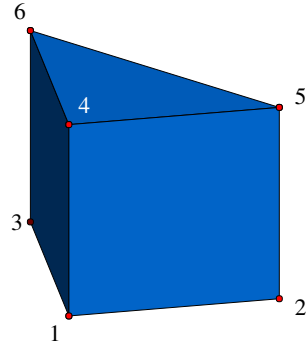


FIGURE 6.2: A regular subdivision of a planar point set, and an associated convex lifting function. The coordinates were taken from [80].

Regular triangulations correspond in a one-to-one fashion to the vertices of a convex polytope  $\Sigma(\mathcal{A})$  that only depends on the point configuration, the so-called *secondary polytope*

of  $\mathcal{A}$ . Moreover, this correspondence is not just bijective, but structural: Two regular triangulations  $T$  and  $T'$  are connected by a flip if and only if the corresponding vertices  $v_T$  and  $v_{T'}$  lie on an edge of the convex hull of  $\Sigma(\mathcal{A})$ . It turns out that this correspondence extends to the whole face lattice of the secondary polytope, so that to each face  $F$  of  $\Sigma(\mathcal{A})$  there corresponds some regular subdivision  $\sigma(F)$  of  $\mathcal{A}$ . Furthermore, if  $F \subset G$  are two faces of  $\Sigma(\mathcal{A})$ , then  $\sigma(F)$  is a *refinement* of  $\sigma(G)$ , which means that any cell of  $\sigma(G)$  is the union of cells of  $\sigma(F)$ .

As an example, let us construct the secondary polytope of the point configuration  $\mathcal{A}$  formed by the vertices of a prism  $P$  over a triangle. The homogeneous coordinates of  $P$  are given by the columns of the following matrix.

$$A = \begin{pmatrix} 0 & 1 & 0 & 0 & 1 & 0 \\ 0 & 0 & 1 & 0 & 0 & 1 \\ 0 & 0 & 0 & 1 & 1 & 1 \\ 1 & 1 & 1 & 1 & 1 & 1 \end{pmatrix}$$


Any triangulation of  $P$  must contain one of the tetrahedra formed by the base  $\{1, 2, 3\}$  and one vertex  $i$  in the set  $\{4, 5, 6\}$ , where the point labels correspond to the column indices of  $A$ . This leaves two choices for the apex of the tetrahedron with base  $\{4, 5, 6\}$ , and each one determines the last tetrahedron of the triangulation uniquely. We see that there are six distinct triangulations of  $P$  in total, namely,

$$\begin{aligned} & \{\{1, 2, 3, 4\}, \{2, 3, 4, 5\}, \{3, 4, 5, 6\}\}, & \{\{1, 2, 3, 4\}, \{2, 3, 4, 6\}, \{2, 4, 5, 6\}\}, \\ & \{\{1, 2, 3, 5\}, \{1, 3, 4, 5\}, \{3, 4, 5, 6\}\}, & \{\{1, 2, 3, 5\}, \{1, 3, 5, 6\}, \{1, 4, 5, 6\}\}, \\ & \{\{1, 2, 3, 6\}, \{1, 2, 4, 6\}, \{2, 4, 5, 6\}\}, & \{\{1, 2, 3, 6\}, \{1, 2, 5, 6\}, \{1, 4, 5, 6\}\}. \end{aligned}$$

These triangulations all turn out to be regular, and therefore correspond to vertices of  $\Sigma(\mathcal{A})$ .

One way to construct the secondary polytope is to start by calculating a basis for the (right) kernel of  $A$ , i.e., a matrix  $B$  with  $AB = 0$ . Since  $A$  has full rank, its kernel has dimension 2, and one possible basis is given by the rows of the following matrix  $B$ :

$$B = \begin{pmatrix} 1 & -1 & 0 & -1 & 1 & 0 \\ 1 & 0 & -1 & -1 & 0 & 1 \end{pmatrix}.$$

By interpreting the *columns* of  $B$  as six points  $b_1, b_2, \dots, b_6$  in  $\mathbb{R}^2$ , we arrive at the *Gale transform*  $\mathcal{A}^*$  of  $\mathcal{A}$  (see also the discussion in Section 4.1, where we used  $B^T$  instead of  $B$ ). In general, if  $\mathcal{A}$  consists of  $n$  points in  $d$ -space (and  $\mathcal{A}$  does not lie in any lower-dimensional subspace), then  $\mathcal{A}^*$  is made up of  $n$  points in  $(n - d - 1)$ -space. Now consider the set  $\mathcal{C}(\mathcal{A})$

of all full-dimensional positive cones spanned by the points in  $\mathcal{A}^*$  with apex in 0, together with the set  $R$  of all their facets. The *chamber complex*  $\tilde{\mathcal{C}}(\mathcal{A})$  of  $\mathcal{C}(\mathcal{A})$  is the union of all full-dimensional polyhedral cones whose facets are facets of cones in  $\mathcal{C}(\mathcal{A})$ , but whose relative interior is not crossed by any member of  $R$ . In our two-dimensional example, the set  $R$  consists of the six rays  $\text{cone}(b_i)$ ,  $1 \leq i \leq 6$ , so  $\tilde{\mathcal{C}}(\mathcal{A})$  is given by the following list of cones. See Figure 6.3 (left).

$$\tilde{\mathcal{C}}(\mathcal{A}) = \left\{ \text{cone}(b_1, b_6), \text{cone}(b_6, b_2), \text{cone}(b_2, b_4), \text{cone}(b_4, b_3), \text{cone}(b_3, b_5), \text{cone}(b_5, b_1) \right\}$$

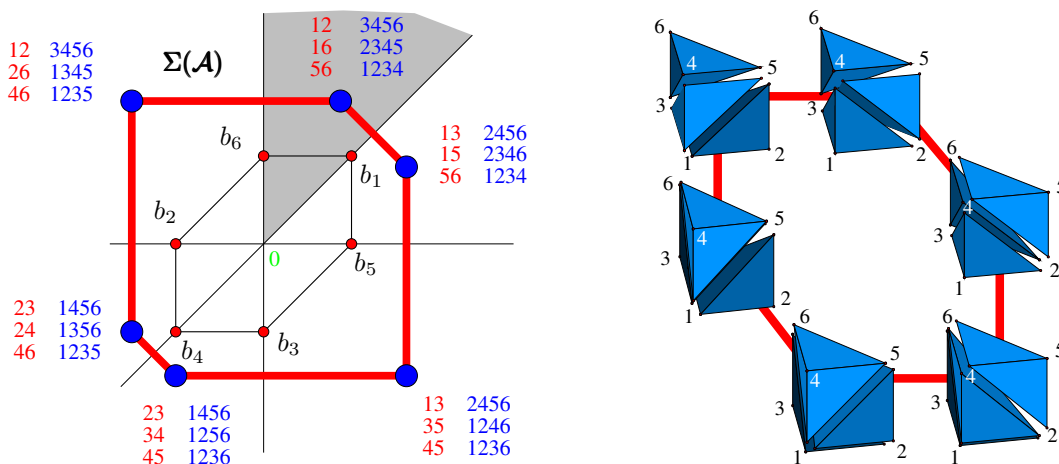


FIGURE 6.3: The hexagon as the secondary polytope of the prism  $P$ . *Left*: One maximal cone of the secondary fan is highlighted. Pairs of digits inside such a cone  $\sigma$  index vertices  $b_i$  in whose positive span  $\sigma$  lies, and the complementary 4-tuples label the simplices of the triangulation of  $\mathcal{A}$  that  $\sigma$  corresponds to. *Right*: Triangulations corresponding to vertices of  $\Sigma(P)$ . The edges of  $\Sigma(P)$  represent flips between triangulations.

We now consider each cone  $\sigma \in \tilde{\mathcal{C}}(\mathcal{A})$  in turn, and write down the generators of all cones in  $\mathcal{C}(\mathcal{A})$  that contain  $\sigma$ . For instance,  $\sigma = \text{cone}(b_1, b_6)$  lies in the cones  $\text{cone}(b_5, b_6)$ ,  $\text{cone}(b_1, b_6)$ , and  $\text{cone}(b_1, b_2)$  of  $\mathcal{C}(\mathcal{A})$ , and the *complements*  $\{1, 2, 3, 4\}$ ,  $\{2, 3, 4, 5\}$ , and  $\{3, 4, 5, 6\}$  of these index sets correspond precisely to a triangulation of  $P$ ! Since there are six maximal cones in  $\tilde{\mathcal{C}}(\mathcal{A})$ , we expect each one to correspond to one of the six regular triangulations of  $P$ .

In fact this is true, and even more: The set  $\tilde{\mathcal{C}}(\mathcal{A})$  is a *complete polyhedral fan*, which means that the cones in  $\tilde{\mathcal{C}}(\mathcal{A})$  intersect precisely in common faces, and together span all of  $\mathbb{R}^{n-d-1}$ . This fan is called the *secondary fan* of  $\mathcal{A}$ . It has the additional property that it is the *normal fan* of a certain polytope in  $\mathbb{R}^{n-d-1}$ , which says that the vectors contained in a fixed cone of  $\tilde{\mathcal{C}}(\mathcal{A})$  are just the normal vectors of hyperplanes supporting exactly one face of this polytope. It now comes as no surprise that one defines this polytope to be the *secondary polytope*  $\Sigma(\mathcal{A})$  of  $\mathcal{A}$ . Of course, this construction only determines  $\Sigma(\mathcal{A})$  up to

*normal equivalence*, i.e., any polytope with the same normal fan is also a secondary polytope of  $\mathcal{A}$ . In any case, passing from one maximal cone of  $\widetilde{\mathcal{C}}(\mathcal{A})$  to an adjacent one corresponds to going from one vertex of the secondary polytope to the next, and therefore to a flip between these triangulations. This is illustrated in Figure 6.3 (right). We summarize our discussion in the following theorem.

**Theorem 6.1** (Gel'fand, Kapranov, and Zelevinsky [28])

- (1) *The dimension of the secondary polytope  $\Sigma(\mathcal{A})$  of a full-dimensional configuration of  $n$  points in  $\mathbb{R}^d$  is  $n - d - 1$ .*
- (2) *The faces of  $\Sigma(\mathcal{A})$  correspond to the regular subdivisions of  $\mathcal{A}$ .*
- (3) *If  $F \subset G$  are faces of  $\Sigma(\mathcal{A})$ , then the subdivision of  $\mathcal{A}$  corresponding to  $F$  refines the subdivision corresponding to  $G$ . In particular, the vertices of  $\Sigma(\mathcal{A})$  encode the regular triangulations of  $\mathcal{A}$ .*

## 6.2 Hypergeometric Differential Equations

In this section, we briefly present the connection between secondary polytopes and certain systems of partial differential equations. This material is largely taken from [84].

To the matrix  $A$  from the preceding section we can associate the following ideal in the (commutative) polynomial ring of differential operators  $k[\partial] = k[\partial_1, \partial_2, \dots, \partial_n]$  with  $n = 6$ :

$$\begin{aligned} I_A &= \langle \partial^u - \partial^v : Au = Av, u, v \in \mathbb{N}^6 \rangle \\ &= \langle \partial_1 \partial_5 - \partial_2 \partial_4, \partial_1 \partial_6 - \partial_3 \partial_4, \partial_3 \partial_5 - \partial_2 \partial_6 \rangle, \end{aligned}$$

which corresponds to the system of differential equations

$$\begin{aligned} \frac{\partial^2}{\partial x_1 \partial x_5} f(x_1, x_2, \dots, x_6) &= \frac{\partial^2}{\partial x_2 \partial x_4} f(x_1, x_2, \dots, x_6), \\ \frac{\partial^2}{\partial x_1 \partial x_6} f(x_1, x_2, \dots, x_6) &= \frac{\partial^2}{\partial x_3 \partial x_4} f(x_1, x_2, \dots, x_6), \\ \frac{\partial^2}{\partial x_3 \partial x_5} f(x_1, x_2, \dots, x_6) &= \frac{\partial^2}{\partial x_2 \partial x_6} f(x_1, x_2, \dots, x_6) \end{aligned} \tag{6.2}$$

for a (formal) power series  $f$  in six variables. Notice how the differential operators that generate  $I_A$  correspond to elements of the kernel of  $A$ . The general theory developed in [84] tells us that a first step in constructing a series solution of (6.2) is to calculate the initial ideals  $\text{in}_\omega(I_A)$  for all term orders  $\prec_\omega$  on  $k[\partial]$  induced by weight vectors  $\omega \in \mathbb{Z}^n$ . The positive hull of the weight vectors that select a given initial ideal of  $I_A$  is a polyhedral cone in  $\mathbb{R}^n$ , and it is readily seen that the set of all such cones forms a polyhedral fan, the *Gröbner fan* of  $I_A$ . It is then also clear that the weight vectors in the *maximal* cones of the Gröbner fan

select *monomial* initial ideals, while those in lower-dimensional cones lead to initial ideals whose generators have more than one term.

Just as for the secondary fan, there exists an equivalence class of polytopes whose normal fan coincides with the Gröbner fan. Any representative from this class is called a *state polytope* [101, Chapter 2] of  $\mathcal{A}$ . By the preceding paragraph, the vertices of the state polytope exactly correspond to the monomial initial ideals of  $I_{\mathcal{A}}$ .

In general [101, Prop. 8.15], the Gröbner fan refines the secondary fan; an equivalent way of putting this is to say that the secondary polytope is a *Minkowski summand* of the state polytope. However, for a certain subclass of point configurations it is known that the Gröbner fan coincides with the secondary fan, and that therefore also the state polytope and the secondary polytope are the same (up to normal equivalence). These are the *unimodular* point configurations: those configurations *all* of whose triangulations are unimodular, i.e., entirely made up of simplices of unit volume (appropriately normalized for the dimension of the ambient space).

Therefore, for differential ideals coming from unimodular point configurations  $\mathcal{A}$ , we can calculate the Gröbner fan via geometrical techniques. We only need to enumerate all triangulations  $T$  of  $\mathcal{A}$ , and for each of them construct the following ideal, called the *Stanley-Reisner ideal* of  $T$ :

$$\left\langle \prod_{j \in J} \partial_j : J \text{ does not index a face of } T \right\rangle = \bigcap_{\sigma \in T} \langle \partial_j : j \notin \sigma \rangle \subset k[\partial].$$

By unraveling definitions, this is exactly the initial ideal of  $I_{\mathcal{A}}$  selected by any weight vector in the cone of the secondary fan which is dual to the vertex  $v_T$  of  $\Sigma(\mathcal{A})$ ; see Figure 6.4. Note that this initial ideal is square-free by construction.

If the point configuration is not unimodular, i.e., if it admits some triangulation with at least one simplex of non-unit volume, then as we saw above the Gröbner fan is a proper refinement of the secondary fan. The Stanley-Reisner ideal of such a triangulation  $T$  is then only the *radical* of the initial ideals selected by weight vectors in those Gröbner cones that refine the cone corresponding to  $T$ . However, knowing the number of regular triangulations of  $\mathcal{A}$  at least gives a lower bound for the number of monomial initial ideals of  $I_{\mathcal{A}}$ .

### 6.3 The GKZ vectors

The original construction of the secondary polytope—presented by Gelfand and Zelevinsky in 1989—was somewhat mysterious; as we will see, it gives rise to a straightforward recipe for calculating secondary polytopes, but it is not at all so straightforward to understand what is happening geometrically. In 1992, Billera and Sturmfels [9] finally presented secondary polytopes as the *fiber polytopes* of the projection of the  $(n - 1)$ -dimensional simplex to a configuration  $\mathcal{A}$  of  $n$  points. We will not develop this theory here, but instead refer the interested reader to [9], where also the formulation in terms of Gale transforms was first given, and especially to Chapter 9 of [103].

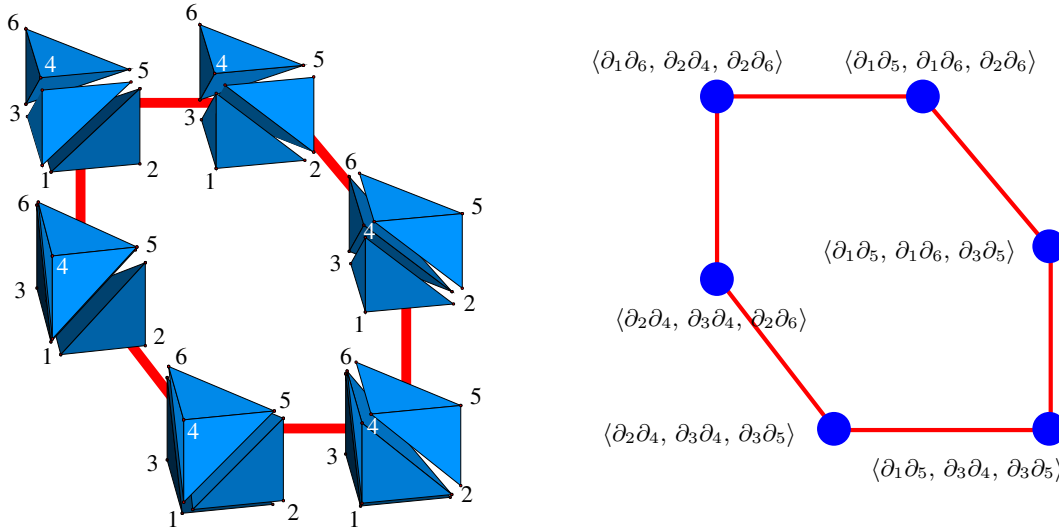


FIGURE 6.4: How to construct geometrically the six initial ideals of the unimodular ideal  $I_{\mathcal{A}} = \langle \partial_1 \partial_5 - \partial_2 \partial_4, \partial_1 \partial_6 - \partial_3 \partial_4, \partial_3 \partial_5 - \partial_2 \partial_6 \rangle$ : The generators of each initial ideal are precisely the minimal non-faces of the corresponding regular triangulation of  $\mathcal{A}$ .

The GKZ construction proceeds as follows. We associate an  $n$ -dimensional vector  $v_T$  to any given triangulation  $T$  of  $\mathcal{A}$ , in such a way that the  $i$ -th coordinate of  $v_T$  is the sum of the volumes of all simplices in  $T$  incident to the point  $i$ .

$$(v_T)_i = \sum_{\sigma: \sigma \in T, i \in \sigma} \text{vol conv } \sigma$$

This gives us one  $n$ -dimensional vector for each triangulation of  $\mathcal{A}$ . The *secondary polytope*  $\Sigma(\mathcal{A}) \subset \mathbb{R}^n$  of  $\mathcal{A}$  is then defined as the convex hull of all such vectors obtained by considering every possible triangulation of  $\mathcal{A}$ .

$$\Sigma(\mathcal{A}) = \text{conv} \{v_T : T \text{ triangulation of } \mathcal{A}\}$$

It turns out that the secondary polytope defined in this way is not full-dimensional, but resides in an  $(n - d - 1)$ -dimensional subspace. However, the fact that this polytope coincides, up to scaling and normal equivalence, with the secondary polytope as defined earlier definitely comes as a surprise!

## 6.4 Implementation: How to find the face lattice of the secondary

We briefly describe our approach to calculate an embedding and the face lattice of the secondary polytope of a point configuration in  $\mathbb{R}^d$ . We are not claiming that this is a particularly efficient strategy!

First, we calculate a placing triangulation  $\mathcal{T}$  of  $\mathcal{A}$  (which is known to be regular), and generate the connected component of the flip graph that contains  $\mathcal{T}$ . Since flips correspond to edges of the secondary polytope, and the 1-skeleton of any convex polytope of dimension at least 2 is connected, we know that this component contains at least all regular triangulations of  $\mathcal{A}$ —possibly along with some non-regular ones.

Next, we embed the nodes of the flip graph in  $\mathbb{R}^n$  via their GKZ coordinates, project the resulting point configuration to  $\mathbb{R}^{n-d-1}$ , and calculate (the vertex-facet incidence matrix of) the convex hull of the result. Because we now have an embedding of the regular component of the flip graph, we can investigate, for example, the *flip distance* of a non-regular triangulation to the nearest regular one. Of course, this procedure misses all connected components of the flip graph that do not contain any regular triangulation.

We implemented this procedure using the POLYMAKE rule base and client programs to convert between the data structures of TOPCOM and POLYMAKE. To calculate the secondary polytope of a configuration  $\mathcal{A}$  of  $n$  points in  $\mathbb{R}^d$ , the POLYMAKE client requests from TOPCOM a list of all triangulations of  $\mathcal{A}$ , and for each one calculates the coordinates of its GKZ embedding in  $\mathbb{R}^n$ . Next, the client asks for these points to be projected to  $\mathbb{R}^{n-d-1}$ , and then to calculate the convex hull of these projected points. These requests are all answered by the POLYMAKE server, which in turn calls the appropriate clients for each task as specified in the rule base. Finally, the `secondary` client outputs the flip graph of  $\mathcal{A}$  both with its embedding and as an abstract (`.gml`)-graph, and marks points corresponding to non-regular triangulations. If dimension permits, this embedded flip graph can then be visualized, e.g. with *Javaview* [76].

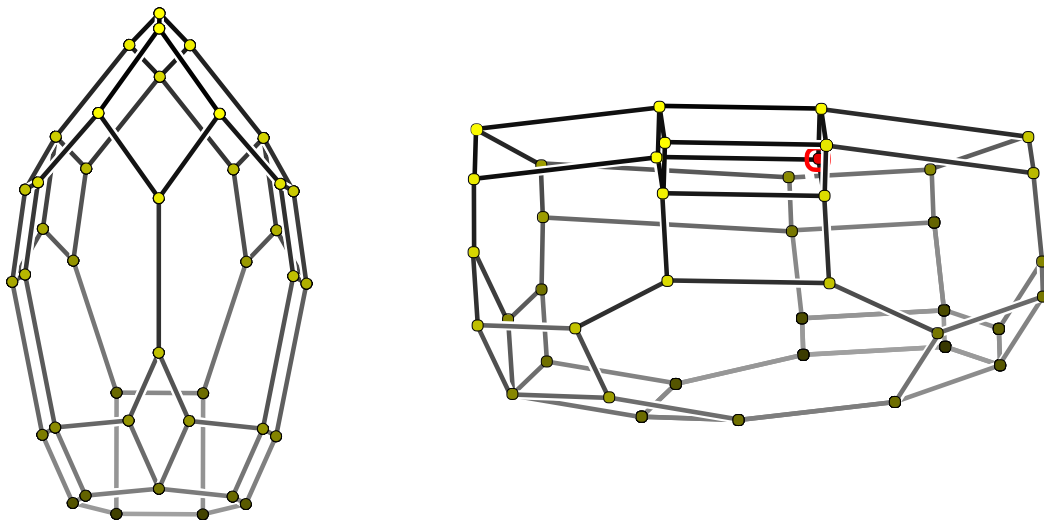


FIGURE 6.5: *Left*: Secondary polytope of the cyclic 4-polytope with 8 vertices. All 40 triangulations are regular. *Right*: Secondary of a different neighborly 4-polytope with 8 vertices [31, Ch. 7], which has one nonregular triangulation (circled; in the interior of the convex hull) among 41.



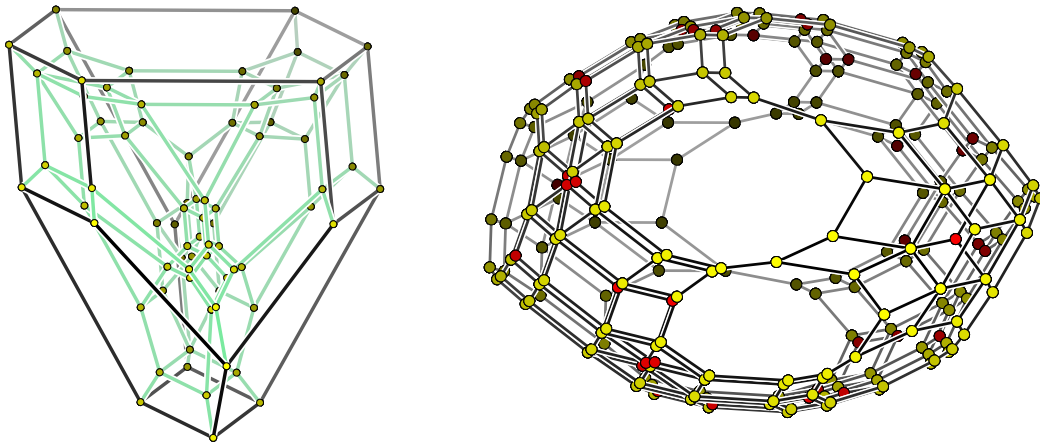


FIGURE 6.6: *Left*: Schlegel diagram of the secondary polytope of the 3-cube [73]. All 74 triangulations are regular. *Right*: Secondary of the cyclic 8-polytope with 12 vertices, realized on the Carathéodory curve [72]. There are 42 nonregular triangulations among 244 in all. Note that this polytope is not a zonotope, since it has facets with an odd number of vertices.

In Figures 6.5 and 6.6, we present the results of four such calls to **secondary**. All running times, excluding the computation of the convex hull, remained well under one minute on a Sun Blade. The bottleneck is calculating the convex hull: The longest such computation with **cdd** [25] for the secondary of the cyclic 8-polytope with 12 vertices realized on the Carathéodory curve took 2 minutes.

With a view towards future developments, we remark that the computation of the entire vertex-facet incidence matrix of the secondary polytope seems wasteful if all one is interested in is the information which edges of the embedded flip graph actually lie on the convex hull of the secondary polytope. Moreover, while TOPCOM is fine-tuned to exploit symmetries of a point configuration, at this moment there is no convex hull code available that could do likewise. However, implementing an algorithm that simultaneously inserts all points of an orbit under a given symmetry group may well prove to be a non-trivial task. In the future, perhaps it will be possible to exploit the fact that TOPCOM not only provides a list of points corresponding to triangulations, but in fact a connected component of the flip-graph that includes the entire 1-skeleton of the polytope.

Let us note that there have been other approaches to computing the edge graph of the secondary polytope by reverse search [61]. Unfortunately, we do not have access to any code based on these algorithms. If memory limitations dominate then reverse search is certainly the method of choice.

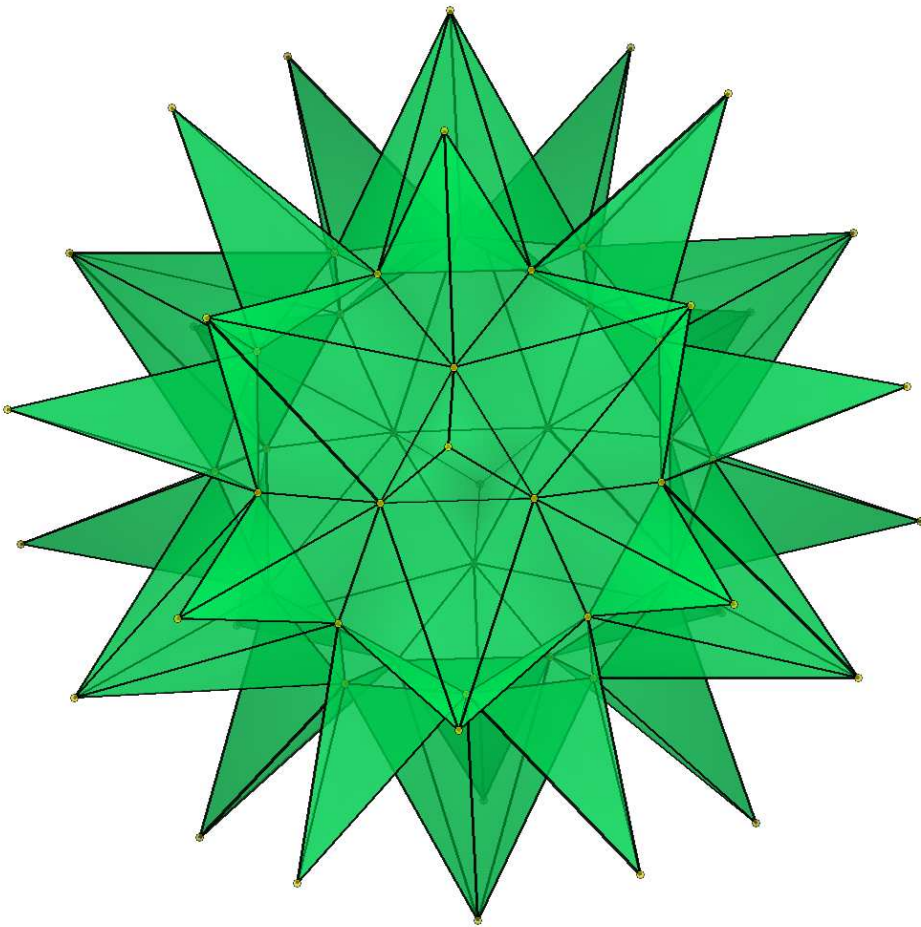






## Part II

# Spheres





## Chapter 7

# Overview

### 7.1 Many triangulated 3-spheres

Chapters 8 and 9 of this thesis focus on convex realizability of simplicial spheres. In general, we expect that a ‘generic’ pure  $d$ -dimensional simplicial complex will be ‘too complicated’ to permit a convex embedding in  $\mathbb{R}^{d+1}$ , but the question gains interest if we only consider ‘nice’ complexes such as simplicial spheres.

Nonrealizability of spheres can happen from dimension 3 onward: 1-dimensional spheres are trivial to realize, and Steinitz’ famous theorem [97], [98] from the beginning of the 20th century asserts that *all* 2-spheres, including the non-simplicial ones, are polytopal (i.e., they arise as boundary complexes of 3-dimensional polytopes). However, it is well known that this is not at all the case in higher dimensions.

The first example—the so-called *Brückner sphere*—of a 3-dimensional simplicial sphere that is *not* the boundary complex of any 4-polytope was inadvertently found by Brückner [13] in 1910 in an attempt to enumerate all combinatorial types of 4-polytopes with 8 facets. As noted in 1967 by Grünbaum and Sreedharan [32], one of the complexes that Brückner thought to represent a polytope is in fact *not* realizable in a convex way in  $\mathbb{R}^4$ . As the (polytopal) complex Brückner considered (cf. Chapter 2) is simple (any vertex is contained in exactly 4 facets), its combinatorial dual is a simplicial 3-sphere. Incidentally, in their new enumeration Grünbaum and Sreedharan also discovered the first examples of polytopes that are neighborly but not cyclic; this phenomenon was important in Chapter 5.

Another known ‘sporadic’ example of a non-polytopal simplicial sphere is *Barnette’s sphere* [4], which is nicely explained in [24, Chapter III.4]. From these two examples one can build infinite series, but apart from such sporadic families, no substantial number of non-polytopal spheres on a fixed number of vertices was known until 1988.

In that year, Kalai [44] adapted a construction by Billera and Lee [8] to show that for  $d \geq 4$ , there exist *far* more simplicial  $d$ -spheres than simplicial  $(d+1)$ -polytopes on  $n$  vertices. (Asymptotically optimal upper bounds for the number of such polytopes had been derived in 1986 by Goodman and Pollack [29], [30].) This proves that in a very strong sense, *most* simplicial spheres are not realizable. However, Kalai’s argument is by sheer number: given any concrete  $d$ -sphere his construction produces, we have (as yet) no way of telling whether it is actually polytopal or not.

Since Billera and Lee’s idea underlies Kalai’s construction and will also be important for our purposes, we briefly digress to present its context.

### 7.1.1 The $g$ -Theorem

In 1971, McMullen [64] boldly conjectured a characterization of the  $f$ -vectors of  $d$ -dimensional simplicial spheres  $\mathcal{S}$  arising as boundary complexes of  $(d+1)$ -dimensional simplicial polytopes in terms of the so-called  $g$ -vector of  $\mathcal{S}$ . To understand this encoding, first define the  $h$ -vector  $h(\mathcal{S}) = (h_0, h_1, \dots, h_{d+1})$  of  $\mathcal{S}$  by

$$h_k = \sum_{i=0}^k (-1)^{k-i} \binom{d+1-i}{d+1-k} f_{i-1}, \quad \text{for } k = 0, 1, \dots, d+1.$$

The  $h$ -vector of any simplicial sphere satisfies the *Dehn-Sommerville equations*  $h_k = h_{d+1-k}$  for  $k = 0, 1, \dots, \lfloor d/2 \rfloor$ . Now the  $g$ -vector of  $\mathcal{S}$  is  $g(\mathcal{S}) = (g_0, g_1, \dots, g_{\lfloor (d+1)/2 \rfloor})$ , where  $g_0 := h_0 = 1$  and  $g_k := h_k - h_{k-1}$  for  $k = 1, 2, \dots, \lfloor (d+1)/2 \rfloor$ . We say that  $g(\mathcal{S})$  forms an  $M$ -sequence if  $g_0 = 1$  and  $g_{k-1} \geq \partial^k(g_k)$  for  $k = 1, \dots, \lfloor (d+1)/2 \rfloor$ , where

$$\partial^k(g_k) = \binom{a_k - 1}{k-1} + \binom{a_{k-1} - 1}{k-2} + \dots + \binom{a_2 - 1}{1} + \binom{a_1 - 1}{0},$$

and the integers  $a_k > a_{k-1} > \dots > a_2 > a_1 \geq 0$  are determined by the *binomial expansion*

$$g_k - 1 = \binom{a_k}{k} + \binom{a_{k-1}}{k-1} + \dots + \binom{a_2}{2} + \binom{a_1}{1}$$

of  $g_k - 1$  with respect to  $k$ . See [103, Chapter 8] for more details. We can now state McMullen's conjecture [64]:

**Theorem** ( $g$ -Conjecture/Theorem) [64, 95, 8] *An integer vector  $g = (g_0, g_1, \dots, g_{\lfloor (d+1)/2 \rfloor})$  is the  $g$ -vector of the boundary complex of a simplicial  $(d+1)$ -dimensional polytope  $P$  if and only if it is an  $M$ -sequence.*

In the same year, 1979, Stanley [95] proved the necessity and Billera and Lee [8] the sufficiency of McMullen's conditions. Stanley's proof that the  $g$ -vector of any simplicial polytope is an  $M$ -sequence used the Hard Lefschetz Theorem for the cohomology of projective toric varieties, but in the meantime a simpler proof by McMullen using his *polytope algebra* [65, 66] is available.

Billera and Lee invented an ingenious construction to produce, for every  $M$ -sequence  $g$ , a simplicial  $d$ -polytope with this  $g$ -vector. Very briefly, they first find a shellable ball  $B$  as a collection of facets of a cyclic polytope  $C$ , such that the  $g$ -vector of  $\partial B$  is the given  $M$ -sequence. Then they construct a realization of  $C$  and a point  $z$  that sees exactly the facets in  $B$ , and obtain a realization of  $\partial B$  as a simplicial polytope by taking the vertex figure at  $z$  of  $\text{conv}(\{z\} \cup C)$ ; see Figure 7.1.

### 7.1.2 Many triangulated $d$ -spheres

Next, we outline Kalai's 1988 extension of Billera and Lee's construction, by which he built so many simplicial spheres that *most* of them (in a sense to be made precise below) fail to be polytopal.



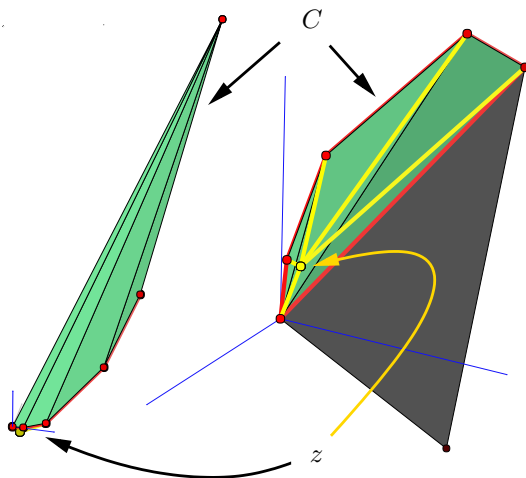


FIGURE 7.1: Billera and Lee's construction [8] in the case of a 3-dimensional cyclic polytope  $C = C_3(6)$  on 6 vertices.  $C$  is realized on the moment curve (with one vertex in the origin) and seen from two different viewpoints, together with the coordinate axes, an 'observation' point  $z$  and the facets of  $C$  that  $z$  sees.

Kalai built “many triangulated  $d$ -spheres” [44] by giving a rule to produce many lists  $I$  of  $(d + 2)$ -tuples of vertices, which span pure simplicial complexes  $B(I)$ . The underlying space of every such complex turns out to be a simplicial, shellable  $(d + 1)$ -ball, which he called a *squeezed ball*, and therefore the boundary  $S(I)$  of  $B(I)$  is a simplicial PL  $d$ -sphere, a *squeezed sphere*. (It was shown by Lee [58] that Kalai's squeezed spheres are shellable.)

To see what Kalai's construction implies about the relative number of simplicial spheres vs. simplicial polytopes, let  $s(d, n)$  denote the number of simplicial  $d$ -spheres,  $sq(d, n)$  the number of squeezed  $d$ -spheres, and  $c(d, n)$  the number of combinatorial types of simplicial  $d$ -polytopes with  $n$  labeled vertices. In 1987, Goodman and Pollack [29, 30] derived the upper bound

$$\log c(d, n) \leq d(d + 1)n \log n \quad (7.1)$$

using a theorem of Milnor that bounds the sum of the Betti numbers of real algebraic varieties. Note that in 1982, Shemer [91] had already constructed  $2^{\Omega(n \log n)}$  *neighborly*  $d$ -polytopes for fixed  $d \geq 4$ .

In contrast, Kalai's squeezed spheres provide the following lower bound for  $s(d, n)$ :

$$\begin{aligned} \log s(d, n) \geq \log sq(d, n) &\geq \frac{1}{(n - d - 1)(d + 2)} \binom{n - \lfloor (d + 1)/2 \rfloor - 1}{\lfloor d/2 \rfloor + 1} \\ &= \Omega(n^{\lfloor d/2 \rfloor}) \quad \text{for fixed } d. \end{aligned}$$

These bounds reveal that  $\lim_{n \rightarrow \infty} c(d + 1, n)/sq(d, n) = 0$  for  $d \geq 4$ , which means that for  $d \geq 4$  *most* of Kalai's  $d$ -spheres are not polytopal—there are simply too many of them!

- Remark 7.1** (1) For  $d \geq 4$ , we cannot (yet) make any assertion about the polytopality of any concrete  $d$ -sphere of Kalai's family.
- (2) Up to now, we have learned nothing for  $d \leq 3$ : We will prove in Proposition 8.3 that  $sq(3, n) \leq 2^{n-5}n!$  for  $n \geq 5$ , which by (7.1) is strictly less than the upper bound for  $c(4, n)$  for all  $n \geq 5$ . That in fact the number of simplicial 3-spheres *is* far greater than the number of 4-polytopes is the content of Chapter 9 of this thesis.

## 7.2 New results in this thesis

In dimension 3, Kalai's construction is not as successful as in higher dimensions: We prove in Theorem 8.1 that all of his 3-spheres *do* arise as boundary complexes of simplicial 4-polytopes. As an added bonus, we use the insight gained to provide a shorter proof (Theorem 8.8 in Section 8.5) for Hebble and Lee's result [35] that Kalai's 3-spheres are Hamiltonian, i.e. their dual skeleton admits a Hamiltonian path. These results were published in [74].

In Chapter 9, we put together a venerable construction from the dawn of topology by Heffter [36] from 1898 with a modern idea of Eppstein [22] from 2002, and finally prove in Theorem 9.1 that on sufficiently many vertices, there *do* exist far more triangulated 3-spheres than simplicial 4-polytopes. This is joint work with Günter M. Ziegler.

Finally, we prove in Theorem 10.1 of Chapter 10 that there exist no *neighborly centrally symmetric star-shaped simplicial  $d$ -spheres* with  $2d + 4$  vertices, for even  $d \geq 4$  and odd  $d \geq 11$ . See Chapters 1 and 10 for more details.

## 7.3 Open problems

**Question 7.2** Can the method used in Theorem 8.1 to prove the polytopality of Kalai's 3-spheres be extended to prove the polytopality of a 'substantial number' of his  $d$ -spheres, for  $d \geq 4$ ?

**Question 7.3** Can one prove directly the non-polytopality of the 'many triangulated 3-spheres' arising from Heffter's and Eppstein's constructions? Is it true that 'many' of them are not shellable?

**Question 7.4** Do there exist neighborly centrally symmetric star-shaped simplicial  $d$ -spheres with  $2d + 4$  vertices for  $d = 5, 7, 9$ ? These are the cases left open in Theorem 10.1.





## Chapter 8

# Kalai's squeezed 3-spheres are polytopal

This chapter is devoted to proving that all 3-spheres arising from Kalai's construction can be realized as polytopes. We first introduce some notation; for the poset terminology, cf. [96].

Define a partial order  $\preceq$  on  $\binom{[n]}{d+2}$  by  $\{i_1, i_2, \dots, i_{d+2}\} < \preceq \{j_1, j_2, \dots, j_{d+2}\}$  if  $i_k \leq j_k$  for every  $k = 1, \dots, d+2$ . Here the notation  $A = \{a_1, \dots, a_r\} <$  means that the elements of the set  $A$  are listed in increasing order.

For an even integer  $d \geq 0$  and  $n \in \mathbb{N}$ , let  $\mathcal{F}_d(n)$  be the collection of  $(d+2)$ -subsets of  $[n] := \{1, 2, \dots, n\}$  of the form  $\{i_1, i_1+1\} \cup \{i_2, i_2+1\} \cup \dots \cup \{i_e, i_e+1\}$ , where  $e = (d+2)/2$ ,  $i_1 \geq 1$ ,  $i_e < n$ , and  $i_{j+1} \geq i_j + 2$  for all relevant  $j$ . Let  $I'$  be an initial set (order ideal) of  $\mathcal{F}_d(n)$  with respect to the partial order  $\preceq$  on  $\binom{[n]}{d+2}$ . Informally,  $f' \preceq g'$  for  $f', g' \in \mathcal{F}_d(n)$  if  $f'$  arises from  $g'$  by pushing some elements in  $g'$  to the left. For odd  $d \geq 1$ , put  $\mathcal{F}_d(n) = \{\{0\} \cup f' : f' \in \mathcal{F}_{d-1}(n)\} =: 0 * \mathcal{F}_{d-1}(n)$  with the induced partial order, and set  $I := 0 * I'$ . (Our notation differs from that in [44], but it is consistent with Chapter 9.)

Finally, let  $B(I)$  resp.  $B(I')$  denote the simplicial complex *spanned* by  $I$  resp.  $I'$  (i.e., given by the sets in  $I$  resp.  $I'$  and their subsets), and denote the boundaries of these complexes by  $S(I)$  resp.  $S(I')$ . By [44],  $B(I)$  resp.  $B(I')$  are shellable  $(d+1)$ -dimensional balls (Kalai calls them *squeezed  $(d+1)$ -balls*), and therefore  $S(I)$  resp.  $S(I')$  are simplicial PL  $d$ -spheres (*squeezed  $d$ -spheres*). We can now state the main theorem of this chapter:

**Theorem 8.1** (Squeezed 3-spheres are polytopal) [74] *Every squeezed 3-sphere  $S(I)$  given by an order ideal  $I$  in the poset  $(\mathcal{F}_3(n), \preceq)$  with  $n \geq \max \bigcup I$  can be realized as the boundary complex of a simplicial convex 4-polytope.*

**Remark 8.2** The construction shows the stronger result that every squeezed 4-ball  $B(I)$  can be realized as a regular triangulation of a convex 4-polytope.

We first collect some facts about Kalai's 3-spheres and *cyclic polytopes*, an essential ingredient of our proof. After proving Theorem 8.1 in Section 8.4, we use the pictures made along the way to give a shorter proof of Hebble and Lee's result [35] that the dual graphs of squeezed 3-spheres are Hamiltonian.

## 8.1 Kalai's 3-spheres

To specialize Kalai's construction to  $d = 3$ , we first study squeezed 3-balls. Take  $n \geq 4$  in  $\mathbb{N}$ , write  $(i, j)$  for an element  $\{i, i+1, j, j+1\} \subset [n]$  of  $\mathcal{F}_2(n)$ , and define the *gap* of  $(i, j) \in \mathcal{F}_2(n)$  to be the number  $j - i - 2$  of integers between  $i+1$  and  $j$ . From the fact

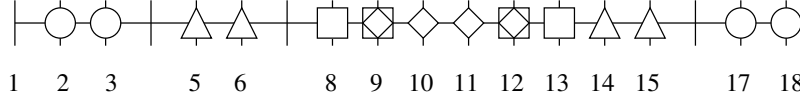
that any two elements of  $\mathcal{F}_2(n)$  with the same gap are translates of each other and therefore comparable with respect to the partial order  $\preceq$ , we conclude that any  $\preceq$ -antichain in  $\mathcal{F}_2(n)$  can be linearly ordered by increasing gap, and denote this order by  $\sqsubset$ . We remark that the difference between the gaps of any two elements in a  $\preceq$ -antichain must be at least 2, as otherwise the two elements would be  $\preceq$ -comparable. In particular, the maximal number of elements of a  $\preceq$ -antichain in  $\mathcal{F}_2(n)$  is  $\lceil (n-3)/2 \rceil$ .

Any order ideal  $I' \subset \mathcal{F}_2(n)$  for  $n \in \mathbb{N}$  is generated by the set  $G' = \{g'_1, g'_2, \dots, g'_r\}_{\sqsubset}$  of its maximal elements, for some  $r \leq \lceil (n-3)/2 \rceil$ . By our discussion, the  $g'_k = (i_k, j_k)$  satisfy

- (1)  $j_k \geq i_k + 2$  for  $k = 1, \dots, r$ , and
- (2)  $i_k > i_{k+1}$  and  $j_k < j_{k+1}$  for  $k = 1, \dots, r-1$ .

As an example, let  $I'$  be the ideal generated by

$$G' = \{(9, 11), (8, 12), (5, 14), (2, 17)\}_{\sqsubset} :$$



Note that if  $g' \sqsubset h' \in G'$ , then  $g'$  is nested inside  $h'$  (possibly with overlap). From Figure 8.1 below, we will read off the structure of the 3-ball  $B(I')$  generated by  $G'$ , and its boundary  $S(I')$ .

Now put  $\mathcal{F}_3(n) = 0 * \mathcal{F}_2(n)$  with the induced partial order, and  $I = 0 * I'$ . The 4-ball  $B(I)$  spanned by  $I$  is a cone over the 3-ball  $B(I')$ , whose boundary complex is the squeezed 3-sphere  $S(I)$ .

**Proposition 8.3** There are at most  $2^{n-4}(n+1)!$  squeezed 3-spheres with  $n+1 \geq 5$  labeled vertices. In particular,  $\log sq(4, n) = \Theta(n \log n)$ .

*Proof.* By [44, Proposition 3.3], distinct 4-balls  $B(I)$  whose vertices are labeled according to their construction give rise to distinct 3-spheres  $S(I)$  labeled in this way, and distinct initial sets  $I \subset \mathcal{F}_3(n)$  obviously induce distinct such 4-balls. Every initial set  $I$  is of the form  $0 * I'$  for a unique order ideal  $I' \subset \mathcal{F}_2(n)$ . Therefore, by relabeling vertices,  $sq(4, n+1)$  is at most  $(n+1)!$  times the number of distinct order ideals in  $\mathcal{F}_2(n)$ , depending on the combinatorial symmetries of  $S(I)$ . By Figure 8.1, every such order ideal can be represented by a lattice path of length  $n-4$  taking steps only in the positive  $i$ - or negative  $j$ -directions, and starting at  $(i, j) = (1, n-1)$ . There are  $2^{n-4}$  of these, and they all give rise to distinct ideals.  $\square$

## 8.2 Interlude: Some facts on cyclic polytopes

The convex hull of  $n$  distinct points on the image of the *moment curve*  $\mu_d : t \mapsto (t, t^2, \dots, t^d)$  in  $\mathbb{R}^d$  is called a  $d$ -dimensional *cyclic polytope* with  $n$  vertices. The combinatorial type of this polytope is independent of the choice of the  $n$  points on  $\mu_d$  [103, Chapter 0], and so one can talk about *the* cyclic polytope  $C_d(n)$ . In fact, any  $d$ -dimensional order  $d$  curve also gives rise to the same combinatorial types of polytopes [100].



In the following, we switch from  $d$  and  $n$  to  $d+1$  and  $n+1$ . Consider a set  $X = \{x_0 = \mu(t_0), \dots, x_n = \mu(t_n)\}$  of  $n+1$  distinct points on the moment curve  $\mu_{d+1} =: \mu$ , ordered by their first coordinates. For any  $f \subset \{0, 1, \dots, n\}$ , write  $F_f$  for the subset of  $X$  indexed by  $f$ , and  $i(F)$  for the indices of a subset  $F$  of  $X$ . The supporting hyperplane  $H(F)$  of a  $(d+1)$ -subset  $F \subset X$  is given by  $H(F) = \{x \in \mathbb{R}^{d+1} : \gamma(F) \cdot x = -\gamma_0(F)\}$ , where  $\gamma(F) = (\gamma_1(F), \dots, \gamma_{d+1}(F)) \in \mathbb{R}^{d+1}$  and  $\gamma_0(F) \in \mathbb{R}$  are defined by

$$0 = \prod_{i \in i(F)} (t - t_i) = \sum_{j=0}^{d+1} \gamma_j(F) t^j = \gamma_0(F) + \gamma(F) \cdot \mu(t). \quad (8.1)$$

Observe that  $\gamma_{d+1}(F) = 1$ ; we say that  $\gamma(F)$  *points upwards*.

Gale's *evenness criterion* [26], [103, Chapter 0] tells us which  $(d+1)$ -subsets  $F$  of  $X$  are vertex sets of facets of the cyclic polytope  $C = \text{conv}(X)$ : For any  $i, j \in \{0, 1, \dots, n\} \setminus i(F)$ , the number of elements of  $i(F)$  between  $i$  and  $j$  must be even.

We also need to know whether a given facet  $F$  of a cyclic polytope whose vertices lie on a moment curve is an “upper” or “lower” facet with respect to the “up” direction given by the positive coordinate axis  $e_{d+1}$ . For this, we define the *end set*  $W_{\text{end}}$  of  $F_f \subset X$  as the right-most contiguous block  $\{r_f + 1, \dots, \max f\}$  of the indices  $f$  of  $F$ , where we have used the notation  $r_f = \max\{i \in \mathbb{N} : i < \max f, i \notin f\}$ . Let  $F$  be a facet of  $C$  and take  $x_j = \mu(t_j) \in X \setminus F$ . If the cardinality of the end set of  $F$  is odd, we get  $\prod_{i \in i(F)} (t_j - t_i) < 0$  because  $j \notin i(F)$ , and therefore  $\gamma(F) \cdot x_j < -\gamma_0(F)$ . Since  $\gamma_{d+1}(F) = 1$ , we conclude that the whole cyclic polytope  $C$  is *below*  $F$ , and call  $F$  an *upper facet* of  $C$ . If  $\#W_{\text{end}}$  is even, we analogously call  $F$  a *lower facet* of  $C$ . Finally, we define the *outer normal vector*  $\alpha(F)$  of a facet  $F$  of  $C$  to be  $\alpha(F) = \gamma(F)$  resp.  $\alpha(F) = -\gamma(F)$  if  $F$  is an upper resp. lower facet of  $C$ , and set  $\alpha_0(F) = -\gamma_0(F)$  resp.  $\alpha_0(F) = \gamma_0(F)$ . In this way, we obtain  $C \subset \{x \in \mathbb{R}^{d+1} : \alpha(F) \cdot x \leq \alpha_0(F)\}$  for all facets  $F$  of  $C$ .

### 8.3 A bird's-eye view of the realization construction

By Gale's Evenness Criterion, every  $f \in I$  indexes a lower facet  $F_f$  of a cyclic polytope. Adapting the ideas of Billera and Lee, we will realize any  $S(I)$  as boundary complex of a 4-dimensional polytope  $P$  by appropriately realizing a cyclic 5-polytope  $C$ , and choosing a viewpoint  $v$  close to the negative  $e_5$ -axis that sees exactly the facets of  $C$  in  $B(I)$ . The convex 4-polytope  $P$  is then the vertex figure at  $v$  of  $\text{conv}(C \cup \{v\})$ , and  $S(I)$  its boundary.

Specifically, let  $\mu = \mu_5 : \mathbb{R} \rightarrow \mathbb{R}^5$ ,  $t \mapsto (t, t^2, \dots, t^5)$  be the moment curve in dimension 5. Given an order ideal  $I = 0 * I'$  in  $\mathcal{F}_3(n)$  where  $n = \max \bigcup I$ , we execute the following steps:

- (1) Choose  $N' > 0$  and place  $0 = t_0 < t_1 < \dots < t_n \in \mathbb{R}_{\geq 0}$  such that

$$\begin{aligned} \prod_{i \in f \setminus \{0\}} t_i &< N' \quad \text{for all } f \in I, \quad \text{and} \\ \prod_{i \in f \setminus \{0\}} t_i &> N' \quad \text{for all } f \in \mathcal{F}_3(n) \setminus I. \end{aligned} \quad (S1)$$



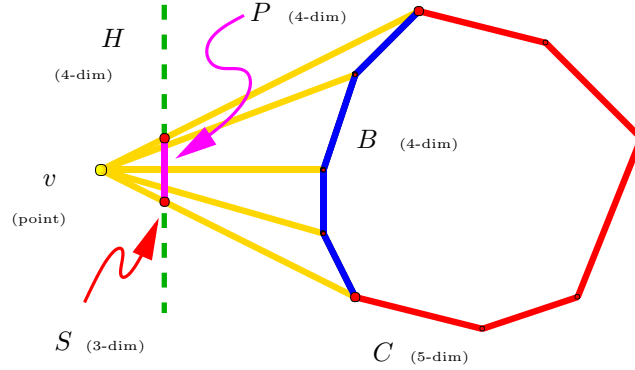


FIGURE 8.2: We first find the simplicial complex underlying each Kalai sphere as the boundary of a shellable 4-ball in the boundary of a 5-dimensional cyclic polytope  $C$ , and obtain a convex realization by intersecting the cone over this 4-ball with a hyperplane.

Solutions of (S1) exist with  $t_1 > 0$  arbitrarily small. We will find one by processing the elements of  $E' = G' \cup H'$  in  $\sqsubset$ -order, where  $G'$  is the set of  $\preceq$ -maximal elements of  $I'$ , and  $H'$  is the set of  $\preceq$ -minimal elements of  $\mathcal{F}_2(n) \setminus I'$ .

- (2) Make sure that the viewpoint to be defined will not see any upper facets of  $C = C_5(n+1) = \text{conv}\{0, \mu(t_1), \mu(t_2), \dots, \mu(t_n)\}$  that contain 0, by choosing  $t_1 > 0$  so small that

$$t_1 t_{n-2} t_{n-1} t_n < N'. \quad (\text{S2})$$

- (3) Choose  $\varepsilon$ , with  $0 < \varepsilon < t_1$ , so small that for all  $e, f \in \mathcal{F}_3(n)$ ,

$$e \prec f \implies \gamma(F_e) \cdot \mu(\varepsilon) < \gamma(F_f) \cdot \mu(\varepsilon). \quad (\text{S3})$$

- (4) Choose  $\varepsilon > 0$  even smaller, if necessary, such that the viewpoint  $v := \mu(\varepsilon) - \varepsilon N' e_5$  satisfies

$$\begin{aligned} \alpha(F) \cdot v &> \alpha_0(F) && \text{for } f_F \in I, \\ \alpha(F) \cdot v &< \alpha_0(F) && \text{for all lower facets } F \text{ of } C \text{ s.t. } f_F \notin I, \\ \alpha(F) \cdot v &< \alpha_0(F) && \text{for all upper facets } F \text{ of } C, \end{aligned} \quad (\text{S4})$$

where  $\alpha(F)$  is the outer normal vector of  $F$  we defined at the end of Section 8.2.

We conclude that  $v$  sees exactly the facets of  $C$  in  $B(I)$ , and obtain  $S(I)$  as above.

## 8.4 How to realize Kalai's 3-spheres

We now give the details of the construction and prove Theorem 8.1.

Given an ideal  $I \subset \mathcal{F}_3(n)$ , we may assume that  $n = \max \bigcup I$  since  $\mathcal{F}_3(n) \subseteq \mathcal{F}_3(n')$  for all  $n \leq n'$ . Moreover, by definition every order ideal  $I \subset \mathcal{F}_3(n)$  is of the form  $I = 0 * I'$ ,

where  $I' = \langle G' \rangle \subset \mathcal{F}_2(n)$  is generated by its maximal elements  $G' = \{g'_1, g'_2, \dots, g'_r\}$  with  $g'_k = (i_k, j_k)$ . Choose  $N' > 0$ , introduce  $n$  variable points  $0 < t_1 < t_2 < \dots < t_n$  in  $\mathbb{R}_{>0}$ , and consider the set  $H'$  of  $\preceq$ -minimal elements of  $\mathcal{F}_2(n) \setminus I'$ .

**Observation 8.4** Consider any two consecutive elements  $e' = (i, j) \sqsubset f' = (k, \ell)$  of a  $\sqsubset$ -ordered  $\preceq$ -antichain  $G'$  of  $\mathcal{F}_2(n)$ . Then the unique  $\prec$ -minimal element  $m'$  in  $\mathcal{F}_2(n) \setminus \langle G' \rangle$  with  $\text{gap}(e') < \text{gap}(m') < \text{gap}(f')$  exists and is  $m' = (k+1, j+1)$ . In particular, the number of  $\prec$ -minimal elements in  $\mathcal{F}_2(n) \setminus \langle G' \rangle$  is no greater than  $\lfloor (n-3)/2 \rfloor$ .  $\square$

*Sketch of proof.* The first statement follows from Figure 8.1. For the second assertion, note that the set  $H'$  has maximal cardinality if  $G' = \{(i, n-i) : i = 1, 2, \dots, \lfloor (n-3)/2 \rfloor\}$ .  $\square$

Using Observation 8.4, we linearly order  $E' = G' \cup H'$  by  $\sqsubset$ , see Figure 8.1. To carry out Step 1, first choose some small  $\delta > 0$ . Our goal is to place the  $t$ 's in  $\mathbb{R}_{>0}$  such that

$$\prod_{i \in g'} t_i = N' - \delta \quad \text{for } g' \in G' \quad \text{and} \quad \prod_{i \in h'} t_i = N' + \delta \quad \text{for } h' \in H'. \quad (\text{S1}')$$

**Observation 8.5** The cardinality of  $E' = G' \cup H'$  is at most  $n-3$ . In particular, there are fewer equalities in (S1') than there are variables.

*Proof.* Because  $n = \max \bigcup I$ , the largest element of  $(E', \sqsubset)$  is in  $G'$ . By Observation 8.4,

$$\#E' = \#G' + \#H' \leq \left\lceil \frac{n-3}{2} \right\rceil + \left\lfloor \frac{n-3}{2} \right\rfloor = n-3,$$

which proves Observation 8.5.  $\square$

We now begin the construction by placing the  $t$ 's corresponding to the  $\sqsubset$ -smallest element of  $E'$  in such a way in  $\mathbb{R}_{>0}$  that (S1') is satisfied. This is clearly possible. The general step of constructing a solution to (S1') is based on the following lemma.

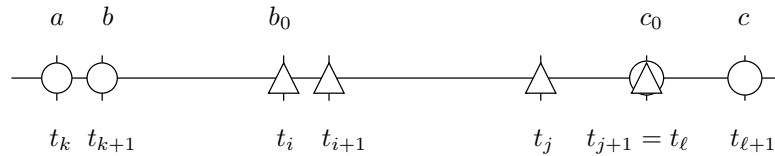
**Lemma 8.6** Let  $e' = (i, j) \sqsubset f' = (k, \ell)$  be two consecutive elements of  $E'$ .

- (a) If  $e' \in G'$  and  $f' \in H'$ , then  $0 < k \leq i$  and  $\ell = j+1$ . If  $e' \in H'$  and  $f' \in G'$ , then  $k = i-1$  and  $j \leq \ell < n$ . (See Figure 8.1.)
- (b) Suppose that the points  $\{t_i, t_{i+1}, t_j, t_{j+1}\}$  have been placed already, but not all of the points  $\{t_k, t_{k+1}, t_\ell, t_{\ell+1}\}$ . Then these latter  $t$ 's may be placed in such a way in  $\mathbb{R}_{>0}$  that  $0 < t_k < t_{k+1} < t_\ell < t_{\ell+1}$ , and the equality

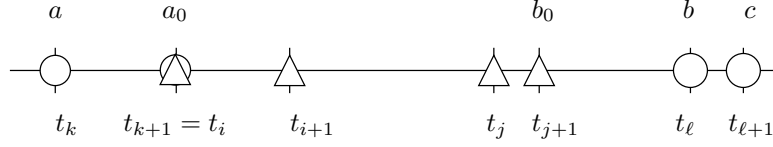
$$t_k t_{k+1} t_\ell t_{\ell+1} = M \quad (8.2)$$

is satisfied, where  $M := N' - \delta$  if  $f' \in G'$  and  $M := N' + \delta$  if  $f' \in H'$ .

*Sketch of proof for (b).* Suppose that  $e' \in G'$  and  $f' \in H'$ . We then have the following situation:



It is straightforward to verify that for any  $0 < k \leq i$ , the points  $a, b, c$  may be placed in such a way that  $0 < a < b < b_0 < c_0 < c$  and  $abc_0c = N' + \delta$ . Similarly, if  $e' \in H'$  and  $f' \in G'$ ,



for any  $j \leq \ell < n$  we may place  $a, b, c$  with  $0 < a < a_0 < b_0 < b < c$  and  $aa_0bc = N' - \delta$ .  $\square$

We complete Step 1 by applying Lemma 8.6 to all members of  $E'$  in  $\sqsubset$ -order. The definition of  $\preceq$  tells us that because the  $f' \in E'$  satisfy (S1'), in fact all  $f \in \mathcal{F}_3(n)$  satisfy (S1).

If in Step 1 there was some  $e' \in E'$  with  $1 \in e'$ , then necessarily  $e' = \{1, 2, n-1, n\} \in G'$ , which imposed the inequality  $t_1 t_2 t_{n-1} t_n < N'$ . This inequality in turn remains satisfied if we choose  $t_1$  even small enough to verify (S2). If  $1 \notin e'$  for all  $e' \in E'$ , we are free to do the same. We have completed Step 2, and place any remaining unassigned  $t$ 's such that  $0 = t_0 < t_1 < \dots < t_n$ .

**Observation 8.7** (a)  $\gamma_0(F_f) = 0$  for any 5-element subset  $f \subset \{0, 1, \dots, n\}$  containing 0.

(b) For all choices of  $t_1 < \dots < t_n$ , one can find  $\varepsilon > 0$  small enough such that the implication (S3) holds for all  $f, g \in \mathcal{F}_3(n)$ .

*Proof of (b).* The definition (8.1) of the  $\gamma$ 's implies that for  $f = \{0, s_1, \dots, s_4\}$ ,

$$\gamma(F_f) \cdot \mu(\varepsilon) = \varepsilon(\varepsilon - s_1) \cdots (\varepsilon - s_4) = \varepsilon s_1 s_2 s_3 s_4 \pm o(\varepsilon). \quad (8.3)$$

This means that  $\gamma(F_f) \cdot \mu(\varepsilon) < \gamma(F_g) \cdot \mu(\varepsilon)$  by definition of  $\prec$ , for  $\varepsilon$  small enough.  $\square$

Take  $0 < \varepsilon < t_1$  as in Observation 8.7(b), tentatively set  $z := \mu(\varepsilon)$ , and let  $f \in \mathcal{F}_3(n)$ . If  $f \in I$ , there exists some  $g \in G := 0 * G'$  with  $f \preceq g$ , and by (8.3), we have

$$\gamma(F_f) \cdot z \leq \gamma(F_g) \cdot z = \varepsilon \prod_{i \in g \setminus \{0\}} t_i + O(\varepsilon^2) = \varepsilon(N' - \delta) \pm o(\varepsilon).$$

If  $f \notin I$ , then there is some  $h \in H := 0 * H'$  with  $f \succeq h$ , and we obtain in a similar way that

$$\gamma(F_f) \cdot z \geq \varepsilon(N' + \delta) \pm o(\varepsilon).$$

Thus, we finally choose  $0 < \varepsilon < t_1$  so small that with  $z := \mu(\varepsilon)$  and  $N := \varepsilon N'$ , we have  $\gamma(F_f) \cdot z < N$  for  $f \in I$ , and  $\gamma(F_f) \cdot z > N$  for  $f \notin I$ . Step 3 is now complete.

We proceed to verify that  $v := \mu(\varepsilon) - \varepsilon N' e_5 = z - N e_5$  satisfies the inequalities (S4). For this, recall that all  $F_f$  with  $f \in \mathcal{F}_3(n)$  satisfy Gale's Evenness Criterion, which means that  $\mathcal{F}_3(n)$  is exactly the set of lower facets of the cyclic polytope  $C = \text{conv}(X)$  that contain  $x_0 = 0$ . However, *any*  $F \subset X$  of odd cardinality satisfying Gale's Evenness Criterion with even end-set must contain 0, and therefore  $\mathcal{F}_3(n)$  is in fact the set of *all* lower facets of  $C$ .

Recall from Section 8.2 that  $\alpha(F) = \gamma(F)$  and  $\alpha_0(F) = -\gamma_0(F)$  if  $F$  is an upper facet of  $C$ , and that  $\alpha(F) = -\gamma(F)$  and  $\alpha_0(F) = \gamma_0(F)$  if  $F$  is a lower facet of  $C$ . We discuss all facets  $F_f$  of  $C$  in turn.

- ▷ Lower facets of  $C$ :
  - ▷ If  $f \in I \subset \mathcal{F}_3(n)$ , then by construction  $\gamma(F_f) \cdot z < N$ , and this implies  $\gamma(F_f) \cdot v < 0$  (remember that  $\gamma_5(F) = 1$  for all  $F$ ) and  $\alpha(F_f) \cdot v > 0 = \alpha_0(F_f)$ , which means that  $F_f$  is visible from  $v$ .
  - ▷ If  $f \in \mathcal{F}_3(n) \setminus I$ , we conclude from  $\gamma(F_f) \cdot z > N$  that  $\alpha(F_f) \cdot v < 0 = \alpha_0(F_f)$ , which says that  $F_f$  is not visible from  $v$ .
- ▷ Upper facets of  $C$ :
  - ▷ If  $0 \notin f = \{s_1, \dots, s_5\}$ , then it follows from (8.1) and  $\varepsilon < t_1$  that

$$\gamma(F_f) \cdot z + \gamma_0(F_f) = \prod_{i=1}^5 (\varepsilon - s_i) < 0,$$

which in turn implies that

$$\alpha(F_f) \cdot v = \gamma(F_f) \cdot v = \gamma(F_f) \cdot z - N < -\gamma_0(F_f) - N < -\gamma_0(F_f) = \alpha_0(F_f).$$

- ▷ If  $0 \in f$ , then  $\gamma_0(F_f) = 0$  and  $f = \{0, 1\} \cup \{i, i+1\} \cup \{n\}$  with  $2 \leq i \leq n-2$ . By inequality (S2) and the definition of  $\prec$ , we conclude that necessarily  $\gamma(F_f) \cdot z < N$  and

$$\alpha(F_f) \cdot v = \gamma(F_f) \cdot z - N < 0 = \alpha_0(F_f).$$

We have verified the inequalities (S4) and completed the proof of Theorem 8.1.  $\square$

### 8.5 A shorter proof that squeezed 3-spheres are Hamiltonian

In 1973, Barnette [83] conjectured that all simple 4-polytopes admit a Hamiltonian circuit. In [35], Hebble and Lee prove that squeezed 3-spheres are (dual) Hamiltonian by explicitly constructing a Hamiltonian circuit in the dual graph; however, their proof goes through extensive case analysis. A referee of [74] suggested that it might be possible to obtain a simpler proof of this result. We followed his or her suggestion and obtained a “proof by picture” with fewer case distinctions, which moreover only depend on parity conditions.

**Theorem 8.8** (Hebble and Lee, 2000 [35]) *The dual graphs of Kalai’s 4-polytopes admit a Hamiltonian circuit. In particular, the (simple) duals of these 4-polytopes satisfy Barnette’s conjecture.*

*New proof.* Recall from Section 8.1 that the set of facets of  $S(I)$  is  $B(I') \cup (0 * S(I'))$ . We continue to write  $(i, j) = \{i, i+1, j, j+1\}$  for facets of  $S(I)$  in  $B(I')$ , and introduce the notation  $(i + \frac{1}{2}, j) := \{0, i+1, j, j+1\}$  and  $(i, j + \frac{1}{2}) := \{0, i, i+1, j+1\}$  for facets of  $S(I)$  in  $0 * S(I')$ . Also, recall from Section 8.1 the definition of the order relations  $\preceq$  and  $\sqsubset$ , and number the set  $G'$  of  $\preceq$ -maximal elements  $(i_k, j_k)$  of  $B(I')$  in ascending  $\sqsubset$ -order, starting with  $k = 1$ . Finally, define the difference operators  $\Delta j_k = j_{k+1} - j_k$  and  $\Delta i_k = i_{k+1} - i_k$ .

We start our Hamiltonian circuit in the dual graph of  $S(I)$  at the facet  $(i_0, j_0) = (1, 3) = \{1, 2, 3, 4\} \in B(I')$ . While walking through the other facets of  $B(I')$ , we will also pick up

the facets of the form  $(i + \frac{1}{2}, j)$  and  $(i, j + \frac{1}{2})$  with  $i, j \geq 1$  of  $S(I')$ , and then return to  $(1, 3)$  via the set of facets  $\{(0, j) : 2 \leq j \leq n - 1\}$ . In our circuit, we repeatedly go through certain steps, and in the figures we will mark the end of one step and the beginning of the next by a square. In all steps, if all facets in  $G'$  are processed, go to step *Down* (and then to *Finish*).

- (1) *Over the top*: Start at  $(i_0, j_0) = (1, 3)$ . If  $j_1 - j_0$  is odd, continue as in Figure 8.3(a). If  $j_1 - j_0$  is even, proceed as in Figure 8.3(b). In both cases, go on until  $(i_1 + \frac{1}{2}, j_1)$ . Set  $k = 1$ , and go to step *Down*.

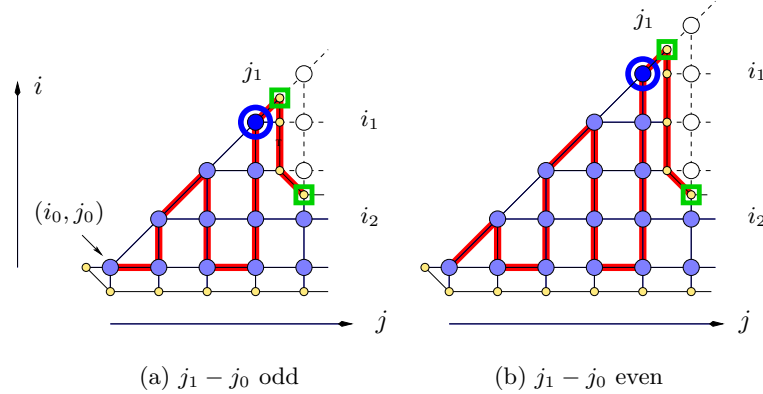


FIGURE 8.3: Steps *Over the top* and *Down*. The circled facet is  $(i_1, j_1)$ , the upper  $\square$  represents  $(i_1 + \frac{1}{2}, j_1)$ , and the lower  $\square$  is  $(i_2 + \frac{1}{2}, j_1 + 1)$ .

- (2) *Down*: If there are no more generators to be processed, go down along the facets  $\{(i_\ell, j_k + \frac{1}{2}) : \ell = k, k - 1, \dots, 1\}$  and continue with step *Finish*. Otherwise, if  $\Delta i_k > 0$ , continue downwards as in Figure 8.3 until  $(i_{k+1} + \frac{1}{2}, j_k + 1)$ . If  $i_{k+1} = i_k$ , do nothing. In both cases, increment  $k$  by 1, and continue to step *Across*.
- (3) *Across*: If  $\Delta j_k$  is even, continue as in Figure 8.4(a). If  $\Delta j_k$  is odd and not 1 and  $i_{k+1} - i_0$  is even, continue as in Figure 8.4(b); if  $\Delta j_k \neq 1$  and  $i_{k+1} - i_0$  are both odd, as in Figure 8.4(c).  
If  $\Delta j_k = 1$  and  $\Delta i_{k+1}$  is even, proceed as in Figure 8.5(a), if  $\Delta i_{k+1}$  is odd, as in Figure 8.5(b). In any case, increment  $k$  by one, and repeat from step *Down* or *Across* as necessary, depending on whether the facet surrounded by a dashed circle in Figure 8.5 is in  $G$  or not.
- (4) *Finish*: Now the only thing left to do is to return to  $(1, 3)$  via the set of facets  $\{(0, j) : n - 1 \geq j \geq 2\}$ , as in Figure 8.6.

This completes the proof of Theorem 8.8.  $\square$

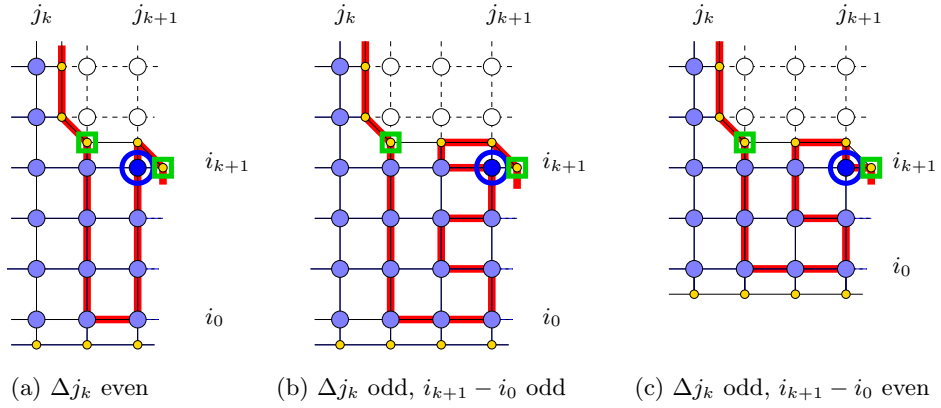


FIGURE 8.4: Step *Across* in case  $\Delta j_k$  is even. The circled facet is  $(i_{k+1}, j_{k+1})$ .

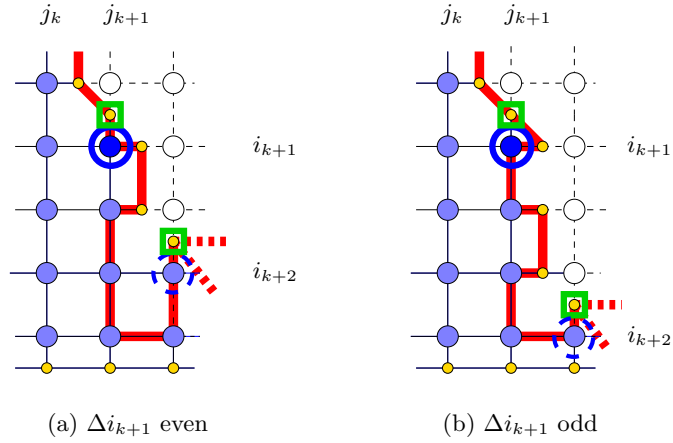


FIGURE 8.5: Step *Across* in case  $\Delta j_k = 1$ . The circled facet is  $(i_{k+1}, j_{k+1})$ . Depending on whether the facet surrounded by a dashed circle in Figure 8.5 is in  $G$  or not, the next step will be *Down* or *Across*, respectively.

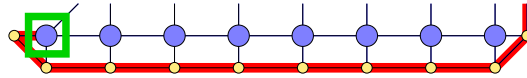


FIGURE 8.6: Step *Finish*.







## Chapter 9

# Many triangulated 3-spheres

In Chapter 7, we saw that Kalai’s idea [44] for building “many triangulated  $d$ -spheres” works just admirably for  $d \geq 4$ , producing far more combinatorial types of spheres than there can possibly be types of polytopes. However, it was the content of Theorem 8.1 that for  $d = 3$ , his construction only yields *polytopal* spheres.

In this chapter we show that there *do* exist far more combinatorial types of triangulated 3-spheres than the  $2^{\Theta(n \log n)}$  types of 4-polytopes guaranteed by (7.1) and [91]. More precisely, we prove the following theorem:

**Theorem 9.1** *There are at least*

$$s(3, n) \geq 2^{\Omega(n^{5/4})}$$

*combinatorially non-isomorphic simplicial 3-spheres on  $n$  vertices.*

In brief, we prove Theorem 9.1 by producing a cellulation  $\mathcal{S}$  of  $S^3$  with  $n$  vertices and  $\Theta(n^{5/4})$  octahedral facets, and triangulating each octahedron independently. The cellulation  $\mathcal{S}$  is constructed from a Heegaard splitting  $S^3 = H_1 \cup H_2$  of  $S^3$  of high genus (see Section 9.3 below) by appropriately subdividing the thickened boundary surface  $(H_1 \cap H_2) \times [0, 1]$ .

**Remark 9.2** (a) The fact that *most* of our spheres are combinatorially distinct follows from their sheer number: There can be at most  $n!$  spheres combinatorially isomorphic to any given one, where  $n! < n^n = 2^{n \log n} \ll 2^{n^c}$  holds for  $c > 1$ .  
 (b) The only known upper bound for  $s(3, n)$  is the rather crude estimate  $\log s(3, n) = O(n^2 \log n)$  obtained from Stanley’s proof of the upper bound theorem for spheres [94].

We assemble the ingredients for our construction in Sections 9.1–9.3, and devote Section 9.4 to the proof of Theorem 9.1.

## 9.1 Heffter’s embedding of the complete graph

In 1898, Heffter [36] constructed remarkable cellulations of closed orientable surfaces:

**Proposition 9.3** Let  $q = 4k + 1$  be a prime power, and  $\alpha$  be any generator of the cyclic group  $\mathbb{F}_q^*$  of invertible elements of the finite field  $\mathbb{F}_q$  on  $q$  elements. Then there exists a regular but not strongly regular cellulation  $\mathcal{C}_q^\alpha$  of the closed orientable surface  $S_g$  of genus  $g = q(q - 5)/4 + 1$  with  $f$ -vector  $(q, \binom{q}{2}, q)$ , all of whose 2-cells are  $(q - 1)$ -gons.  $\mathcal{C}_q^\alpha$  can be refined to a strongly regular triangulation  $\mathcal{T}_q^\alpha$  of  $S_g$  with  $f$ -vector  $(2q, \binom{q}{2} + q(q - 1), q(q - 1))$ .

*Proof:* There exist infinitely many *prime* numbers  $q$  of the form  $q = 4k + 1$ ; see [23]. For any prime *power*  $q$  of this form, take as vertices of the cellulation  $\mathcal{C}_q^\alpha$  the elements of  $\mathbb{F}_q$ , and as 2-cells the  $(q - 1)$ -gons (compare Figure 9.1, left)

$$F^\alpha(s) = \left\{ v^\alpha(s, k) = s + \frac{\alpha^k - 1}{\alpha - 1} : 0 \leq k \leq q - 2 \right\} \quad \text{for } s \in \mathbb{F}_q.$$

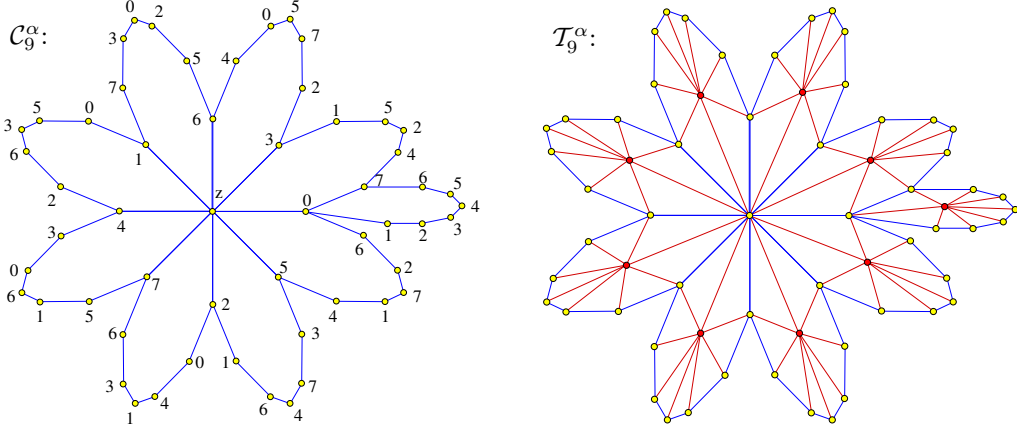


FIGURE 9.1: *Left:* The Heffter cellulation  $\mathcal{C}_9^\alpha$  of a surface  $S_g$  of genus  $g = 10$  for  $\alpha = 2x + 2 \in \mathbb{F}_9 \cong \mathbb{F}_3[x]/\langle x^2 + x + 2 \rangle$ . The vertex  $z$  corresponds to  $0 \in \mathbb{F}_9$ , and vertices labeled  $i$  to the element  $\alpha^i$ . Note that any two of the  $q = 9$  vertices are adjacent, and that all vertices in any given one of the 9 polygons are distinct. However, the link of every vertex contains identified vertices, and so the vertex stars are not embedded. *Right:* After subdividing the surface to the triangulation  $\mathcal{T}_q^\alpha$  using  $q$  new vertices, all stars are embedded disks.

It is straightforward to check (see [36] and [22, Lemma 12]) that this cellulation is *regular* (all vertices in each  $F(s)$  are distinct), *neighborly* (any two vertices are connected by an edge), and *closed* (any edge is shared by exactly two polygons), but not *strongly regular* (any two polygons share  $q - 2$  vertices). An Euler characteristic calculation yields the genus of the underlying surface  $S_g$  of  $\mathcal{C}_q^\alpha$ . By subdividing each polygon as in Figure 9.1 (right), the cellulation becomes strongly regular with the stated  $f$ -vector.  $\square$

**Remark 9.4** This cellulation was independently obtained in [22] as an abelian covering of the canonical one-vertex cellulation of  $S_g$ .

**Remark 9.5** Heffter’s original construction involved only prime numbers. As it turns out, allowing prime powers becomes necessary for symmetric embeddings: According to Biggs [7], if the complete graph  $K_n$  embeds into a closed orientable surface in a symmetric way (i.e., there exists a “rotary” or “chiral” combinatorial automorphism, see [102]), then  $n$  is the power of a prime number, and James & Jones [38] showed that *any* such embedding of  $K_n$  is actually one from Heffter’s family.

**Remark 9.6** Two cellulations  $\mathcal{C}_q^\alpha$  and  $\mathcal{C}_q^\beta$  are combinatorially distinct for  $\beta \neq \alpha, 1/\alpha \in \mathbb{F}_q$ : By [36], the only automorphisms of  $\mathcal{C}_q^\alpha$  are induced by affine maps  $\varphi : \mathbb{F}_q \rightarrow \mathbb{F}_q, x \mapsto ax + b$  with  $a \in \mathbb{F}_q^*, b \in \mathbb{F}_q$ . An easy calculation shows that requiring  $\varphi(v^\alpha(s, k + i)) = v^\beta(t, \ell + i)$  resp.  $\varphi(v^\alpha(s, k + i)) = v^\beta(t, \ell - i)$  for  $t \in \mathbb{F}_q, 0 \leq \ell \leq q - 2$  and  $i = 0, 1, 2$  already implies  $\beta = \alpha$  resp.  $\beta = 1/\alpha$ .

## 9.2 The E-construction

**Proposition 9.7** [22] Given a cellulation  $\mathcal{C}$  of a  $d$ -dimensional manifold  $M$  with boundary with  $f$ -vector  $(f_0, f_1, \dots, f_d)$  and  $f_{d-1}^{\text{in}}$  interior ridges, there exists a cellulation  $E(\mathcal{C})$  of  $M$  with  $f_0 + f_d$  vertices consisting of  $f_{d-1}^{\text{in}}$  bipyramids and  $f_{d-1} - f_{d-1}^{\text{in}}$  pyramids.

*Proof:* Cone a new vertex to the inside of each  $d$ -cell  $F$  of  $M$  to create  $f_{d-1} + f_{d-1}^{\text{in}}$  pyramids, then combine each pair of pyramids over the same interior ridge to a bipyramid.  $\square$

**Example 9.8** Let  $\mathcal{C}$  be a cellulation of a closed orientable surface  $S$  with  $f$ -vector  $(f_0, f_1, f_2)$ . Then applying Proposition 9.7 to  $\mathcal{C} \times [0, 1]$  yields a cellulation of the prism  $S \times [0, 1]$  with  $2f_0 + f_2$  vertices consisting of  $f_1$  octahedra and  $2f_2$  pyramids; see Figure 9.2.

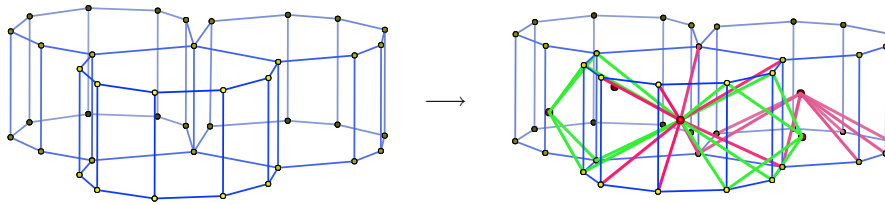


FIGURE 9.2: The E-construction applied to  $\Pi = \mathcal{C}_9^\alpha \times [0, 1]$ . *Left:* Three of the nine prisms of  $\Pi$ . *Right:* Three of the 18 octagonal pyramids and two out of  $\binom{9}{2}$  octahedra of  $E(\Pi)$ .

## 9.3 Heegaard splittings

**Proposition 9.9** (see [99, Section 8.3.2]) For any  $g \geq 1$ , the 3-sphere may be decomposed into two solid handlebodies  $S^3 = H_1 \cup H_2$  that are identified along a surface  $S_g = H_1 \cap H_2$  of genus  $g$ . Conversely, any 3-manifold can be split into handlebodies  $H_1, H_2$  and is determined up to homeomorphism by the images  $h(m_1), \dots, h(m_{2g})$  on  $H_2$  of the canonical meridians  $m_1, \dots, m_{2g}$  of  $H_1$  under the identification map  $h : \partial H_1 \rightarrow \partial H_2$ .  $\square$

**Theorem 9.10** (Lazarus et al. [56, Theorem 1]) Any triangulation  $\mathcal{T}$  of a closed orientable surface of genus  $g$  with a total of  $f = f_0 + f_1 + f_2$  cells can be refined to a triangulation  $\tilde{\mathcal{T}}$  with  $O(fg)$  vertices that contains representatives of the canonical homology generators in its 1-skeleton. These representatives only intersect in a single vertex, and each one uses  $O(f)$  vertices and edges.  $\square$

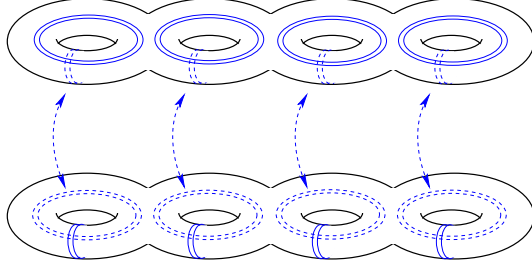


FIGURE 9.3: Heegaard splitting of  $S^3$  of genus  $g = 4$ . The complement of one solid handlebody in the 3-sphere is the other solid handlebody of the same genus. One copy of each doubled solid (resp. dashed) homology generator on the upper handlebody  $H_1$  is identified with one copy of the solid (resp. dashed) one on the lower handlebody  $H_2$  as indicated by the arrows, and the union of all copies of the generators induces a cellulation of  $H_1$  (resp.  $H_2$ ) into one 3-ball and  $g$  solid cylinders.

#### 9.4 Many triangulated 3-spheres

*Proof of Theorem 9.1:* We build a cellular decomposition  $\mathcal{S}$  of  $S^3$  with  $n$  vertices and  $\Theta(n^{5/4})$  octahedral facets from two triangulated handlebodies and a stack of prisms over a Heffter surface. The theorem then follows by independently triangulating the octahedra.

We begin with a Heegaard splitting  $S^3 = H_1 \cup H_2$  of  $S^3$  of genus  $g = q(q-5)/4 + 1$  as in Proposition 9.9, for any prime power  $q$  of the form  $q = 4k + 1$  for  $k \geq 1$ . We replace the boundary  $S_g = H_1 \cap H_2$  of the handlebodies by the prism  $\Pi_g = S_g \times [0, 1]$ , pick a generator  $\alpha$  of  $\mathbb{F}_q^*$ , and embed a copy of the Heffter triangulation  $\mathcal{T}_q^\alpha$  on  $S_g \times \{0\}$  and  $S_g \times \{1\}$ .

- ▷ *The triangulated handlebodies.* Use Theorem 9.10 to refine each copy of  $\mathcal{T}_q^\alpha$  to a triangulation of  $S_g$  that contains representatives of the canonical homology generators  $\{a_i, b_i : 1 \leq i \leq g\}$  in its 1-skeleton, such that the  $a_i$ 's span meridian disks in  $H_1$  and the  $b_i$ 's do the same in  $H_2$ . This introduces  $O(q^2g) = O(q^4)$  new vertices. Double all generators as in Figure 9.3 using another  $O(q^4)$  vertices to obtain a triangulation  $\mathcal{T}'$  of  $S_g$ , and in each handlebody triangulate the meridian disks spanned by all these polygonal curves (using a total of  $O(q^2g)$  triangles, but no new vertices). Then cone the boundary of each of the  $2g$  solid cylinders bounded by the meridian disks to a new vertex (introducing a total of  $O(q^2g)$  tetrahedra), and cone the triangulated boundary of each of the remaining two 3-balls to another new vertex. This last step uses  $2g + 2$  new vertices and  $O(q^4)$  tetrahedra. The total  $f$ -vector of this triangulation  $\mathcal{T}''$  of  $H_1 \cup H_2$  is

$$f(\mathcal{T}'') = (O(q^4), O(q^4), O(q^4), O(q^4)).$$

- ▷ *The stack of prisms.* Let  $\mathcal{C}_q^\alpha \times I_m$  cellulate the manifold with boundary  $\Pi_g = S_g \times [0, 1]$ , where  $I_m$  is the subdivision of  $[0, 1]$  into  $m = \Theta(q^3)$  closed intervals, and refine each of  $\mathcal{C}_q^\alpha \times \{0\}$  and  $\mathcal{C}_q^\alpha \times \{1\}$  into the triangulation  $\mathcal{T}'$ . This refined cellulation  $\mathcal{C}$  is composed of  $\Theta(q^4)$  prisms over  $(q-1)$ -gons and  $2q$  3-cells whose boundary consists of  $q-1$  4-gons, one  $(q-1)$ -gon, and on average  $O(q^3)$  triangles that together triangulate another  $(q-1)$ -gon.

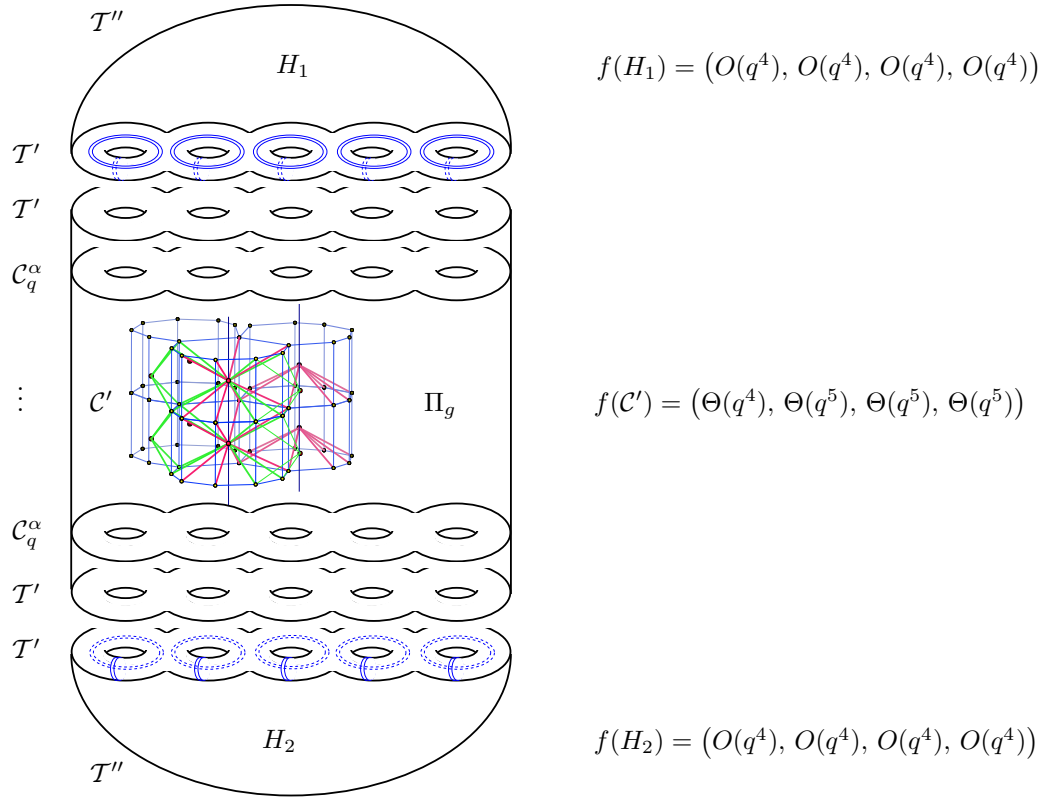


FIGURE 9.4: The thickened Heegaard splitting  $S^3 = H_1 \cup C' \cup H_2$  of  $S^3$ . Not shown is the triangulation of the handlebodies  $H_1$  and  $H_2$ . Independently triangulating the  $\Theta(n^{5/4})$  octahedral 3-cells of  $C'$  in different ways yields “many triangulated 3-spheres”.

The boundary of  $\mathcal{C}$  consists of the union of these  $O(q^4)$  triangles, and the  $f$ -vector of  $\mathcal{C}$  is

$$\begin{aligned} f(\mathcal{C}) &= \Theta(q^3) \cdot (\Theta(q), \Theta(q^2), \Theta(q^2), \Theta(q)) + (O(q^4), O(q^4), O(q^4), 0) \\ &= (\Theta(q^4), \Theta(q^5), \Theta(q^5), \Theta(q^4)). \end{aligned}$$

Apply the E-construction (Proposition 9.7) to  $\mathcal{C}$ , using  $\Theta(q^4)$  new vertices, to arrive at a cellulation  $E(\mathcal{C})$  of  $\Pi_g$  into  $\Theta(q^4)$  simplices (pyramids over the boundary triangles),  $\Theta(q^4)$  bipyramids over  $(q-1)$ -gons, and  $\Theta(q^5)$  octahedra. Now triangulate the bipyramids by joining each main diagonal to each edge of the base  $(q-1)$ -gon. This cellulation  $\mathcal{C}'$  of  $\Pi_g$  consists of  $\Theta(q^5)$  simplices and  $\Theta(q^5)$  octahedra (Figure 9.4). Its total  $f$ -vector is

$$f(\mathcal{C}') = (\Theta(q^4), \Theta(q^5), \Theta(q^5), \Theta(q^5)).$$

The desired cellulation of  $S^3$  is  $\mathcal{S} = \mathcal{T}'' \cup \mathcal{C}'$ . □



## Chapter 10

# Neighborly centrally symmetric fans

### 10.1 Introduction

A polytope  $P \subset \mathbb{R}^d$  is *centrally symmetric* or a *cs-polytope* if, after a suitable translation,  $P = -P$ . In view of the existence of neighborly polytopes, a natural question is to ask for the maximal number of  $k$ -faces that a cs-polytope with  $2n$  vertices can have. By convexity, no face of a  $d$ -dimensional cs-polytope with  $d > 1$  can contain two antipodal vertices (i.e., two vertices  $v, w$  with  $w = -v$ ). Therefore, one modifies the usual definition of neighborliness and defines a cs-polytope  $P$  on  $n$  vertices to be  *$k$ -neighborly centrally symmetric* [67] or  *$k$ -cs-neighborly* if every subset of  $k$  vertices of  $P$  not containing two antipodal vertices is the vertex set of a  $(k-1)$ -simplex which is a face of  $P$ . Equivalently,  $P = -P$  is  $k$ -cs-neighborly if

$$f_i = \binom{n}{i+1} 2^{i+1} \quad \text{for all } 0 \leq i \leq k-1, \quad (10.1)$$

where  $f_i$  counts the number of  $i$ -dimensional faces of  $P$ . A  $d$ -dimensional cs-polytope is called *neighborly centrally symmetric* or *cs-neighborly* if (10.1) holds for  $k = \lfloor d/2 \rfloor$ .

The  $d$ -dimensional cross-polytope with  $n = 2d$  vertices is cs-neighborly for all  $d \geq 2$ , and Grünbaum gave an example for a  $d$ -dimensional cs-neighborly cs-polytope  $P$  with  $n = 2d + 2$  vertices for all  $d \geq 2$ , namely  $P = \text{conv}\{\pm e_i, \pm \mathbf{1}\}$ , where  $\mathbf{1}$  denotes the all-1 vector.

In sharp contrast to these examples, Grünbaum proved in Section 6.4 of his 1967 classic [31] that there is *no* convex 4-dimensional cs-neighborly cs-polytope with  $12 = 2 \cdot 4 + 4$  vertices. By reverse induction on the number of vertices, this implies that there exists *no* 4-dimensional cs-neighborly cs-polytope on  $n$  vertices, for all  $n \geq 12$ .

In 1968, McMullen and Shephard [67] gave an analogue of the Gale transform for centrally symmetric point sets. Namely, if  $P = \text{conv}\{\pm x_1, \pm x_2, \dots, \pm x_n\} \subset \mathbb{R}^d$ , take the Gale transform  $G^* = \{x_1^*, x_2^*, \dots, x_n^*\} \subset \mathbb{R}^{n-d}$  of  $\{x_1, x_2, \dots, x_n\}$ , and define the *cs-Gale transform* of  $P$  as  $P^\diamond := G^* \cup -G^*$ . Much as in the usual Gale transform, the combinatorics of  $P$  is encoded via *cs-circuits* and *cs-cocircuits*; see Definition 10.6 and Proposition 10.12 below.

Using the cs-Gale transform, McMullen and Shephard investigated cs-polytopes on few vertices, and proved that a  $d$ -dimensional cs-polytope on  $2(d+\ell)$  vertices can be cs-neighborly only for  $\ell = 0, 1$ , and is at most  $\lfloor (d+1)/3 \rfloor$ -cs-neighborly for  $\ell \geq 2$ . (Grünbaum's result is the case  $d = 4$ .)

In 1975, Schneider [86] provided an asymptotic *lower* bound for the possible cs-neighborliness of cs-polytopes by constructing a family of cs-Gale transforms of  $k$ -cs-neighborly cs-

polytopes. More specifically, he proved that

$$\liminf_{d \rightarrow \infty} \frac{k(d, \ell)}{d + \ell} > 0.239 \quad \text{for all } \ell \geq 2,$$

where  $k(d, \ell)$  is the greatest integer  $k$  such that there exists a  $d$ -dimensional  $k$ -cs-neighborly cs-polytope with  $2(d + \ell)$  vertices. Compare this with McMullen and Shephard's result, which states that  $k(d, \ell)/(d + \ell) < 1/3$  for  $\ell \geq 2$ .

For fixed dimension  $d$ , cs-neighborliness is an even more restrictive property: In 1991, Burton provided a half-page proof [15] that for all dimensions  $d \geq 2$ , there exists an integer  $N(d)$  such that any  $d$ -dimensional cs-polytope with more than  $N(d)$  vertices is not even 2-cs-neighborly!

We now pass to the larger class of spheres. A *centrally symmetric* simplicial sphere or *cs-sphere* is defined via a combinatorial abstraction of the non-antipodality property, namely, the vertex set must admit an involution that does not fix any face.

Stanley observed (cf. [39]) that just as the upper bound theorem is valid for spheres [94], the maximal number of faces of a  $d$ -dimensional cs-sphere is the same as that of a  $(d + 1)$ -dimensional cs-polytope. In 1993, Jockusch [39] gave an inductive construction of 3- and 4-dimensional cs-neighborly cs-spheres on  $n$  vertices for all even  $n \geq 8$  resp.  $n \geq 10$ , and Lutz [60] in 2002 provided an explicit construction for 3-dimensional cs-neighborly cs-spheres with a transitive cyclic group action on  $4m$  vertices, for all  $m \geq 2$ .

In this chapter, we focus on an intermediate class of objects, namely *neighborly centrally symmetric star-shaped spheres*, also called *cs-neighborly fans*. For this, define a *simplicial cone*  $\sigma$  in  $\mathbb{R}^d$  to be the non-negative hull

$$\sigma = \text{cone}(v_1, v_2, \dots, v_k) = \left\{ \sum_{i=1}^k \lambda_i v_i : \lambda_i \geq 0, i = 1, 2, \dots, k \right\}$$

of  $k$  affinely independent points in  $\mathbb{R}^d$ , for  $0 \leq k \leq d$ . (We set  $\text{cone}(\emptyset) = \{0\}$ .) A *simplicial fan* is a finite collection  $\Sigma = \{\sigma_j : j \in J\}$  of simplicial cones such that the intersection between any two is contained in  $\Sigma$ , where we can assume that  $\dim \text{lin } \Sigma = d$ . Cones of maximal dimension are called *facets*. A simplicial fan  $\Sigma$  is *complete* if  $\bigcup \Sigma = \mathbb{R}^d$ . By intersecting a complete simplicial fan with  $S^{d-1}$ , we get a simplicial cell decomposition of  $S^{d-1}$ , and any simplicial sphere that arises in this way is called a *star-shaped* simplicial sphere. The definition of a *centrally symmetric* star-shaped sphere should now be clear: we require the defining complete simplicial fan  $\Sigma$  to be centrally symmetric (a *cs-fan*), i.e., to satisfy the condition  $\Sigma = -\Sigma$ . We observe the following hierarchy:

$$\{\text{cs-polytopes}\} \subsetneq \{\text{cs-fans}\} = \{\text{cs-star-shaped spheres}\} \subseteq \{\text{cs-spheres}\}$$

Without the prefix “cs-”, both inclusions are strict in all dimensions  $d \geq 3$ . An example for the first one is *Schönhardt's polyhedron* [87], a well-known non-regular subdivision of a triangular prism, and to get a non-star-shaped sphere glue together two copies of *Barnette's sphere* [24, Theorem III.5.5].



In the centrally symmetric case, the first inclusion is seen to be strict by taking the cone  $C$  over some non-regular triangulation of a point set, and completing  $C \cup (-C)$  to a cs-fan.

When we add the adjective “*cs-neighborly*”, we have seen that the first set is ‘quite small’, while there exist infinite families in the last one. We take a step towards investigating the middle set by proving the following theorem.

**Theorem 10.1** *For all even  $d \geq 4$  and for all odd  $d \geq 11$ , there are no cs-neighborly centrally symmetric  $d$ -dimensional fans on  $2d + 4$  rays.*

In sharp contrast to polytopes, the combinatorics of a fan is not at all specified by giving generators for the 1-dimensional rays. Our strategy for proving Theorem 10.1 is to first calculate the number of facets of a cs-neighborly simplicial sphere (Proposition 10.4); here we use the fact that the Dehn-Sommerville equations hold for simplicial spheres, so the number  $n$  of vertices already determines the number  $f_{d-1}^{\mathcal{S}}(d, n)$  of facets of a cs-neighborly  $(d-1)$ -dimensional sphere  $\mathcal{S}$ .

We then use McMullen and Shephard’s [67] technique of centrally symmetric Gale diagrams (Section 10.3) to bound from above the number  $f_d^{\Sigma}(d, d+2)$  of facets of a centrally symmetric neighborly  $d$ -dimensional fan on  $2(d+2)$  rays, and conclude that  $f_{d-1}^{\mathcal{S}}(d, d+2) > f_d^{\Sigma}(d, d+2)$  for even  $d \geq 4$  and odd  $d \geq 11$ .

## 10.2 The number of facets of a cs-neighborly cs-fan

**Proposition 10.2** The number of facets of a  $(d-1)$ -dimensional simplicial sphere  $\mathcal{S}$  whose  $f$ -vector  $f(\mathcal{S}) = (f_0, f_1, \dots, f_{\lfloor d/2 \rfloor}, \dots, f_{d-1})$  is known up to dimension  $\lfloor d/2 \rfloor$  is

$$f_{d-1} = \begin{cases} \sum_{i=0}^{d/2} (-1)^{d/2+i} \frac{i}{d-i} \binom{d-i}{d/2} f_{i-1} & \text{if } d \text{ is even,} \\ \sum_{i=0}^{(d-1)/2} (-1)^{(d-1)/2+i} \binom{d-i-1}{(d-1)/2} f_{i-1} & \text{if } d \text{ is odd.} \end{cases}$$

*Proof.* The  $h$ -vector  $h(\mathcal{S}) = (h_0, h_1, \dots, h_d)$  of  $\mathcal{S}$  satisfies the Dehn-Sommerville equations  $h_k = h_{d-k}$  for  $k = 0, 1, \dots, d$ , where

$$h_k = \sum_{i=0}^k (-1)^{k+i} \binom{d-i}{d-k} f_{i-1}.$$

We use  $d - \lceil (d+1)/2 \rceil = \lfloor (d-1)/2 \rfloor$ ,  $\lceil (d+1)/2 \rceil - 1 = \lceil (d-1)/2 \rceil = \lfloor d/2 \rfloor$  and Iverson’s

notation  $[p]$ , which stands for 1 if the statement  $p$  is true and for 0 otherwise. Now

$$\begin{aligned}
f_{d-1} &= 2 \sum_{k=0}^{\lfloor (d-1)/2 \rfloor} h_k + h_{d/2} [d \text{ is even}] \\
&= 2 \sum_{k=0}^{\lfloor (d-1)/2 \rfloor} \sum_{i=0}^k (-1)^{k+i} \binom{d-i}{d-k} f_{i-1} + h_{d/2} [d \text{ is even}] \\
&= 2 \sum_{k=0}^{\lfloor (d-1)/2 \rfloor} (-1)^i f_{i-1} \sum_{k=i}^{\lfloor (d-1)/2 \rfloor} (-1)^k \binom{d-i}{d-k} + h_{d/2} [d \text{ is even}] \\
&= 2 \sum_{k=0}^{\lfloor (d-1)/2 \rfloor} (-1)^i f_{i-1} \sum_{k=\lceil (d+1)/2 \rceil}^{d-i} (-1)^{d-k} \binom{d-i}{k} + h_{d/2} [d \text{ is even}]
\end{aligned}$$

We use the identity  $\sum_{k \leq m} (-1)^k \binom{r}{k} = (-1)^m \binom{r-1}{m}$  to simplify the inner sum to

$$\begin{aligned}
\sum_{k=\lceil (d+1)/2 \rceil}^{d-i} (-1)^{d+k} \binom{d-i}{k} &= 0 - (-1)^d \sum_{k=\lceil (d+1)/2 \rceil - 1} (-1)^k \binom{d-i}{k} \\
&= (-1)^{d-1} (-1)^{\lceil (d+1)/2 \rceil - 1} \binom{d-i-1}{\lceil (d+1)/2 \rceil - 1} \\
&= (-1)^{\lfloor (d-1)/2 \rfloor} \binom{d-i-1}{\lceil (d-1)/2 \rceil},
\end{aligned}$$

and obtain

$$f_{d-1} = 2 \sum_{k=0}^{\lfloor (d-1)/2 \rfloor} (-1)^{\lfloor (d-1)/2 \rfloor + i} \binom{d-i-1}{\lfloor d/2 \rfloor} f_{i-1} + h_{d/2} [d \text{ is even}],$$

so the formula for odd  $d$  follows. For even  $d$ , we finish by calculating

$$\begin{aligned}
f_{d-1} &= 2 \sum_{k=0}^{d/2-1} (-1)^{d/2-1+i} \binom{d-i-1}{d/2} f_{i-1} + \sum_{i=0}^{d/2} (-1)^{d/2+i} \binom{d-i}{d/2} f_{i-1} \\
&= \sum_{i=0}^{d/2-1} (-1)^{d/2+i} \underbrace{\left[ \binom{d-i}{d/2} - 2 \binom{d-i-1}{d/2} \right]}_{\frac{(d-i)!}{(d/2)!(d/2-i)!} \left( 1 - 2 \frac{d/2-i}{d-i} \right)} f_{i-1} + f_{d/2} \quad (10.2) \\
&= \sum_{i=0}^{d/2} (-1)^{d/2+i} \frac{i}{d-i} \binom{d-i}{d/2} f_{i-1}. \quad \square
\end{aligned}$$

To calculate the number of facets of a centrally symmetric neighborly simplicial  $(d-1)$ -dimensional sphere  $\mathcal{S}$  on  $2n$  vertices, we need the following identity.

**Lemma 10.3** (Eric Sparla, 1997 [93, Lemma 2.4])

$$\sum_{i=0}^{\ell} (-1)^{\ell+i} \binom{2\ell-i}{\ell} \binom{m}{i} 2^i = \binom{(m-1)/2}{\ell} 2^{2\ell}. \quad (10.3)$$

*Method of Proof.* This can be proved either using Zeilberger's algorithm [71] or by regarding both sides of the identity as polynomials in  $m$ , noting that both have degree  $\ell$  and their leading coefficients agree, and using the Residue Theorem to check that the left-hand side vanishes on all  $\ell$  zeros  $\{2j+1 : j = 0, 1, \dots, \ell-1\}$  of the right-hand side.  $\square$

**Proposition 10.4** The number of facets of a centrally symmetric neighborly simplicial  $(d-1)$ -dimensional sphere  $\mathcal{S}$  on  $2(d+k)$  vertices is

$$f_{d-1}^{\mathcal{S}}(d, d+k) = \binom{\lfloor d/2 \rfloor + k/2}{\lfloor d/2 \rfloor} 2^d.$$

*Proof.* Since  $\mathcal{S}$  is neighborly centrally symmetric,  $f_i = \binom{d+k}{i+1} 2^{i+1}$  for  $i = -1, 0, \dots, \lfloor d/2 \rfloor$ . For odd  $d$ , substitute (10.3) with  $\ell = (d-1)/2$  into the formula of Proposition 10.2. For even  $d$ , we continue the calculation from (10.2):

$$\begin{aligned} f_{d-1} &= \sum_{i=0}^{d/2} (-1)^{d/2+i} \left[ \binom{d-i}{d/2} - 2 \binom{d-i-1}{d/2} \right] \binom{d+k}{i} 2^i \\ &= \sum_{i=0}^{d/2} (-1)^{d/2+i} \binom{d-i}{d/2} \binom{d+k}{i} 2^i + \sum_{i=0}^{d/2} (-1)^{d/2+i+1} \binom{d-i-1}{d/2} \binom{d+k}{i} 2^{i+1}. \end{aligned}$$

Using the identity  $\binom{d+k}{i-1} + \binom{d+k}{i} = \binom{d+k+1}{i}$ , the second sum equals

$$\begin{aligned} \sum_{i=1}^{d/2+1} (-1)^{d/2+i} \binom{d-i}{d/2} \binom{d+k}{i-1} 2^i &= \\ \sum_{i=1}^{d/2} (-1)^{d/2+i} \binom{d-i}{d/2} \binom{d+k+1}{i} 2^i - \sum_{i=1}^{d/2} (-1)^{d/2+i} \binom{d-i}{d/2} \binom{d+k}{i} 2^i, \end{aligned}$$

so by using (10.3) with  $\ell = d/2$ , we obtain

$$f_{d-1} = (-1)^{d/2} \binom{d}{d/2} + \binom{(d+k)/2}{d/2} 2^d - (-1)^{d/2} \binom{d}{d/2}. \quad \square$$

### 10.3 Centrally symmetric Gale diagrams

**Definition 10.5** Write  $[\pm n] := \{\pm 1, \pm 2, \dots, \pm n\}$ , and let  $X = \{\pm x_1, \pm x_2, \dots, \pm x_n\} \subset \mathbb{R}^d$  be a spanning centrally symmetric point configuration in  $\mathbb{R}^d$ . Also, set  $x_{-i} := -x_i$  for  $i \in [n]$ .

- (a) Let  $[\pm n] = C^+ \cup C^0 \cup (-C^+)$  be a partition of  $[\pm n]$  such that  $C^+ \neq \emptyset$  and  $C^0 = -C^0$ . Then  $\mathcal{C} = (C^+, C^0)$  is a *cs-vector* of  $X$  if there exist  $\lambda_i > 0$  for all  $i \in C^+$  such that  $\sum_{i \in C^+} \lambda_i x_i = 0$ . A *cs-vector*  $\mathcal{C} = (C^+, C^0)$  is a *cs-circuit* of  $X$  if  $C^+ \neq \emptyset$  is minimal with respect to inclusion. In this case,  $C^+$  is a minimal positively dependent set of vectors for some non-trivial linear subspace.
- (b) Let  $[\pm n] = H^+ \cup H^0 \cup (-H^+)$  be a partition of  $[\pm n]$  such that  $H^+ \neq \emptyset$  and  $H^0 = -H^0$ . We call  $\mathcal{H} = (H^+, H^0)$  a *cs-covector* of  $X$  if there exists an  $a \in \mathbb{R}^d \setminus \{0\}$  such that  $a^T x_j > 0$  resp.  $a^T x_k = 0$  for all  $j \in H^+$  resp.  $k \in H^0$ . Equivalently, there is a linear hyperplane  $L \subset \mathbb{R}^d$  such that  $\{x_j : j \in H^+\} \subset L^{\geq 0}$  and  $\{x_k : k \in H^0\} \subset L$ . If  $H^+ \neq \emptyset$  is minimal with respect to inclusion, then  $\mathcal{H} = (H^+, H^0)$  is a *cs-cocircuit* of  $X$ . In this case,  $H^0$  spans a hyperplane.

**Definition 10.6** Let  $X = \{\pm x_1, \pm x_2, \dots, \pm x_n\} \subset \mathbb{R}^d$  be a centrally symmetric point configuration in  $\mathbb{R}^d$ , and let  $X_+^* = \{x_1^*, x_2^*, \dots, x_n^*\} \subset \mathbb{R}^{n-d}$  be the Gale transform of  $X_+ := \{x_1, x_2, \dots, x_n\}$ . The *cs-Gale transform*  $X^\diamond$  of  $X$  is  $X^\diamond = X_+^* \cup (-X_+^*)$ .

- Remark 10.7** (a) The cs-Gale transform of  $X$  is well-defined: replacing  $x_i$  by  $-x_i$  in the definition of  $X_+$  above amounts to applying a linear transform to  $X$  (extend  $x_i$  to a basis of  $\mathbb{R}^d$ ), and Gale transforms are only defined up to linear transformations.
- (b) The set  $X_+$  is in general linear position (i.e., no  $d$  vectors of  $X_+$  are linearly dependent) if and only if  $X_+^*$  is in general linear position [67]. Indeed, any non-trivial linear relation on  $d$  or fewer members of  $X_+$  could be extended to a basis of  $\mathbb{R}^n$ . But then at least  $n - d$  elements of  $X_+^*$  would have a zero entry in the same coordinate, a contradiction.

**Example 10.8** Let  $X_+$  be given by the columns of the matrix  $\begin{pmatrix} 1 & 0 & 2/3 & 2/3 \\ 0 & 1 & 2/3 & -2/3 \end{pmatrix}$ . One possible choice of  $X_+^*$  is then given by the columns of  $\begin{pmatrix} 2/3 & 2/3 & -1 & 0 \\ 2/3 & -2/3 & 0 & -1 \end{pmatrix}$ , so that we arrive at the representations of  $X = \pm X_+$  and  $X^\diamond$  shown in Figure 10.1.

**Proposition 10.9**  $\mathcal{C} = (C^+, C^0)$  is a cs-circuit of a centrally symmetric point configuration  $X$  if and only if  $\mathcal{C}$  is a cs-cocircuit of  $X^\diamond$ .

*Proof.* Choose  $Y^0 \subset [\pm n]$  such that  $C^0 = Y^0 \cup (-Y^0)$ , and set  $Y := Y^0 \cup C^+$ . Then, in the notation of Definition 4.3,  $\mathcal{C}' = (C^+, \emptyset, Y^0)$  is a non-negative circuit of  $Y$ , so by Gale duality  $\mathcal{C}'$  is a non-negative cocircuit of  $Y^*$ . But  $X^\diamond$  is linearly equivalent to  $Y^* \cup (-Y^*)$ , so  $\mathcal{C}$  is a cs-cocircuit of  $X^\diamond$ .  $\square$

**Observation 10.10** If a centrally symmetric point configuration  $X$  is in linearly general position and  $\mathcal{C} = (C^+, C^0)$  is a cs-circuit of  $X$ , then  $|C^+| = d + 1$ , and  $|C^0| = 2(n - d - 1)$ . For cs-cocircuits, we have  $|H^+| = n - d + 1$ , and  $|H^0| = 2(d - 1)$ .

*Proof.* Each second observation follows by general position; the first is then clear.  $\square$

**Definition 10.11** A subset  $I \subset [\pm n]$  is *antipode-free* if  $I \cap (-I) = \emptyset$ .

**Proposition 10.12** Let  $X = \{\pm x_1, \pm x_2, \dots, \pm x_n\} \subset \mathbb{R}^d$  be a centrally symmetric set of points in  $\mathbb{R}^d$  such that  $X_+$  is in linearly general position, let  $\mathcal{I} \subset 2^{[\pm n]}$  be a collection of antipode-free index sets such that  $\mathcal{I}$  is closed under taking subsets, and let  $\Sigma = \{\sigma_I : I \in \mathcal{I}\}$  be the family of cones  $\sigma_I = \text{cone}(x_i : i \in I)$ .

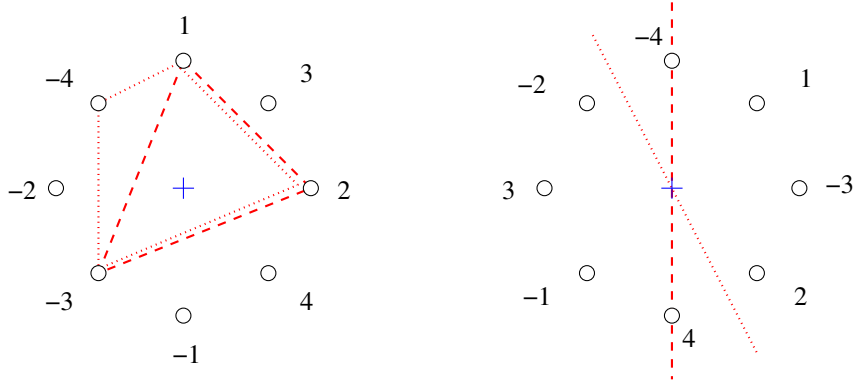


FIGURE 10.1: *Left:* A centrally symmetric point configuration  $X$  of  $2 \cdot 4$  points in  $\mathbb{R}^2$ , along with the cs-vector  $(\{1, 2, -3, -4\}, \emptyset)$  (dotted) and the cs-circuit  $(\{1, 2, -3\}, \{4, -4\})$  (dashed). *Right:* The cs-Gale transform  $X^\diamond$  of  $X$  in  $\mathbb{R}^{4-2} = \mathbb{R}^2$ , along with the corresponding covector (dotted) and cocircuit (dashed).

- (1) The family  $\Sigma$  is a fan if and only if for all  $I, J \in \mathcal{I}$  with  $I \cap J = \emptyset$ , there exists no linear hyperplane in  $\mathbb{R}^{n-d}$  that strictly separates  $\{x_i : i \in I\}$  and  $\{x_j : j \in J\}$ . In other words,  $(I \cup (-J)) \setminus H^+ \neq \emptyset$  for all  $I \neq J \in \mathcal{I}$  and all cs-cocircuits  $H^\diamond = (H^+, H^0)$  of  $X^\diamond$ .
- (2) If there is a cocircuit  $H^\diamond = (H^+, H^0)$  of  $X^\diamond$  and an  $I \in \mathcal{I}$  such that  $|I| = \lceil d/2 \rceil + 1$  and  $I \subset H^+$ , then  $\Sigma$  is not cs-neighborly.
- (3) If  $\Sigma$  is cs-neighborly, then for all cs-cocircuits  $H^\diamond = (H^+, H^0)$  of  $X^\diamond$  and all  $I \in \mathcal{I}$  with  $|I| = \lceil d/2 \rceil + 1$ , we have  $I \setminus H^+ \neq \emptyset$ .

*Proof.* (1) By [78, Proposition 3.2.2] and our assumption of linearly general position, the intersection between any two cones in  $\Sigma$  is again contained in  $\Sigma$  if and only the following condition holds:

$$\text{relint } \sigma_I \cap \text{relint } \sigma_J = \emptyset \quad \text{for all } I, J \in \mathcal{I} \text{ with } I \cap J = \emptyset. \quad (\text{IP})$$

The statement follows from the following chain of equivalences:

$$\begin{aligned} \text{relint } \sigma_I \cap \text{relint } \sigma_J &\neq \emptyset && \text{for some } I, J \in \mathcal{I} \text{ with } I \cap J = \emptyset \\ \iff &&& \text{there exist } \lambda_i > 0, \mu_j > 0 \text{ such that } \sum_{i \in I} \lambda_i x_i - \sum_{j \in J} \mu_j x_j = 0 \\ \iff &&& \mathcal{C} = (I \cup (-J), [\pm n] \setminus (\pm I \cup \pm J)) \text{ is a cs-circuit of } X \\ \iff &&& \mathcal{C} =: (H^+, H^0) \text{ is a cs-cocircuit of } X^\diamond \text{ with } H^+ = I \cup (-J). \end{aligned}$$

(2) Set  $J := -(H^+ \setminus I)$ . Since  $|H^+| = d + 1$  by general position and Observation 10.10, we know that  $|J| = \lfloor d/2 \rfloor$ . If  $\Sigma$  is cs-neighborly, then this means that  $\sigma_J$  is a face of  $\Sigma$ . Now  $I \cup (-J) = H^+$  contradicts (IP) via (1).

(3) By (2), for all such  $H^\diamond$  and  $I$  one has  $G := I \setminus H^+ \neq \emptyset$ . □

## 10.3.1 Centrally symmetric Gale diagrams on few vertices

From now on, let  $X = \{\pm x_1, \pm x_2, \dots, \pm x_n\}$  be a centrally symmetric  $2n$ -set in  $\mathbb{R}^d$  such that  $X_+$  is in linearly general position, and take  $n = d + 2 \geq 4$ . The cs-Gale transform  $X^\diamond = \{\pm x_1^*, \pm x_2^*, \dots, \pm x_n^*\}$  of  $X$  then lies in  $\mathbb{R}^2$ . As is easily checked (see also [92]), the cs-Gale transform of the set  $X_\mu = \{\pm \mu_1 x_1, \pm \mu_2 x_2, \dots, \pm \mu_n x_n\}$  is  $X_\mu^\diamond = \{\pm x_1^*/\mu_1, \pm x_2^*/\mu_2, \dots, \pm x_n^*/\mu_n\}$ , so we may suppose that  $X^\diamond \subset S^1$ . By our assumptions  $d \geq 2$  and general position of  $X_+$ , we may take  $X^\diamond$  to be a centrally symmetric set of  $2n$  distinct points on the unit circle.

**Definition 10.13** Take  $X$  as above. An *almost antipodal pair* (or *aa-pair*) is a pair  $\{i, j\} \subset [\pm n]$  such that  $-x_i^*$  is the (clockwise) neighbor of  $x_j^*$  in  $X$ .

**Proposition 10.14** (1)  $P \setminus H^+ \neq \emptyset$  for any aa-pair  $P$  and any cs-cocircuit  $\mathcal{H} = (H^+, H^0)$  of  $X$ .

- (2) An antipode-free  $d$ -element set  $F \subset [\pm n]$  satisfies  $I \setminus H^+ \neq \emptyset$  for all cs-cocircuits  $H^\diamond$  of  $X$  and all  $(\lceil d/2 \rceil + 1)$ -subsets  $I$  of  $F$  if and only if  $F = \bigcup_{i=1}^{d/2} P_i$  is the disjoint union of  $d/2$  aa-pairs  $P_i$  in case  $d$  is even, or the disjoint union  $F = \bigcup_{i=1}^{\lfloor d/2 \rfloor} P_i \cup \{m\}$  of  $\lfloor d/2 \rfloor$  aa-pairs and one additional index  $m \in [\pm n]$  if  $d$  is odd.

*Proof.* We again use Iverson's notation  $[p]$ . (1) is clear: If  $P \cap H^0 = \emptyset$ , then  $|P \cap H^+| = |P \cap (-H^+)| = 1$ , otherwise  $P \setminus H^+ \supseteq P \cap H^0 \neq \emptyset$ .

For the 'if'-part of (2), let  $I \subset F$  be some subset of cardinality  $\lceil d/2 \rceil + 1$ . Since  $\lceil d/2 \rceil + 1 > \lfloor d/2 \rfloor + [d \text{ odd}]$ ,  $I$  contains at least one pair  $P_j$ , so the assertion follows from (1).

The idea for the other direction is to remove a maximal set of aa-pairs from  $F$ , and find a 'bad' cocircuit under the assumption that some points of  $F$  are still left over. More precisely, we prove that if  $F = \bigcup_{i=0}^k P_i \cup R$  such that  $k$  is maximum and  $|R| = 2\ell + [d \text{ odd}]$  for some  $\ell > 0$ , then we can find a cs-cocircuit  $\mathcal{H} = (H^+, H^0)$  and a  $(\lceil d/2 \rceil + 1)$ -subset  $I$  of  $F$  such that  $I \subset H^+$ . For this, let  $X_R = \{x_i \in X : i \in R\}$  be the points of  $X$  indexed by  $R$ , so that  $\lfloor d/2 \rfloor = k + \ell$ . By a standard sweeping argument,  $X_R$  can be bisected by a line  $H$  passing through the origin. Turn  $H$  counter-clockwise around the origin until it hits a vertex in  $X_R$ . (If  $d$  is odd,  $H$  already passes through a vertex in  $X_R$ ; turn  $H$  nevertheless.) Call this position 1, its antipode  $-1$ , and the line through them  $H_1$ , and do the same for all  $2 \leq i \leq n$  in counter-clockwise order; cf. Figure 10.2 (left).

The three vertices opposite 1 are not in  $X_R$  by maximality of  $k$  and antipode-freeness, so one open half-space  $H_1^-$  of  $H_1$  contains exactly  $\ell - 1$  points from  $X_R$ , and the other  $\ell + [d \text{ odd}]$  points. We turn  $H_1$  one step further to  $H_2$ , and distinguish the following cases:

- (a) If  $2, -2 \notin F$ , then  $|H_2^+ \cap F| = k + \ell + [d \text{ odd}] + 1 = \lceil d/2 \rceil + 1$ , and we are done by setting  $H^+ := H_2^+$  and  $I := H_2^+ \cap F$ .
- (b) If  $2 \in F$ , then  $-2 \notin F$  by non-antipodality, and the same reasoning applies.
- (c) If  $-2 \in F$ , then  $-2, 3 \in F \setminus R$  by maximality of  $k$ , cf. Figure 10.2 (right). In this case, we turn  $H_2$  two steps further to  $H_4$ . If  $-4 \notin F$ , we are done as in (a) by using  $H_4$  instead of  $H_2$ . If  $-4 \in F$ , we continue this process until for some  $5 \leq i \leq n$  there holds  $\pm i \notin F$ . This must happen at some point, since  $|F| = n - 2$ , and then  $|H_i^+ \cap F| = k + \ell + 1 + [d \text{ odd}] = \lceil d/2 \rceil + 1$ .  $\square$

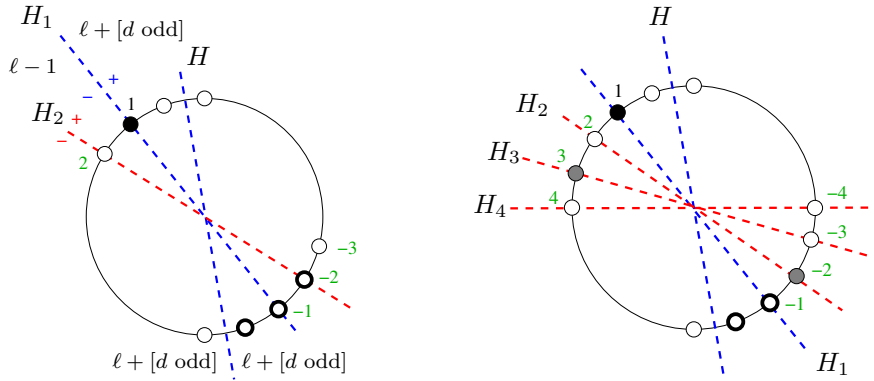


FIGURE 10.2: *Left:* The vertices between the halving line  $H$  and the line  $H_1$  are empty. If  $2, -2 \notin F$ , then  $|H_2^+ \cap F| = \lceil d/2 \rceil + 1$ . *Right:* If  $-2 \in F$ , proceed until  $\pm i \notin F$  for some  $i$ .

#### 10.4 No cs-neighborly cs-fans on few rays

This section is devoted to the proof of Theorem 10.1. For  $d \geq 2$ , we model a cs-Gale diagram  $X^\diamond$  of the set  $X$  of generators of a  $d$ -dimensional cs-fan  $\Sigma$  on  $2d + 4$  rays in the following way. As in the previous section, we may suppose without loss of generality that  $X^\diamond \subset S^1$ , and draw a diameter  $\delta$  through  $S^1$  that does not pass through any point in  $X^\diamond$ . We fix a face  $F$  of  $\Sigma$ , and color the points of  $X^\diamond$  corresponding to the generators of  $F$ . This colored subset  $F^\diamond \subset X^\diamond$  is antipode-free because  $F$  is antipode-free by assumption, and therefore at most one point of any centrally symmetric pair  $\pm x_i^*$  in  $X^\diamond$  is colored. Note that if  $F$  is a facet of  $\Sigma$ , then  $|F^\diamond| = d$ , so by antipode-freeness and  $|X^\diamond| = 2(d + 2)$  we conclude that exactly two antipodal pairs of  $X^\diamond$  remain uncolored.

We model this situation in the following way, cf. Figure 10.3: There are  $n = d + 2$  ‘boxes’ that can be filled either in the ‘high shelf’ or the ‘low shelf’ with a ‘ball’.

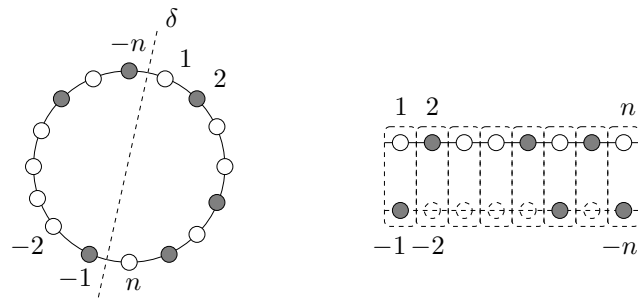


FIGURE 10.3: Modeling a cs-Gale transform of a  $d$ -dimensional cs-fan  $\Sigma$  on  $2d + 4$  rays by  $d + 2$  boxes that may be filled in the high or low shelf with a ball. If the colored points on the left correspond to a facet of  $\Sigma$ , then on the right there are two empty boxes.

- Definition 10.15** (a) A box with a ball in the high shelf is called a *high box* and abbreviated by  $h$ , one with a ball in the low shelf a *low box*  $\ell$ . High and low boxes together comprise *filled boxes*, a box without a ball is an *empty box*  $e$ . An *aa-pair*  $p$  is an ordered pair  $h\ell$  or  $\ell h$  of boxes.
- (b) For  $d \geq 2$ , a  $d$ -*configuration* of boxes is an ordered sequence of  $\lfloor d/2 \rfloor$  aa-pairs (and one filled box if  $d$  is odd) and 2 empty boxes. Transforming a  $d$ -configuration via  $h\sigma \leftrightarrow \sigma\ell$ ,  $\ell\sigma \leftrightarrow \sigma h$  and  $e\sigma \leftrightarrow \sigma e$ , for some ordered sequence  $\sigma$  of boxes, corresponds to different choices of the diameter  $\delta$ .

#### 10.4.1 Even dimension

**Proposition 10.16** Let  $d \geq 2$  be even. Then there are exactly

$$G_{\text{even}}(d) = 2^{d/2} f_{d-1}(C_d(d+2)) = 2^{d/2} \left(\frac{d}{2} + 1\right)^2$$

$d$ -configurations of boxes.

*Proof.* A  $d$ -configuration fulfills Gale's Evenness Criterion (there is an even number of filled boxes between the two empty boxes), and there are two choices for filling each of the  $d/2$  aa-boxes.  $\square$

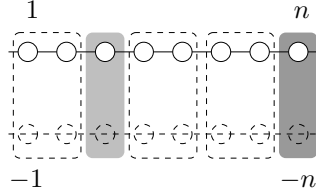


FIGURE 10.4: The partition of  $X$  into  $d/2$  aa-boxes and two empty boxes.

**Corollary 10.17** By the cs-Gale transform and Proposition 10.14,

$$f_{d-1}^{\Sigma}(d, d+2) \leq G_{\text{even}}(d),$$

where  $f_{d-1}^{\Sigma}(d, d+2)$  is the number of facets of a  $d$ -dimensional cs-neighborly cs-fan on  $2d+4$  rays.  $\square$

*Proof of Theorem 10.1 for even  $d \geq 4$ .* Observe that in this case,

$$f_{d-1}^{\Sigma}(d, d+2) = \left(\frac{d}{2} + 1\right) 2^d > G_{\text{even}}(d) \quad \text{for } d \geq 4,$$

so we are done by Corollary 10.17. Note that  $f_{d-1}^{\Sigma}(2, 4) = 8 = G_{\text{even}}(2)$ .  $\square$



## 10.4.2 Odd dimension

In odd dimension  $d \geq 3$ , we have to work a little harder, as not every  $d$ -configuration corresponds to a possible facet of a cs-neighborly cs-fan. Denote by  $t(C)$  resp.  $b(C)$  the number of balls on high resp. low shelves of a  $d$ -configuration  $C$ . Then

$$|t(C) - b(C)| \in \{1, 3\}, \quad (10.4)$$

where  $|t(C) - b(C)| = 3$  implies that the diameter  $\delta$  separates an aa-pair.

**Definition 10.18** For odd  $d \geq 3$ , the set  $\mathcal{C}_{axb}^d$  consists of the representatives of the following  $d$ -configurations:

$$f^{2i} e \ell h f^{(d-5)/2-2i} h h \ell e, \quad \text{for } 0 \leq i \leq (d-5)/2,$$

where ‘ $f$ ’ denotes a filled box. The last ‘ $\ell$ ’-box is called the  $v$ -box, cf. Figure 10.5.

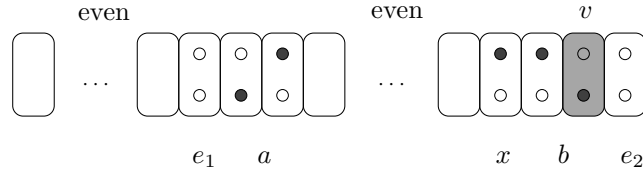


FIGURE 10.5: A typical element of  $\mathcal{C}_{axb}^d$ . The letters below the figure will be explained shortly.

**Lemma 10.19** No configuration in  $\mathcal{C}_{axb}^d$  corresponds to a facet of a  $d$ -dimensional cs-neighborly cs-fan.

*Proof.* Suppose that  $C \in \mathcal{C}_{axb}^d$  does correspond to a facet  $F$  of such a fan, and denote by  $C_v$  the sequence of boxes obtained from  $C$  by replacing the  $v$ -box with an empty box. Then the ridge  $\tau$  of  $F$  that corresponds to  $C_v$  must be contained in exactly one other facet. We try to complete  $C_v$  to a different  $d$ -configuration  $C'$  by placing a ball into one of the two empty boxes  $e_1, e_2$  different from  $v$ . But note the following:

- ▷ If we add the new ball to the high shelf of any empty box, then  $C'$  violates (10.4).
- ▷ If  $e_1$  remains empty,  $C'$  is not a  $d$ -configuration because it does not contain  $\lfloor d/2 \rfloor$  aa-pairs, and thus violates condition (b) of Definition 10.15.
- ▷ If the new ball goes to the bottom of the box  $e_1$ , this condition is also violated.

This completes the proof.  $\square$

**Definition 10.20** (a) A  $d$ -configuration  $C$  is called *valid* if it does not belong to  $\mathcal{C}_{axb}$ .  
 (b) For  $\ell \geq 3$ , let  $\mathcal{W}_\ell$  be the set of words of length  $\ell$  in the alphabet  $\mathcal{A} = \{a, b, e, x, y\}$ , such that

- (1) each  $w \in \mathcal{W}_\ell$  contains exactly two letters  $e$
- (2) each  $w \in \mathcal{W}_\ell$  contains exactly one  $x$  or exactly one  $y$

(3) the following words in  $\mathcal{W}_\ell$  are considered equivalent:

$$\begin{aligned} \sigma xa\tau &\sim \sigma bx\tau & \text{and} \\ \sigma yb\tau &\sim \sigma ay\tau, \end{aligned} \tag{10.5}$$

where  $\sigma$  and  $\tau$  are words in  $\mathcal{W}_i$  for  $0 \leq i \leq \ell - 2$ . (We define  $\mathcal{W}_0 = \emptyset$ .)

**Proposition 10.21** For odd  $d \geq 3$ , set  $\ell := (d - 1)/2 + 3$ . Then there is a bijection between the set  $\mathcal{C}_d$  of  $d$ -configurations and  $\mathcal{W}_\ell$ . Only those words in  $\mathcal{W}_\ell$  correspond to a valid  $d$ -configuration (and are called *valid*) that do not contain  $a\sigma xb$  as a subword.

*Proof.* The dictionary from  $\mathcal{C}_d$  to  $\mathcal{W}_\ell$  is given by Figure 10.6.

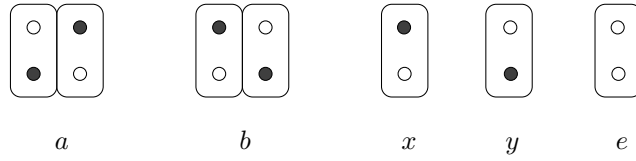


FIGURE 10.6: The dictionary between  $\mathcal{C}_d$  and  $\mathcal{W}_\ell$ .

The two letters  $e$  correspond to the two empty boxes in  $\mathcal{C}_d$ , the letters  $a$  and  $b$  to the possible matchings between balls on adjacent high and low shelves, and the single  $x$  or  $y$  to the remaining box. The rules for equivalence are due to the difficulties in translation depicted in Figure 10.7. For the last statement, cf. Figure 10.5.  $\square$

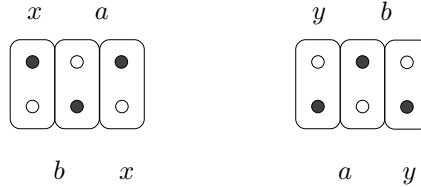


FIGURE 10.7: The reason for identifying the words  $\sigma xa\tau \sim \sigma bx\tau$  and  $\sigma yb\tau \sim \sigma ay\tau$ .

**Lemma 10.22** (a) There are  $I_{ab}(k) = 2^k$  words of length  $k \geq 0$  on the alphabet  $\{a, b\}$ .  
 (b) The number of equivalence classes of words of length  $k \geq 1$  on the alphabet  $\mathcal{A}' := \{a, b, x\}$  that contain exactly one letter  $x$  but no subsequence  $axb$ , and such that two words are equivalent under the rule (10.5), is  $I_{\mathcal{A}'}(k) = 2^k - 1$ .

*Proof.* (a) is clear. Given a word  $w$  as in (b), we use (10.5) to commute the letter  $x$  to the right as far as possible, so that  $w$  is transformed to  $w' = x$  if  $k = 1$ , or  $w' = \sigma xb\tau$  if  $k > 1$ , where  $\sigma$  and  $\tau$  are possibly empty words in  $\mathcal{A}'$ . Suppose that  $k > 1$  and that the letter  $x$  is at position  $i$  counting from the left, with  $1 \leq i \leq k - 1$ ; then there is a letter  $b$  at position  $i + 1$ . Because  $w$  contains no subsequence  $axb$ , we see that  $a \notin \sigma$  and therefore  $\sigma = b^{i-1}$ . This leaves  $2^{k-1-i}$  possible choices for  $w'$ , see Figure 10.8 (top).

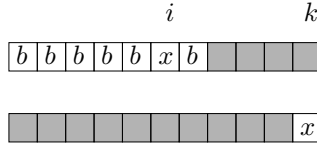


FIGURE 10.8: *Top*: Possible choices for  $w'$ . *Bottom*: One remaining case. In each picture, a shaded box may be filled with either  $a$  or  $b$ .

If we can commute  $x$  all the way to the end, we may choose either  $a$  or  $b$  to fill each of the positions before  $x$ , see Figure 10.8 (bottom). The number we are looking for is therefore

$$I_{\mathcal{A}'}(k) = \sum_{i=1}^{k-1} 2^{k-1-i} + 2^{k-1} = 2^k - 1. \quad \square$$

**Proposition 10.23** For odd  $d \geq 3$ , there are

$$G_{\text{odd}}(d) = (d-1)(d+2)2^{(d+1)/2} + 2(d+2)$$

$d$ -configurations of boxes.

*Proof.* We use the bijection from Proposition 10.21, and count the number of valid  $d$ -configurations by counting the number of words in  $\mathcal{W}_\ell$ , for  $\ell = (d-1)/2 + 3$ . We will first count the number  $N_x(d)$  of words in  $\mathcal{W}_\ell$  beginning with  $e$  and containing one letter  $x$ . The number of words beginning with  $e$  and containing  $y$  is the same by symmetry. Then  $G_{\text{odd}}(d) = \frac{1}{2} 2(d+2)N_x(d) = (d+2)N_x(d)$ , because by Figure 10.9 there are  $d+2$  choices for the position of the first empty box  $e$ , and every word is counted twice that way.

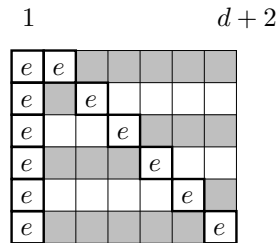


FIGURE 10.9: Possible positions of the empty boxes in a sequence of boxes of length  $d+2$ . The shaded subsequences of odd length  $k$  can be filled in  $I_{\mathcal{A}'}(k)$  ways, and the white ones in  $I_{ab}(k)$  ways.

For  $m \in \{2, 3, \dots, d+2\}$ , build a valid sequence of boxes of length  $d$  by fixing the first empty box  $e$  in position 1, placing the second empty box in position  $m$ , and filling in the remaining positions with one letter  $x$  and  $(d+1)/2$  letters  $a, b$  to create a valid word. Now

by Figure 10.9,

$$\begin{aligned}
N_x(d) &= 2 \sum_{\substack{1 \leq k \leq d \\ k \text{ odd}}} I_{\mathcal{A}'}\left(\frac{k+1}{2}\right) I_{ab}\left(\frac{d-k}{2}\right) = 2 \sum_{\substack{1 \leq k \leq d \\ k \text{ odd}}} (2^{(k+1)/2} - 1) 2^{(d-k)/2} \\
&= 2 \frac{d+1}{2} 2^{(d+1)/2} - 2 \sum_{j=0}^{(d-1)/2} 2^j = (d+1) 2^{(d+1)/2} - 2 (2^{(d+1)/2} - 1) \\
&= (d-1) 2^{(d+1)/2} + 2. \quad \square
\end{aligned}$$

*Proof of Theorem 10.1 for odd  $d$ .* For odd  $d \geq 11$ ,

$$f_{d-1}^S(d, d+2) = \frac{d-1}{2} 2^d > G_{\text{odd}}(d). \quad \square$$

**Remark 10.24** The values of  $f_{d-1}^S(d, d+2)$ ,  $G_{\text{odd}}(d)$  and  $G_{\text{even}}(d)$  for small values of  $d$  are

$d$	1	2	3	4	5	6	7	8	9	10	11
$f_{d-1}^S(d, d+2)$	2	8	16	48	96	256	512	1280	2560	6144	12288
$G_{\text{odd}}(d)$	6		50		238		882		2838		8346
$G_{\text{even}}(d)$		8		36		128		400		1152	





# Bibliography

Numbers at the end of the entries refer to the page(s) on which these are cited

- [1] MANUEL ABELLANAS, *Always in first place.* vii
- [2] NOGA ALON, *The number of polytopes, configurations and real matroids*, *Mathematika*, **33** (1986), 62–71. Zbl. 0591.05014. 8
- [3] NINA AMENTA and GÜNTER M. ZIEGLER, *Deformed products and maximal shadows of polytopes*, in *Advances in Discrete and Computational Geometry. Proceedings of the 1996 AMS-IMS-SIAM joint summer research conference on discrete and computational geometry: ten years later*, South Hadley, MA, USA, July 14–18, 1996, Bernard Chazelle, Jacob E. Goodman, and Richard Pollack, eds., vol. 223 of *Contemporary Mathematics*, Amer. Math. Soc., Providence, RI, 1999, 57–90. Zbl. 0916.90205. 17, 22, 23
- [4] DAVID W. BARNETTE, *Diagrams and Schlegel diagrams*, in *Combinatorial Structures and Their Applications*, Proc. Calgary Internat. Conference 1969, New York, 1970, Gordon and Breach, 1–4. Zbl. 0245.52005. 77
- [5] ———, *A family of neighborly polytopes*, *Isr. J. Math.*, **39** (1981), 127–140. Zbl. 0471.52004. 43, 44
- [6] ALEXANDER BELOW, *Complexity of Triangulation*, PhD thesis, No. 14672, ETH Zürich, 2002. 20
- [7] NORMAN BIGGS, *Automorphisms of imbedded graphs*, *J. Comb. Theory Ser. B*, **11** (1971), 132–138. Zbl. 0187.20901. 96
- [8] LOUIS J. BILLERA and CARL W. LEE, *A proof of the sufficiency of McMullen’s conditions for  $f$ -vectors of simplicial convex polytopes*, *J. Comb. Theory, Ser. A*, **31** (1981), 237–255. Zbl. 0479.52006. 9, 77, 78, 79
- [9] LOUIS J. BILLERA and BERND STURMFELS, *Fiber polytopes*, *Annals of Math.*, **135** (1992), 527–549. Zbl. 0762.52003. 68
- [10] ROBERT E. BIXBY, *Solving real-world linear programs: a decade and more of progress*, *Operations Research*, (to appear). <http://www.caam.rice.edu/caam/trs/2001/TR01-20.pdf>. 6, 17
- [11] ANDERS BJÖRNER, *Topological methods*, in *Handbook of Combinatorics*, Ronald Graham, Martin Grötschel, and László Lovász, eds., vol. 2, Elsevier Science B.V., 1995, 1819–1871. Zbl. 0833.05001. 11
- [12] ANDERS BJÖRNER, MICHEL LAS VERGNAS, BERND STURMFELS, NEIL WHITE, and GÜNTER M. ZIEGLER, *Oriented Matroids*, second ed., vol. 46 of *Encyclopedia of Mathematics*, Cambridge University Press, Cambridge, 1993. Zbl. 0944.52006. 40
- [13] (JOHANNES) MAX BRÜCKNER, *Über die Ableitung der allgemeinen Polytope und die nach Isomorphismus verschiedenen Typen der allgemeinen Achtzelle (Oktatope)*, *Verhand. Konik. Akad. Wetenschap, Erste Sectie*, **10** (1910). announced in JfM 39.0629.01. 77

- [14] HEINZ BRUGGESSER and PETER MANI, *Shellable decompositions of cells and spheres*, *Math. Scand.*, (1971). 30
- [15] GEOFFREY R. BURTON, *The non-neighborliness of centrally symmetric convex polytopes having many vertices*, *J. Comb. Theory Ser. A*, **58** (1991), 321–322. Zbl. 0738.52012. 102
- [16] CGAL, *Computational Geometry Algorithms Library*. <http://www.cgal.org>. 39
- [17] HAROLD SCOTT MACDONALD COXETER, *Regular Polytopes*, third ed., Dover, 1973. 5
- [18] CPLEX. <http://www.ilog.com/products/cplex/>. 39
- [19] GEORGE B. DANTZIG, *Maximization of a linear function of variables subject to linear inequalities*, in *Activity Analysis of Production and Allocation*, Tj. C. Koopmans, ed., Wiley, New York, 1951, ch. XXI, 339–347. Zbl. 0045.09802. 6
- [20] ———, *Linear Programming and Extensions*, Princeton University Press, Princeton, New Jersey, 1963. Zbl. 0997.90504. 6
- [21] DAVID EISENBUD and SORIN POPESCU, *The projective geometry of the Gale transform*, *J. Algebra*, **230** (2000), 127–173. Zbl. pre01523168. 27
- [22] DAVID EPPSTEIN, GREG KUPERBERG, and GÜNTER M. ZIEGLER, *Fat 4-polytopes and fatter 3-spheres*, in *Discrete Geometry: In honor of W. Kuperberg's 60th birthday*, A. Bezdek, ed., Pure and Applied Mathematics. A series of Monographs and Textbooks, Marcel Dekker Inc., 2003 (to appear), 239–265. [arXiv:math.CO/0204007](https://arxiv.org/abs/math.CO/0204007). 9, 80, 96, 97
- [23] PAUL ERDŐS, *Über die Primzahlen gewisser arithmetischer Reihen (German)*, *Math. Z.*, (1935), 473–491. Zbl. 0010.29303. 96
- [24] GÜNTER EWALD, *Combinatorial Convexity and Algebraic Geometry*, vol. 168 of Graduate Texts in Mathematics, Springer, 1996. Zbl. 0869.52001. 12, 77, 102
- [25] KOMEI FUKUDA, *cdd—an implementation of the double description method with LP solver*. [http://www.cs.mcgill.ca/~fukuda/soft/cdd\\_home/cdd.html](http://www.cs.mcgill.ca/~fukuda/soft/cdd_home/cdd.html). 71
- [26] DAVID GALE, *Neighboring vertices on a convex polyhedron*, *Ann. Math. Stud.*, **38** (1956), 255–264. Zbl. 0072.37805. 86
- [27] BERND GÄRTNER, JOZSEF SOLYMOSSI, FALK TSCHIRSCHNITZ, PAVEL VALTR, and EMO WELZL, *One line and  $n$  points*, in *Proc. 33rd Ann. ACM Symp. on the Theory of Computing (STOC)*, 2001, 306–315. <http://www.ti.inf.ethz.ch/ew/research/papers/2001/gstvw-olnp-stoc01.ps>. 22, 27, 29
- [28] ISRAEL M. GELFAND, MIKHAIL M. KAPRANOV, and ANDREI V. ZELEVINSKY, *Discriminants, Resultants, and Multidimensional Determinants*, Birkhäuser, 1994. Zbl. 0827.14036. 67
- [29] JACOB E. GOODMAN and RICHARD POLLACK, *There are asymptotically far fewer polytopes than we thought*, *Bull. Amer. Math. Soc.*, **14** (1986), 127–129. Zbl. 0585.52003. 8, 77, 79
- [30] ———, *Upper bounds for configurations and polytopes in  $\mathbb{R}^d$* , *Discrete Comput. Geom.*, **1** (1986), 219–227. Zbl. 0609.52004. 8, 77, 79
- [31] BRANKO GRÜNBAUM, *Convex Polytopes*, Wiley Interscience, 1967. Zbl. 0163.16603. Second edition by VOLKER KAIBEL, VICTOR KLEE and GÜNTER M. ZIEGLER, Springer Verlag, New York, GTM 221. 9, 20, 22, 23, 27, 33, 39, 70, 101



- [32] BRANKO GRÜNBAUM and V.P. SREEDHARAN, *An enumeration of simplicial 4-polytopes with 8 vertices*, *J. Comb. Theory*, **2** (1967), 437–465. Zbl. 0156.43304. 18, 40, 77
- [33] CHRISTIAN HAASE and GÜNTER M. ZIEGLER, *Examples and counterexamples for the Perles conjecture*, *Discrete Comput. Geom.*, **28** (2002), 29–44. Zbl. pre01784794. 28
- [34] GEORGE W. HART, *Neolithic carved stone polyhedra*.  
<http://www.georgehart.com/virtual-polyhedra/neolithic.html>. 4
- [35] ROBERT L. HEBBLE and CARL W. LEE, *Squeezed 2-spheres and 3-spheres are Hamiltonian*. Preprint <http://www.ms.uky.edu/~lee/ham.pdf>, 15 pages, December 4, 2000. 9, 80, 83, 90
- [36] LOTHAR HEFFTER, *Ueber metacyklische Gruppen und Nachbarconfigurationen. (German)*, *Math. Ann.*, **50** (1898), 261–268. Facsimile available at JfM 29.0117.01. 9, 80, 95, 96, 97
- [37] FRED HOLT and VICTOR KLEE, *A proof of the strict monotone 4-step conjecture*, *Contemp. Math.*, **223** (1999), 201–216. Zbl. 0916.90206. 21
- [38] LYNNE D. JAMES and GARETH A. JONES, *Regular orientable imbeddings of complete graphs*, *J. Comb. Theory Ser. B*, **39** (1985), 353–367. Zbl. 0584.05028. 96
- [39] WILLIAM JOCKUSCH, *An infinite family of nearly neighborly centrally symmetric 3-spheres*, *J. Comb. Theory Ser. A*, **72** (1995), 318–321. Zbl. 0844.52006. 9, 102
- [40] MICHAEL JOSWIG and EWGENIJ GAWRILOW, *polymake—a versatile tool for the algorithmic treatment of polytopes and polyhedra*. 8, 25, 39, 64
- [41] ———, *polymake: A framework for analyzing convex polytopes*, vol. 29 of DMV Semin., Birkhäuser, 2000, 43–73. Zbl. 0960.68182. 8, 64
- [42] MICHAEL JOSWIG, VOLKER KAIBEL, and FRIEDERIKE KÖRNER, *On the  $k$ -systems of a simple polytope*, *Isr. J. Math.*, **129** (2002), 109–117. Zbl. pre01760709. 52
- [43] VOLKER KAIBEL and MARC E. PFETSCH, *Some algorithmic problems in polytope theory*, Tech. report, TU Berlin, February 2002. 25 pages, [arXiv:math.CO/0202204](http://arxiv.org/abs/math.CO/0202204). To appear in: *Algebra, Geometry, and Software Systems*. M. Joswig and N. Takayama (eds.), Springer. See also <http://www.zib.de/pfetsch/apropo/>. 20
- [44] GIL KALAI, *Many triangulated spheres*, *Discrete Comput. Geom.*, **3** (1988), 1–14. Zbl. 0631.52009. 8, 77, 79, 83, 84, 95
- [45] ———, *A simple way to tell a simple polytope from its graph*, *J. Comb. Theory, Ser. A*, **49** (1988), 381–383. Zbl. 0673.05087. 20
- [46] ———, *A subexponential randomized simplex algorithm*, in *Proc. 24th ACM Symposium on the Theory of Computing (STOC)*, ACM Press, 1992, 475–482. 18
- [47] LEONID V. KANTOROVICH, *Mathematical Methods of Organising and Planning Production*, Publication House of the Leningrad State University, Leningrad, 1939. English translation: *Management Science* **5** (1958–59), 1–4. 6
- [48] ———, *My journey in science* (proposed report to the Moscow Mathematical Society) (Russian, English), *Russ. Math. Surv.*, **42** (1987), 233–270. translation from *Usp. Mat. Nauk* **42**, No. 2(254) (1987), 183–213, Zbl. 0631.01025. 6
- [49] NARENDRA KARMARKAR, *A new polynomial-time algorithm for linear programming*, *Combinatorica*, **4** (1984), 373–395. Zbl. 0557.90065. 6, 18

- [50] LEONID G. KHACHIYAN, *Polynomial algorithms in linear programming (Russian)*, Zhurnal Vychislitel'noi Matematiki i Matematicheskoi Fiziki, **20** (1980), 51–68. Zbl. 0431.90043; English translation: U.S.S.R. Comput. Math. Math. Phys. **20** (1980), 53–72, Zbl. 0459.90047. 6, 18
- [51] VICTOR KLEE, *Heights of convex polytopes*, J. Math. Anal. Appl., **11** (1965), 176–190. Zbl. 0133.15904. 18
- [52] ———, *Paths on polyhedra II*, Pacific J. Math., **17** (1966), 249–262. Zbl. 0141.21303. 7
- [53] VICTOR KLEE and PETER KLEINSCHMIDT, *The  $d$ -step conjecture and its relatives*, Math. of Op. Research, **12** (1987), 718–755. Zbl. 0632.52007. 17
- [54] VICTOR KLEE and GEORGE J. MINTY, *How good is the simplex algorithm?*, in Inequalities III, Proc. 3rd Symp., Los Angeles 1969, O. Shisha, ed., Academic Press, New York, 1972, 159–175. Zbl. 0297.90047. 3, 7, 17
- [55] ULRICH KORTENKAMP, *Every simplicial polytope with at most  $d + 4$  vertices is a quotient of a neighborly polytope*, Discrete Comput. Geom., **18** (1997), 455–462. Zbl. 0898.52009. 40
- [56] FRANCIS LAZARUS, MICHEL POCCHIOLA, GERT VEGTER, and ANNE VERROUST, *Computing a canonical polygonal schema of an orientable triangulated surface*, in Proc. 17th Ann. ACM Sympos. Comput. Geom., 2001, 80–89. 97
- [57] CARL W. LEE, *Subdivisions and triangulations of polytopes*, in Handbook of Discrete and Computational Geometry, CRC Press, 1997, ch. 14, 271–290. 64
- [58] ———, *Kalai's squeezed spheres are shellable*, Discrete Comput. Geom., **24** (The Branko Grünbaum Birthday Issue, 2000), 391–396. 79
- [59] FRANK H. LUTZ, *Triangulated manifolds with few vertices and vertex-transitive group actions*, PhD thesis, TU Berlin, 1999. Shaker Verlag, Aachen, Zbl. 0977.57030. 12
- [60] ———, *Nearly neighborly centrally symmetric 3-spheres with cyclic group action on  $4m$  vertices*. Preprint, 5 pages, 2002. 9, 102
- [61] TOMONARI MASADA, HIROSHI IMAI, and KEIKO IMAI, *Enumeration of regular triangulations*, in Proc. 12th Ann. ACM Sympos. Comput. Geom. (Philadelphia, PA, USA), ACM Press, 1996, 224–233. <http://www-imai.is.s.u-tokyo.ac.jp/PAPERS/MasImaIma.ps>. 71
- [62] JIŘÍ MATOUŠEK, *Lectures on Discrete Geometry*, Graduate Texts in Mathematics **212**, Springer, 2002. 27
- [63] JIŘÍ MATOUŠEK, MICHA SHARIR, and EMO WELZL, *A subexponential bound for linear programming*, in Proc. Eighth Annual ACM Symp. Computational Geometry, Berlin, 1992, ACM Press, 1–8. 18
- [64] PETER McMULLEN, *The numbers of faces of simplicial polytopes*, Isr. J. Math., **9** (1971), 559–570. Zbl. 0209.53701. 7, 8, 18, 19, 78
- [65] ———, *The polytope algebra*, Adv. Math., **78** (1989), 76–130. Zbl. 0686.52005. 78
- [66] ———, *Separation in the polytope algebra*, Beitr. Algebra Geom., (1993), 15–30. Zbl. 0780.52015. 78
- [67] PETER McMULLEN and GEOFFREY C. SHEPHARD, *Diagrams for centrally symmetric polytopes*, Mathematika, **2** (1968), 123–138. Zbl. 0167.50902. 9, 101, 103, 106

- [68] JED MIHALISIN and VICTOR KLEE, *Convex and linear orientations of polytopal graphs*, *Discrete Comput. Geom.*, **24** (2000), 421–435. Zbl. 0956.05048, doi:10.1007/s004540010046. 20
- [69] THEODORE S. MOTZKIN, *Comonotone curves and polyhedra*, Abstract, *Bulletin Amer. Math. Soc.*, **63** (1957), 35. 18
- [70] MANFRED PADBERG, *Linear Programming*, second ed., vol. 12 of Algorithms and Combinatorics, Springer Verlag, Heidelberg, 1999. 17
- [71] MARKO PETKOVSEK, HERBERT S. WILF, and DORON ZEILBERGER,  $A = B$ , A. K. Peters, 1996. Zbl. 0848.05002. 105
- [72] JULIAN PFEIFLE, *Secondary polytope of a cyclic 8-polytope with 12 vertices*. Electronic Geometry Model No. 2000.09.032, 2000. <http://www.eg-models.de/>, Zbl. pre01682981. 71
- [73] ———, *Secondary polytope of the 3-cube*. Electronic Geometry Model No. 2000.09.031, 2000. <http://www.eg-models.de/>, Zbl. pre01682980. 71
- [74] ———, *Kalai's squeezed 3-spheres are polytopal*, *Discrete Comput. Geom.*, **27** (2002), 395–407. Zbl. 1003.52007, doi:10.1007/s00454-001-0074-3. 9, 80, 83, 90
- [75] JULIAN PFEIFLE and JÖRG RAMBAU, *Computing triangulations using oriented matroids*, in *Algebra, Geometry, and Software Systems*, Michael Joswig and Nobuki Takayama, eds., Springer, 2003, ch. 3, 49–75. ZIB-preprint 02-02. 63
- [76] KONRAD POLTHIER, SAMY KHADEM-AL-CHARIEH, EIKE PREUSS, and ULRICH REITEBUCH, *Javaview*. <http://www-sfb288.math.tu-berlin.de/vgp/javaview/>. 8, 70
- [77] JÖRG RAMBAU, *TOPCOM—a package for computing Triangulations Of Point Configurations and Oriented Matroids*. <http://www.zib.de/rambau/TOPCOM.html>. Software under the Gnu Public Licence. 8, 64
- [78] ———, *Polyhedral Subdivisions and Projections of Polytopes*, PhD thesis, TU Berlin, 1996. Shaker Verlag.  
See also [http://www.zib.de/rambau/Diss/diss\\_MASTER/diss\\_MASTER.html](http://www.zib.de/rambau/Diss/diss_MASTER/diss_MASTER.html). 107
- [79] ———, *Topcom: Triangulations of point configurations and oriented matroids*, Tech. Report 02-17, ZIB-Report, 2002. Proceedings of the International Congress of Mathematical Software, to appear. 8, 64
- [80] ULRICH REITEBUCH, *Rhombicosidodecahedron*. Electronic Geometry Model No. 2000.09.013, <http://www.eg-models.de>. Zbl. pre01683017. 64
- [81] ———, *Soccerball*. Electronic Geometry Model No. 2000.09.019, <http://www.eg-models.de>. Zbl. pre01683023. 3
- [82] JÜRGEN RICHTER-GEERT, *Realization Spaces of Polytopes*, LNM **1643**, Springer, 1996. Zbl. 0866.52009. 19, 20
- [83] M. ROSENFELD and DAVID BARNETTE, *Hamiltonian circuits in certain prisms*, *Discrete Math.*, **5** (1973), 389–394. Zbl. 0269.05114. 90
- [84] MUTSUMI SAITO, BERND STURMFELS, and NOBUKI TAKAYAMA, *Gröbner Deformations of Hypergeometric Differential Equations*, vol. 6 of Algorithms and Computation in Mathematics, Springer, 2000. Zbl. 0946.13021. 67
- [85] LUDWIG SCHLÄFLI, *Theorie der vielfachen Kontinuität*. Denkschriften der Schweizerischen Naturforschenden Gesellschaft **38**, 1901. 1–237. 5

- [86] ROLF SCHNEIDER, *Neighbourliness of centrally symmetric polytopes in high dimensions*, *Mathematika*, **22** (1975), 176–181. Zbl. 0316.52002. 101
- [87] E. SCHÖNHARDT, *Über die Zerlegung von Dreieckspolyedern in Tetraeder (Ggerman)*, *Math. Ann.*, (1927), 309–312. Facsimile available at JfM 53.0576.01. 102
- [88] ALEXANDER SCHRIJVER, *Theory of Linear and Integer Programming*, Wiley Interscience, 1986. Zbl. 0665.90063. 6, 17, 27, 36
- [89] ———, *On the history of the transportation and maximum flow problems*, *Math. Program.*, **91** (2002), 437–445. Zbl. pre01837142, doi:10.1007/s101070100259. 17
- [90] CLAUDIA SCHULTZ, *Schwierige lineare Programme für den Simplex-Algorithmus (German)*. Diplomarbeit, TU Berlin, 2001. 81 pages. 27
- [91] IDO SHEMER, *Neighborly polytopes*, *Isr. J. Math.*, **43** (1982), 291–314. Zbl. 0598.05010. 43, 79, 95
- [92] GEOFFREY C. SHEPHARD, *Diagrams for positive bases*, *J. London Math. Soc.*, **2** (1971), 165–175. Zbl. 0225.15004. 108
- [93] ERIC SPARLA, *Geometrische und kombinatorische Eigenschaften triangulierter Mannigfaltigkeiten (German)*, PhD thesis, Mathematisches Institut B der Universität Stuttgart, 1997. Shaker Verlag, Zbl. 0937.52008. 105
- [94] RICHARD P. STANLEY, *The upper-bound conjecture and Cohen-Macaulay rings*, *Stud. Appl. Math.*, **54** (1975), 135–142. Zbl. 0308.52009. 8, 95, 102
- [95] ———, *The number of faces of a simplicial convex polytope*, *Adv. Math.*, **35** (1980), 236–238. Zbl. 0427.52006. 78
- [96] ———, *Enumerative Combinatorics, Vol. 1*, second ed., vol. 49 of Cambridge Studies in Advanced Mathematics, Cambridge University Press, 1997. Zbl. 0889.05001. 83
- [97] ERNST STEINITZ, *Polyeder und Raumeinteilungen*, in *Encyclopädie der mathematischen Wissenschaften*, Band 3 (Geometrie), Teil 3AB12, , 1922, 1–139. 77
- [98] ERNST STEINITZ and HANS RADEMACHER, *Vorlesungen über die Theorie der Polyeder unter Einschluß der Elemente der Topologie*, vol. 41 of Grundlehren der mathematischen Wissenschaften, Springer-Verlag, Berlin, 1934. Reprint, Springer Verlag 1976, Zbl. 0325.52001. 8, 20, 77
- [99] JOHN STILLWELL, *Classical Topology and Combinatorial Group Theory*, second ed., Graduate Texts in Mathematics **72**, Springer, 1993. Zbl. 0774.57002. 97
- [100] BERND STURMFELS, *Cyclic polytopes and d-order curves*, *Geom. Dedicata*, **24** (1987), 103–107. Zbl. 0628.52008. 84
- [101] ———, *Gröbner Bases and Convex Polytopes*, vol. 8 of University Lecture Series, AMS, 1996. Zbl. 0856.13020. 68
- [102] STEVE WILSON, *Families of regular maps in graphs*, *J. Comb. Theory Ser. B*, **85** (2002), 269–289. 96
- [103] GÜNTER M. ZIEGLER, *Lectures on Polytopes*, vol. 152 of Graduate Texts in Mathematics, Springer, New York, 1995. Revised edition 1998, Zbl. 0823.52002. 11, 18, 27, 29, 30, 46, 52, 68, 78, 84, 86
- [104] ———, *Typical and extremal linear programs*, in “The Sharpest Cut”, Padberg Festschrift, Martin Grötschel and Annegret Wagler, eds., SIAM, 2003, to appear.  
ftp://ftp.math.tu-berlin.de/pub/combi/ziegler/WWW/79padberg.ps.gz. 17





## Kapitel 11

# Zusammenfassung

Teil I dieser Dissertation kreist um die Frage, ob es für jedes  $n > d \geq 4$  eine lineare Zielfunktion  $f : \mathbb{R}^d \rightarrow \mathbb{R}$  und ein  $d$ -dimensionales Polytop  $P$  mit  $n$  Facetten und maximal vielen Ecken gibt, so dass  $f$  auf  $P$  einen strikt aufsteigenden Hamiltonpfad induziert.

Diese Frage ist unter anderem motiviert durch die Existenz der *Klee-Minty-Würfel*: das sind Polytope vom gleichen kombinatorischen Typ wie ein  $d$ -dimensionaler Würfel, die aber so in  $\mathbb{R}^d$  realisiert sind, dass es einen strikt aufsteigenden Pfad durch alle  $2^d$  Ecken gibt. Sie sind für die Theorie der linearen Programmierung deswegen interessant, weil sie den Simplex-Algorithmus mit einigen natürlichen Pivot-Regeln dergestalt in die Irre leiten, dass er das Optimum erst nach Durchlaufen *sämtlicher* Ecken des Würfels erreicht.

Nun kennen wir in jeder Dimension  $d$  die Polytope mit *maximal* vielen Ecken, bei gegebener Facettenzahl: die *polar-nachbarschaftlichen* Polytope. Es stellt sich somit die Frage, ob man für alle  $n > d \geq 4$  ein polar-nachbarschaftliches  $d$ -dimensionales Polytop mit  $n$  Facetten so im  $\mathbb{R}^d$  realisieren kann, dass es einen strikt aufsteigenden Hamiltonpfad zulässt.

In Dimension  $d = 4$  können wir diese Frage vollständig lösen. In Kapitel 4 betrachten wir den Graphen  $G$  des kleinsten interessanten 4-dimensionalen polar-nachbarschaftlichen Polytops  $C_4(7)^\Delta$ , und klassifizieren sämtliche Äquivalenzklassen von  $G$  unter Graphenisomorphie nach ihrer Realisierbarkeit. In Kapitel 5 realisieren wir dann für jedes  $n \geq 5$  ein 4-dimensionales polar-nachbarschaftliches Polytop mit  $n$  Facetten und der maximal möglichen Anzahl  $n(n-3)/2$  von Ecken so im  $\mathbb{R}^4$ , dass es bezüglich der linearen Zielfunktion  $f : \mathbb{R}^4 \rightarrow \mathbb{R}$ ,  $\mathbf{x} \mapsto x_4$  einen strikt aufsteigenden Hamiltonpfad in seinem Graphen gibt.

In Teil II widmen wir uns mehr kombinatorischen Eigenschaften von Simplicialkomplexen, insbesondere der Frage nach der Anzahl kombinatorischer Typen von simplicialen Sphären. Kalai zeigte im Jahr 1988, dass es für alle  $d \geq 4$  deutlich mehr kombinatorische Typen  $d$ -dimensionaler simplicialer Sphären als Typen von  $(d+1)$ -dimensionalen Polytopen gibt, konnte diese Frage aber für  $d = 3$  nicht entscheiden.

Wir zeigen in Kapitel 8, dass Kalais Konstruktion für  $d = 3$  sogar *ausschließlich* polytopale Sphären liefert, indem wir sämtliche Sphären seiner Familie als Randkomplexe simplicialer 4-dimensionaler Polytope realisieren. In Kapitel 9 zeigen wir dann, dass die Antwort für  $d = 3$  trotzdem dieselbe wie für  $d \geq 4$  ist: Es gibt tatsächlich viel mehr kombinatorische Typen von 3-Sphären als von 4-Polytopen! Günter M. Ziegler und ich konstruieren „viele triangulierte 3-Sphären“, indem wir eine Konstruktion von Heffter aus dem Jahr 1898 mit einer Idee von Eppstein von 2002 kombinieren.

In Kapitel 10 schließlich wird gezeigt, dass es für alle geraden  $d \geq 4$  und ungeraden  $d \geq 11$  keine  $d$ -dimensionalen *zentralsymmetrischen sternförmigen Sphären* mit  $2d+4$  Ecken gibt.





# Lebenslauf

Julian Pfeifle

geboren am 23.9.1971 in Innsbruck (Österreich)  
als Sohn von Karl H. A. Pfeifle und Edith Pfeifle

- 1978–1979 Volksschule in Innsbruck (Österreich)
- 1979–1982 Elementary School in Pasco, WA und San Diego, CA (USA)
- 1982–1989 Bundesrealgymnasium Adolf-Pichler-Platz (Innsbruck)
- 1985–1986 Tri-Cities Senior High School in Pasco, WA (USA)
- Mai 1989 Matura mit Auszeichnung in Innsbruck
- 1989–1997 Studium der Mathematik und Physik an der Leopold-Franzens-Universität Innsbruck
  - 1996 ERASMUS-Aufenthalt an der Universidad Complutense de Madrid
  - 1997 Studienabschluss (Mag. rer. nat.) mit Auszeichnung in Mathematik
  - Betreuer der Diplomarbeit: Dr. Herwig Hauser
- 1997–1998 Zivildienst beim Mobilen Hilfsdienst Innsbruck
- 1998–2000 Studienassistent an der Universidad Rey Juan Carlos (Madrid)
  - 2000 *Suficiencia investigadora* der Universidad Politécnica de Madrid
- 2000–2003 Stipendiat des Graduiertenkollegs *Combinatorics, Geometry, and Computation* an der TU Berlin; Betreuer Prof. Günter M. Ziegler



## Eidesstattliche Versicherung

Ich versichere an Eides statt, dass ich die von mir vorgelegte Dissertation selbstständig angefertigt habe und alle benutzten Quellen und Hilfsmittel vollständig angegeben habe. Die Zusammenarbeit mit anderen Wissenschaftlern habe ich kenntlich gemacht. Diese Personen haben alle bereits ihr Promotionsverfahren abgeschlossen.

Teile dieser Arbeit sind bereits veröffentlicht, und zwar:

1. *Many triangulated 3-spheres*  
gemeinsam mit Günter M. Ziegler, [arXiv:math.MG/0212004](#), 7 Seiten, November 2002
2. *Kalai's squeezed 3-spheres are polytopal*  
*Discrete & Computational Geometry* **27** (2002) No. 3, 395-407      Zbl. pre01747949
3. *Computing triangulations using oriented matroids*  
gemeinsam mit Jörg Rambau, ZIB preprint **ZR 02-02**;  
ausserdem in *Algebra, Geometry, and Software Systems*, Michael Joswig and Nobuki Takayama, eds., Springer 2003
4. *Some Secondary Polytopes of Point Configurations*  
in *EG-Models*,      Zbl. pre01682980–Zbl. pre01682986

Die noch nicht endgültig veröffentlichten Artikel können nachgereicht werden.

Eine Anmeldung der Promotionsabsicht habe ich an keiner anderen Fakultät oder Hochschule beantragt.